Industria Textilă

ISSN 1222–5347

6/2014

Revistă **cotată ISI** și inclusă în **Master Journal List** a Institutului pentru Știința Informării din Philadelphia – S.U.A., începând cu vol. 58, nr. 1/2007/
ISI rated *magazine, included in the* ***ISI Master Journal List*** *of the Institute of Science Information, Philadelphia, USA, starting with vol. 58, no. 1/2007*

Editată în 6 nr./an, indexată și recenzată în:
Edited in 6 issues per year, indexed and abstracted in:
Science Citation Index Expanded (SciSearch®), Materials Science Citation Index®, Journal Citation Reports/Science Edition, World Textile Abstracts, Chemical Abstracts, VINITI, Scopus, Toga FIZ technik ProQuest Central

Recunoscută în România, în domeniul Științelor inginerești, de către
Consiliul Național al Cercetării Științifice din Învățământul Superior
(C.N.C.S.I.S.), în **grupa A** /
Aknowledged in Romania, in the engineering sciences domain,
by the ***National Council of the Scientific Research from the Higher Education*** *(CNCSIS), in* ***group A***

Sumar

Contents

Journal edited in colaboration with **Editura AGIR**, 118 Calea Victoriei, sector 1, Bucharest, tel./fax: 021-316.89.92; 021-316.89.93;
e-mail: editura@agir.ro, www.edituraagir.ro

Investigation of wrinkle free treatment of 100% lightweight cotton plain fabric

RUI-HUA YANG CHI-WAI KAN

REZUMAT – ABSTRACT

Investigarea tratamentului antişifonare al ţesăturilor plane uşoare din 100% bumbac

Finisarea prin presare permanentă este o metodă eficientă de producere a ţesăturilor din bumbac neşifonabile, dar cu o pierdere a rezistenţei la rupere a ţesăturilor. În această lucrare au fost realizate experimente factoriale complete şi ortogonale pentru a investiga mecanismul de revenire din şifonare şi rezistenţa la rupere a ţesăturii plane din bumbac. Unghiul de revenire din şifonare (WRA) al mostrei a fost testat prin metoda de testare AATCC 66-2003. Rezistenţa la rupere a ţesăturii, rezistenţa la interţesere şi rezistenţa firului au fost testate înainte şi după tratamentul aplicat cu ajutorul maşinii de testare la tracţiune. Utilizând experimentul factorial complet, s-a ajuns la concluzia că mostra de ţesătură a avut cea mai bună performanţă antişifonare la o temperatură de polimerizare de 110ºC, un timp de polimerizare de 3 minute, un grad de absorbţie de 80% şi o concentraţie a răşinii de 60g/l. S-a descoperit că după tratamentul cu răşină, a existat o îmbunătăţire a unghiului de şifonare (WRA), dar în acelaşi timp rezistenţa la rupere a ţesăturii s-a pierdut din cauza reducerii frecării firului şi a tenacităţii firului.

Cuvinte-cheie: ţesătură plană din bumbac, antişifonare, răşină, rezistenţă la rupere, rezistenţă la interţesere, tenacitatea firului

Investigation of Wrinkle Free Treatment of 100% Lightweight Cotton Plain Fabric

Durable press finishing is an effective way to produce wrinkle-resistant cotton fabrics but with a loss in tearing strength of fabrics. In this paper, full factors and orthogonal experiments were carried out to investigate mechanism between the wrinkle recovery and tearing strength of cotton plain fabric. Wrinkle recovery angle (WRA) of the specimen was tested by AATCC Test Method 66-2003. Fabric tearing strength, interwoven resistance and yarn strength were tested before and after resin treatment by tensile testing machine. With the use of full factors experiment, it can be concluded that the fabric specimen achieved the best wrinkle-free performance at 110ºC curing temperature, 3.0 minutes curing time, 80% pick-up and 60g/l resin concentration. It was revealed that after resin treatment, there was an improvement in the WRA but at the same time fabric lost tearing strength due to reduction in yarn friction and yarn tenacity.

Keywords: Cotton plain fabric, wrinkle-free, resin, tearing strength, interwoven resistance, yarn tenacity

Cotton fibers are the most important natural fibers in the apparel industry. Since cotton can readily absorb moisture, the clothing made of cotton fabrics is the most comfortable garment. Despite the numerous advantages, there are also some disadvantages, such as easy wrinkling of fabric in practical applications [1–5]. As cotton fibers contain large amounts of hydroxyl groups they are highly hydrophilic. In addition, the fiber crystallization is low, so that when cotton fibers absorb water, the bonding force among cellulose molecules is reduced markedly, which causes swelling. Therefore, when cotton fabrics are twisted or rubbed when being washed or worn, the cellulose macromolecules shift and undergo plastic deformation. Consequently, the fabric shrinks and wrinkles. The primary method of minimizing creases in cotton fabrics when washed or worn is to use appropriate agents to cross-link the cellulose molecules in the fiber called durable press finishing or wrinkle free finishing. The finishing used for overcoming wrinkling problems in cotton fabric for some years, involves chemical crosslinking agents that covalently crosslink with hydroxyl groups of adjacent cellulose polymer chains within cotton fibers to prevents the relative displacement of the cellulose molecules in cotton fibers when washed or worn. The chemicals usually involved were mainly dimethyloldihydroxyethylenurea (DMDHEU) and the formaldehyde-free finishing agents for example carboxylic acids such as 1,2,3,4-butanetetracarboxyic acid (BTCA) and citric acid [6–8]. This crosslinking not only results in improving the fabric wrinkle resistance but also impairing fabric strength and other mechanical properties. Several studies show that there was a decrease in mechanical strength of durable press finished cotton fabric [9–10].

100% lightweight cotton plain fabric is defined as fabric weight of less than 115 g/m^2 which is commonly applied on the making shirt in the garment industry. It is good for creating print design and many finishing as the surface is plain and relatively flatter than other weaves. In this study, we aimed to impart durable press functionalities to lightweight cotton plain fabric by a simple pad-dry-cure procedure in order to investigate the effect of durable press treatments on wrinkle free ability and the mechanism between durable press and tearing strength of cotton fabrics. Wrinkle recovery angle (WRA) measurements were performed to evaluate the durable-press efficiency. In addition, fabric tearing strength, yarn tenacity, fabric interwoven resistance were measured in order to explore the mechanism of durable press and fabric tearing strength.

EXPERIMENTAL

Fabric

The lightweight 100% cotton plain woven fabric was used and its specification was listed in table 1. No scouring or washing was required to clean dirt or impurity prior to wrinkle free finishing. The fabrics were conditioned at 21±1ºC with a relative humidity of 65±2% for at least 24 hours prior to use.

Table 1

FABRIC SPECIFICATION	
Fabric weight	105 g/m²
Yarn count	80 s
Fabric density Warp density Weft density	 140 yarns per inch 76 yarns per inch

Wrinkle free finishing

Wrinkle free finishing cotton plain fabric was carried out by pad-dry-cure method using a commercial resin, Fixapret F-ECO (modified dimethyloldihydroxyethylene urea resin) with magnesium chloride as catalyst. Three resin solution concentrations, 30g/l, 45g/l and 60g/l, were used. Three pick-ups, 60%, 70% and 80%, were used and after padding, the fabric specimens were dried completely in the oven at 70ºC. The curing was carried out at 110ºC or 120ºC using three curing times, i.e. 2 minutes, 2.5 minutes and 3 minutes. After wrinkle free finishing, the fabric specimens were conditioned at 21±1ºC with relative humidity of 65±2% for at least 24 hours prior to evaluation. Full factor experiments were used to research the wrinkle free finishing by wrinkle recovery angle.

Table 2

EXPERIMENTAL ARRANGEMENT			
Test Run	**Parameters**		
	Resin concentration (g/l)	**Curing time (minutes)**	**Pick-up (%)**
1	30	2	60
2	30	2.5	80
3	30	3	70
4	45	2	80
5	45	2.5	70
6	45	3	60
7	60	2	70
8	60	2.5	60
9	60	3	80

Orthogonal experiment was used to carry out the effects of the wrinkle free finishing on strength of fabrics and yarns, and the experimental arrangement was shown in table 2.

Wrinkle recovery angles

The wrinkle free property, expressed as wrinkle recovery angle (WRA) was evaluated by AATCC Test Method 66-2003.

Fabric tearing strength

Fabric tearing strength was evaluated by BS EN ISO 13937-2 using a constant-rate-of-extension tensile testing machine – Instron 4411 tensile testing machine (New Jersey, USA), as shown in figure 1.

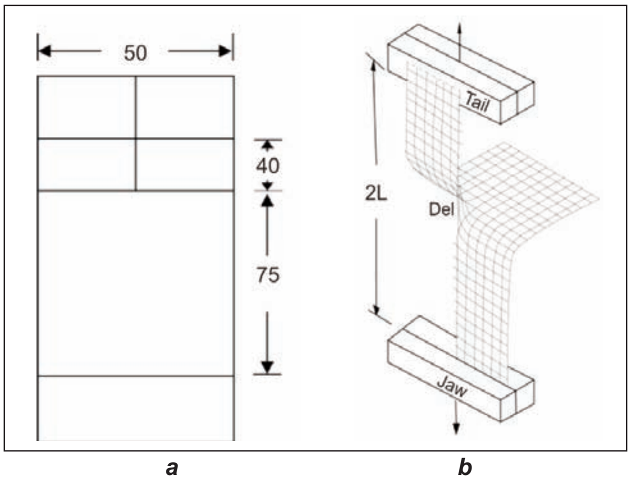

Fig. 1. Fabric tearing method: *a* – geometry diagram (mm), *b* – tear illustration (unit: mm)

Yarn tenacity

Yarns were taken from fabrics with and without durable press finishing and their tenacity were tested by tensile testing machine (Instron 4411 tensile testing machine) with at a test length of 500 mm, extension rate of 250 mm/min and pretension of 0.5 cN/tex.

Interwoven resistance

Interwoven resistance was tested by tensile testing machine (Instron 4411 tensile testing machine), as shown by figure 2. The testing speed was 48±2 mm/min, pulling distance 15 mm, and distance of tong mouth 25 mm.

Scanning electron microscopy (SEM)

The surface morphology of the fabrics was investigated by a scanning electron microscope (JEOL, Model No: JSM-6335F) with a magnification of 1 000X.

RESULTS AND DISCUSSION

Wrinkle recovery angle at 110ºC curing temperature

The results of WRA according to the full factorial experiment with 110ºC curing temperature are shown in figure 3. It can be observed that WRA increases

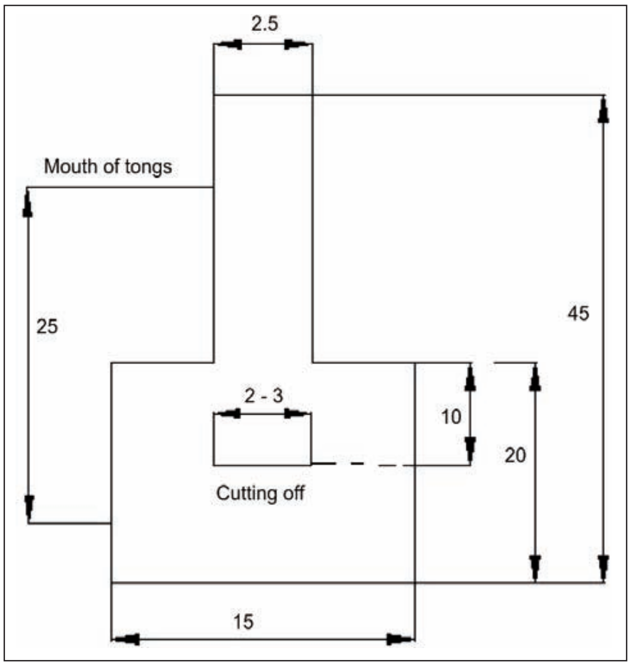

a

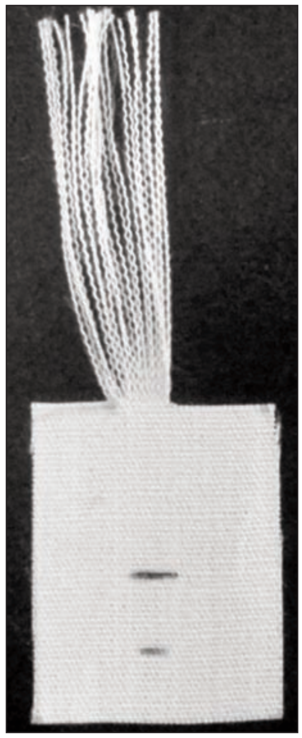

b

Fig. 2. Interwoven resistance testing (unit: mm):
a – geography illusion, *b* – sample before testing)

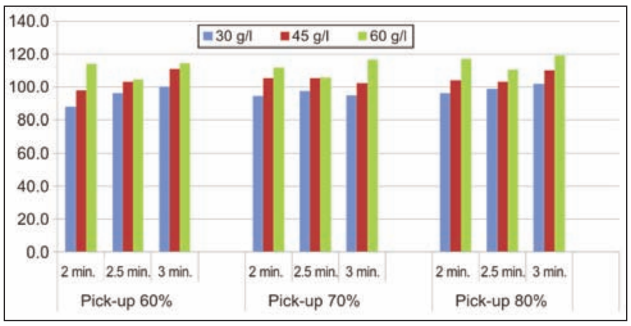

Fig. 3. Winkle recovery angles of cotton plain fabric

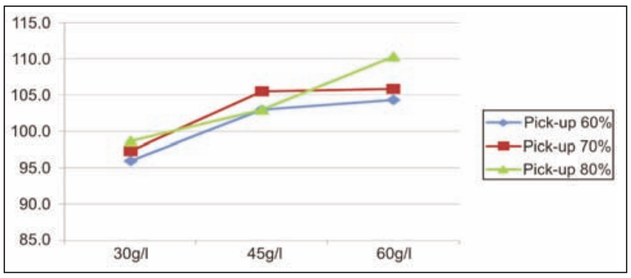

Fig. 4. Wrinkle recovery angles of cotton plain fabric at 2.5 minutes curing time

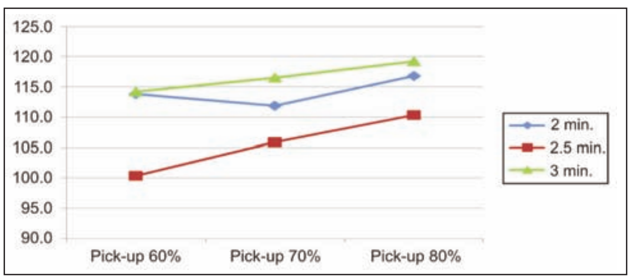

Fig. 5. Wrinkle recovery angles of cotton plain fabric with resin concentration of 60 g/L

with the resin concentrations, pick-up percentages and curing time, regularly. But WRA shows a sudden drop at 80% pick-up and 45 g/L, which is even lower than 60% and 70%, as indicated by figure 4. WRA increases with pick-up percentage, both at 30 g/L and 60 g/L. So maybe 45 g/L has a critical effect on WRA, which needs special attention at engineering. Figure 5 demonstrates that 2.5 minutes curing time gives the lowest WRA value compared with 2 min and 3 min under 60 g/L. But for 30 g/L and 45 g/L, the more curing time, the better is the WRA. The refined details are discussed in the part of tearing strength and orthogonal experiments results.

Wrinkle recovery angle at 120ºC curing temperature

Figure 6 illustrates the results of WRA under the full factorial experiment. It shows that WRA increases with increment in resin concentration. It can be observed from figure 7 that WRA could be improved by higher pick-up percentage. In case of 60% pick-up, WRA of fabric cured for 2.5 minutes achieved the best result followed by 2 and 3 minutes. While at 70% and 80% pick up, WRA increases with increasing curing time. Figure 8 reveals that WRA increases with pick-up percentage and resin concentration at 2.5 minutes curing time. Figures 6 to 8 demonstrate

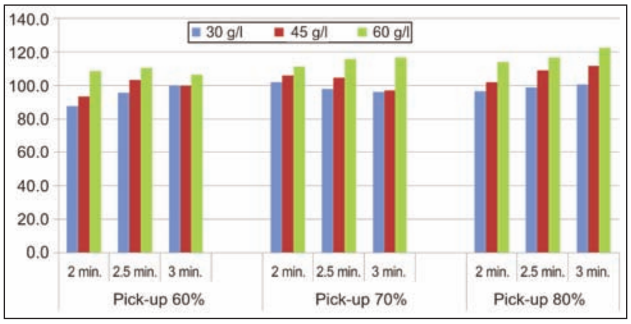

Fig. 6. Wrinkle recovery angles of cotton plain fabric

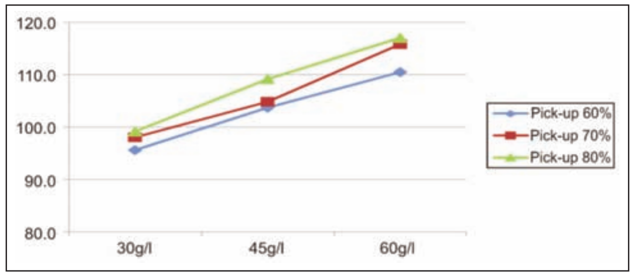

Fig. 8. Wrinkle recovery angles of cotton plain fabric at 2.5 minutes curing time

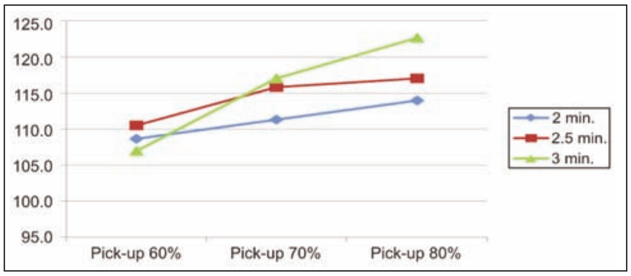

Fig. 7. Wrinkle recovery angles of cotton plain fabric with resin concentration of 60 g/l

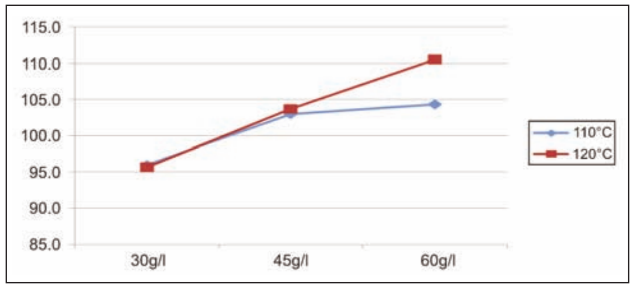

Fig. 9. Wrinkle recovery angles of cotton plain fabric treated with 110°C and 120°C curing temperature with curing time of 2.5 minutes and 60% pick-up

that at 120°C curing time, WRA achieves the best condition with curing time of 3 minutes, 80% pick-up and 60 g/l resin concentration. It is provided with the prediction that longer is curing time, the higher is the resin concentration and high pick-up percentage, brings more crosslinkages and thus improves the wrinkle free property.

Figure 9 shows the WRA values under the condition of curing time 2.5 minutes, 60% pick-up 60% both at 110°C and 120°C curing temperature. It reveals that both at resin concentration of 30 g/l and 45 g/l, WRA values were almost the same at 110°C and 120°C, while at 60g/l, the WRA value at 120°C is higher than 110°C. This might be an indication that temperature is effectively only for high resin concentration solution.

Tearing strength

Figure 10 shows the tearing strength of fabric at warp and weft direction under the full factorial experiments. It is observed that tearing strength decreases with increasing curing time with different pick-up and resin concentration. Figure 11 indicates that in warp direction, the tearing strength is the highest at 70% pick-up percentage with different curing time and resin concentration but opposite effect is noted in the weft direction. Figure 12 shows that tearing strength of resin-treated fabrics decreases with the increment of resin concentration with different pick-up percentage. Figure 13 reveals that tearing strength of resin treated fabrics at 110°C curing temperature is better than 120°C curing temperature while the curing time is 2.5 min and pick-up 70%. By concluding figures 10 to 13, the best condition to achieve a good tearing strength result would be resin concentration of 30 g/l, pick-up of 70%, curing time of 2.5 minutes with 110°C curing temperature. However, if a better complex effect on both WRA and tearing is required, the treatment condition should be resin concentration of 45 g/l, pick-up of 70%, curing time of 2.5 minutes with 110°C curing temperature.

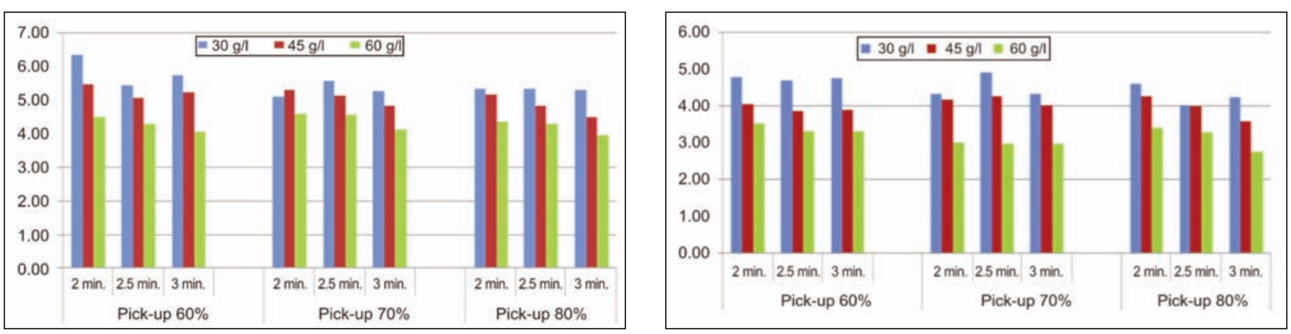

a *b*

Fig. 10. Tearing strength of (a) warp and (b) weft at 110°C

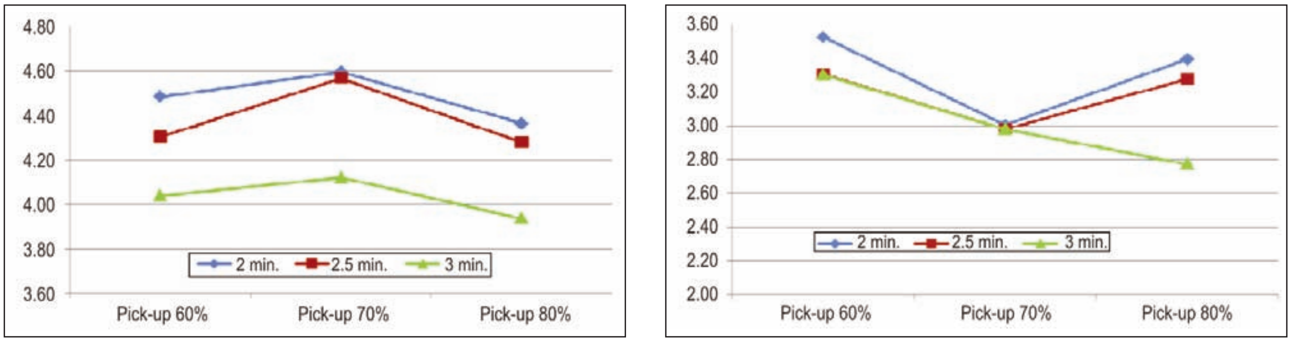

a *b*

Fig. 11. Tearing strength of (a) warp and (b) weft at 110ºC and 60g/l

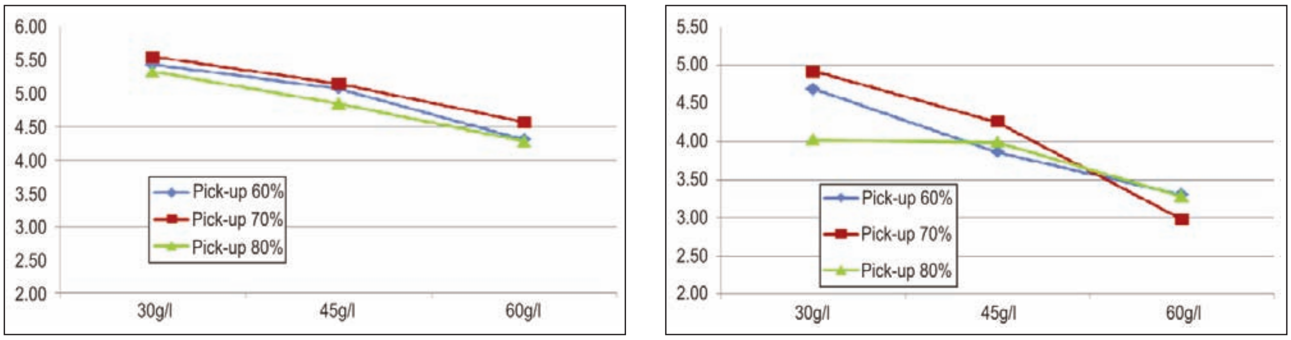

a *b*

Fig. 12. Tearing strength of (a) warp and (b) weft at 110ºC and 2.5 minutes curing time

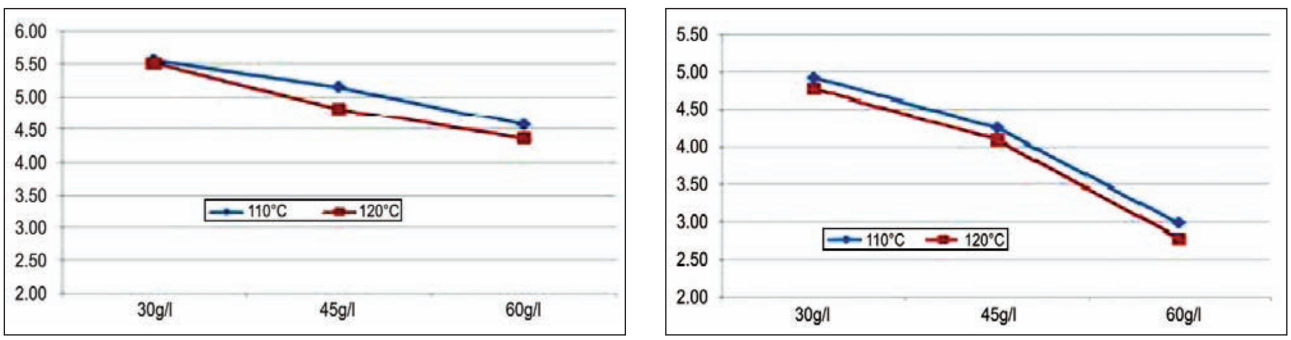

a *b*

Fig. 13. Tearing strength of (a) warp and (b) weft at 110ºC and 120ºC curing temperature, 2.5 minutes curing time

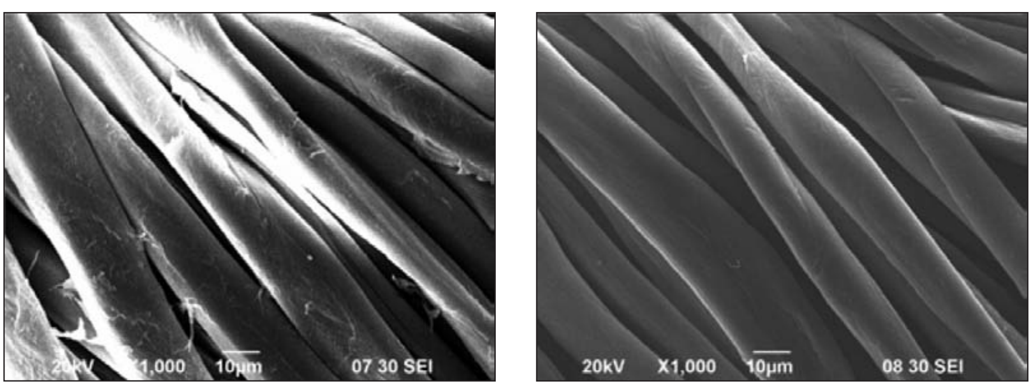

a *b*

Fig. 14. SEM of specimen (a) untreated; (b) resin treated

Table 3

ORTHOGONAL TESTS RESULTS								
		WRA	Tearing strength (Warp) (N)	Tearing strength (Weft) (N)	Single yarn strength (Warp) (cN/tex)	Single yarn strength (Weft) (cN/tex)	Interwoven resistance (Warp) (cN/tex)	Interwoven resistance (Weft) (cN/tex)
1		88.20	5.25	4.48	14.93	13.77	16.61	9.34
2		98.70	5.15	3.95	14.17	12.75	14.15	8.68
3		95.00	5.25	4.00	13.12	12.42	12.53	10.53
4		104.00	4.88	3.71	13.27	11.75	11.99	9.77
5		105.50	4.61	3.34	12.53	10.91	11.74	8.41
6		110.80	4.80	3.50	13.47	10.89	11.86	10.04
7		111.80	4.31	3.06	12.56	10.69	11.71	9.94
8		100.30	4.24	3.17	12.13	10.1	10.94	8.89
9		119.20	4.12	2.86	10.82	9.85	10.24	8.16
Untreated		82.30	7.24	5.89	18.70	17.09	18.13	11.43
CRP[1]	ΣI	281.90#	15.65*	12.42*	42.22*	38.94*	43.29*	28.55*
	ΣII	320.30	14.29	10.55	39.27	33.55	35.59	28.22
	ΣIII	331.30*	12.67#	9.09#	35.51#	30.64#	32.89#	26.99#
	D	49.40	2.98	3.34	6.71	8.30	10.40	0.33
CT[2]	ΣI	304.00#	14.44*	11.24*	40.76*	36.21*	40.31*	29.05*
	ΣII	304.50	14.08#	10.46	39.26	33.76	37.60	25.98#
	ΣIII	325.00*	14.17	10.36#	37.41#	33.16#	34.63#	28.73
	D	21.00	0.36	0.88	1.50	3.05	5.68	3.07
PU[3]	ΣI	299.30#	14.29*	11.14*	40.53*	34.76*	39.41*	28.27
	ΣII	321.90*	14.15#	10.52	38.26	34.35	36.38	26.61#
	ΣIII	312.30	14.17	10.40#	38.21#	34.02#	35.98#	28.88*
	D	22.60	0.14	0.74	2.27	0.41	3.43	2.27

Note: 1. CRP: resin concentration (g/l); 2. CT: curing time (minutes); 3. PU: Pick-up (%); *: the highest value; #: the lowest value

By testing results of WRA and tearing strength of resin treated fabrics, it can be easily found that WRA is improved with the loss in tearing strength. In order to optimize the wrinkle-free treatment parameters, the factors related to tearing strength of fabrics were further investigated. Table 3 is the orthogonal testing results of WRA, tearing strength of fabrics, interwoven resistance of fabrics and yarn tenacity.

From table 3, it can be discovered that the resin treatment has a complex effect on interwoven resistance. CRP and CT affect the interwoven resistance adversely. The higher CRP and CT are, the lower is the interwoven resistance but not in the case of PU. Along with the yarn count, woven density, fiber stype, the main factors that affect the interwoven resistance of fabric are yarn friction and yarn strength. The friction of yarn is reduced after the resin treatment, which means fibers are getting smoother as shown by figure 14. Therefore, the number of yarns in tearing zone is increased, thus the tearing strength of fabric will be increased. The yarn strength would be decreased after the resin treatment as crosslink of fiber is destroyed, which leads to the reducing of fabric tearing strength. Hence, the combination effects of yarn friction and strength of yarn after resin treatment become the main factor of reducing the tearing strength of fabrics.

CONCLUSIONS

Mechanism of wrinkle-free and tearing strength of fabric was explored by full factors and orthogonal experiments. Wrinkle recovery angle (WRA), fabric tearing strength, fabric interwoven resistance and yarn strength were analyzed both before and after the resin treatment. The experimental results revealed that reducing the friction coefficient of yarn by wrinkle-free treatment would be effectively to improve the WRA and at the same time maintain as much of tearing strength of cotton plain fabrics.

Acknowledgments

This work was supported by Natural Science Foundation of Jiangsu Province No. SBK201340440 and the National Natural Science Foundation of China No. 51403085.

BIBLIOGRAPHY

[1] Zampetakis, A; Katsaros, G. *Wear comfort and protective properties of fabrics,* In: Industria textila, 2008, vol. 59, issue 3, pp.118–124

[2] Yuen C. W. M., Kan C. W., Lee H. L., *Improving wrinkle resistance of cotton fabric by montmorillonite,* In: Fibers and Polymers, 2006, vol. 7, issue 2, pp. 139–145

[3] Khoddami, A.; Shokohi, S. S.; Sebdani, Z.M.; *A facile method for anti-bacterial finishing of cotton fabrics using silver nanoparticles*, In: Industria Textila, 2012, vol. 63, issue 1, pp. 20–26

[4] Danko, A.; Popescu, C., Dunca, S., *Improving cotton textile materials properties by treating with chitosan and metallic salts*, In: Industria Textila, 2013, vol.64, issue 4, pp. 204–209

[5] Hashem M., Ibrahim N. A., El-Shafei A., Refaie R., Hauser P., *An eco-friendly-novel approach for attaining wrinkle-free / soft-hand cotton fabric,* In: Carbohydrate Polymers, 2009, vol. 78, issue 4, pp. 690–703

[6] Vahid Ameri Dehabadi; Hans-Jürgen Buschmann; Jochen Stefan Gutmann, *Durable press finishing of cotton fabrics with polyamino carboxylic acids,* In: Carbohydrate Polymers, 2012 vol. 89, issue 2, pp. 558–563

[7] Peng, HT; Yang, CQ; Wang, SY., *Nonformaldehyde durable press finishing of cotton fabrics using the combination of maleic acid and sodium hypophosphite,* In: Carbohydrate Polymers, 2012; vol. 87; issue 1; pp. 491–499

[8] Cook, Fred Leon. *Durable press finishing of cotton fabrics,* School of Textile Engineering, Georgia Institute of Technology, 1991.

[9] Zhou, WL; Yang, CQ; Lickfield, GC., *Mechanical strength of durable press finished cotton fabric part V: Poly(vinyl alcohol) as an additive to improve fabric abrasion resistance,* In: Journal of Applied Polymer Science; 2004, vol.91, issue 6, p. 3940

[10] Schramm, C.; Rinderer, B., *Dyeing and DP treatment of sol-gel pre-treated cotton fabrics,* In: Fibers and Polymers, 2011, vol. 12, issue 2, pp. 226–232.

Author:

RUI-HUA YANG
Key Laboratory of Science & Technology
of Eco-textiles Ministry of Education
Jiangnan University,
1800 Lihu Avenue, Wuxi,
Jiangsu Province, 214122,
P. R. CHINA

CHI-WAI KAN
Institute of Textiles and Clothing,
The Hong Kong Polytechnic University,
Hung Hom, Kowloon,
Hong Kong, China

Corresponding author:
CHI-WAI KAN
E-mail: tccwk@inet.polyu.edu.hk

The influence of the textile materials structure on the screen printed circuits' characteristics

IULIANA DUMITRESCU
LI PIRA NELLO
OVIDIU GEORGE IORDACHE
GIUSEPE BIMA

REZUMAT – ABSTRACT

Influenţa structurii materialelor textile asupra caracteristicilor circuitelor imprimate cu şabloane

Lucrarea prezintă rezultatele cercetărilor privind realizarea circuitelor electrice prin tehnologia de imprimare cu șabloane pe materiale textile. Scopul l-a constituit compararea calității (lațimea și grosimea liniilor imprimate, neuniformitațile marginilor) și a rezistenței electrice a circuitelor obţinute prin imprimare cu pastă de argint (5064 Du Pont) pe țesături poliester neacoperite și acoperite cu straturi polimerice subțiri de poliuretan. Morfologia și procentul de argint al circuitelor electrice au fost analizate prin microscopie optică şi de scanare electronică (SEM), cuplat cu spectrometrul de energie dispersiva cu raze X (EDS).
Structura materialului și direcția de imprimare influențează puternic precizia liniilor imprimate. Straturile subțiri polimerice închid porii și interspațiile existente în țesături, formează o suprafață cu rugozitate scăzută și minimizează pătrunderea pastei în substrat.
Rezultatele demonstrează o acoperire relativ uniformă cu pasta conductivă a țesăturii de poliester acoperită cu poliuretan, precum și o bună definire a marginilor liniilor imprimate.

Cuvinte-cheie: textile, imprimare cu șabloane, circuite electrice

The influence of the textiles materials structure on the screen printed circuits' characteristics

The paper presents the results of the investigation of the electrical circuits manufactured by screen printing technology on textile materials. The aim was to compare the print quality (line width, thickness, edge blurriness) and electrical resistance of the circuits printed by using silver paste (5064 Du Pont) on woven polyester non-coated and coated with thin polyurethane polymeric layers. The morphology and percentage of silver of electrical circuits were analyzed by scanning electron microscope (SEM) with an energy dispersive X-ray (EDS) spectrometer.
Structure of the material and precision printing direction strongly influence the printed lines. Thin polymer layers close pores and existing interspaces between threads, form surfaces with a low roughness and minimize the paste penetration into the substrate.
The results demonstrate a relatively uniform coverage of the conductive paste on the polyester coated with polyurethane as well as good printed line edge definition.

Key-words: textiles, screen printing, electrical circuits

INTRODUCTION

Screen printing is one of the oldest and usual techniques in the textile industry. Nowadays, this technique is used for printing resistors, conductors, dielectrics, sensors, solar cells, displays, etc.

Even if great efforts have been made to adapt this technology to miniaturization and electrical circuit complexity requirements, some sensitive points are not fully solved, such as:

- penetration of the conductive inks into flexible substrates as textiles [1];
- high tendency of conductive inks (e.g. silver) to migrate, especially in the presence of moisture and an electric field [2];
- low resolution of the printed lines limited by the capillarity of the screen and the characteristics of the conductive paste, the incompatibility between the mesh opening and the viscosity of the paste [3];
- non-uniformity of the printed lines due to the non-adapted screen printing parameters (screen mesh count, squeegee durometer, snap-off distance, print speed) to the type of substrate.

The width, thickness and resolution of the printed lines largely depend on the type of process, the fabric parameters (structure type, yarn fineness, surface roughness, porosity, absorbance capacity), conductive paste properties (viscosity,) and the screen printing parameters (the curing temperature, the screen, stencil and the number of printing passes). With roller based systems it is possible to print lines at 50 μm, with screen printing to approximately 75 μm, and pad printing [4] to 10 μm.

The resolution of the printed lines is deeply affected by the surface roughness and surface energy of the textile [5]. Generally, the woven fabrics, being composed by two sets of yarns interlaced at right angles, have a high roughness, significantly influencing the adhesion and performance of printed circuits. A high surface roughness improves the effective contact area between the circuits and the substrate but if the substrate used is too rough, the printed lines are non-uniform due to peaks in the substrate which interrupt the printed tracks.

Therefore, the textiles surface roughness must be designed in such a way to ensure a good ink adhesion to the substrate and avoid tracks interruption. To optimize the surface roughness, two main factors have to be considered: textile material parameters (structure, yarn fineness, density, porosity and thickness) and deposition of a thin polymeric (polyurethane, PVC, rubber) layer onto the fabric.

MATERIALS AND METHODS

Textile materials

For the experiments, three types of substrates were used:

A 100% polyester fabric,

B 100% polyester fabric coated with polyvinylchloride

C 100% polyester fabric coated with polyurethane.

The physical and mechanical properties of polyester material (A), strongly influencing the printing characteristics are listed in table 1.

The polyester coated with polyurethane is characterized by: total weight: 200 g/m^2, textile support weight: 140 g/m^2, polyurethane weight: 60 g/m^2; polyurethane thickness: 0.03 mm.

Conductive inks

5064 Du Pont Silver conductive paste was used to print the electrical lines due its benefits [6]: good printability, outstanding electrical conductivity, high paste coverage (170 cm^2/g), excellent adhesion (5 according to ASTM x-hatch, no material removal) to various substrates such as polyester, polyamide, paper and epoxy glass, low viscosity (10Pa.S) and solids (63–66%).

Screen printing

The silver electrical lines have been screen printed on materials by using a semi-automatic screen printer with a dual squeegee print head, metal screen (200 mesh), with a sieve thickness of 50 µm (45° and 90°). For all the samples, from single to 3 print passes were applied. The printed lines have been cured in a static box oven at 130°C for 20 min in air. In the case of B and C material, the electrical lines were screen printed on the polyvinyl chloride or polyurethane coated side. No packaging as well as protective coatings has been deposited on. In detail the names report respectively fabric type, ink type, amounts of printing passes and sequential trial. As example A5064-1P-2 is A[polyester fabric]5064[ink]-1P[single pass]-2[second test]. The resulted samples are listed in the table 2 (**PVC**: polyvinyl chloride; **PU**: polyurethane).

Table 1

PROPERTIES OF WOVEN POLYESTER FABRIC

Characteristics		Value	Standard
Yarn density/cm	Warp	82	ISO 7211-2
	Weft	30	
Yarn fineness, tex	Warp	7.6	SR 6430/2012
	Weft	36	
Nr. of filaments	Warp	40	ISO 5084
	Weft	96	
Fabric thickness		0.29	SR EN ISO 5084/2001
Weight, g/m^2		140	SR EN 12127/2003; SR EN ISO 5084/2001
Structure		Satin 4/1	
Abrasion, cycles		>100000	SR EN ISO 12947-2/2002

Table 2

SCREEN PRINTED SAMPLES

Sample name		Textile material	No. of printings	Drying temp., °C
A5064	A5064-1P-2	polyester	1	20min@130°C
	A5064-1P-4	polyester	1	20min@130°C
B5064	B5064-3P-4	polyester coated with PVC	3	20min@130°C
	B5064-2P-5	polyester coated with PVC	2	20min@130°C
	B5064-2P-6	polyester coated with PVC	2	20min@130°C
C5064	C5064-1P-1	polyester coated with PU	1	20min@130°C
	C5064-1P-2	polyester coated with PU	1	20min@130°C
	C5064-1P-3	polyester coated with PU	1	20min@130°C

ANALYSES

The morphological characteristics of the conductive paste deposited on textile support have been analysed on scanning electronic microscope, SEM (Quanta 200, FEI, Netherlands) using GSED as detector. The amounts of silver included in the printed lines and on the textile support were measured by X-Rays Energy Dispersive Analysis. The width of the printed lines was approximated by optical microscopy (Carl Zeiss SteREO Discovery.V8) and SEM. The printed samples were washed according to the ISO 105 C06 using a Rotawash washing machine (Atlas, USA) equipped with polyethylene vessels with a capacity of 25 mL. The quantity of silver migrating in washing water was quantified by an atomic absorption spectrophotometer (AAS 880, Varian), equipped with a deuterium arc background corrector and an air-acetylene burner assembly. The electrical resistance of the initial and washed samples was measured by a multi-ohmeter. A static contact angle analysis was per-formed on the printed and non-printed fabrics.

RESULTS AND DISCUSSIONS

Morphological characteristics of the silver conductive paste deposited on the materials

All the materials are covered with silver flakes, presenting irregular forms and different sizes, in random contact each other. In the case of polyester not coated with polymeric layers (A), the flakes are better superimposed, probably due to the better penetration of the conductive paste into materials.
Unlike samples B5064-2P-5 and B5064-2P-6, which are covered by larger flakes and form numerous gaps between them, for sample B5064-3P-4, the flakes are smaller and overlap each other. Also, on the coated polyester polyurethane (C), the flakes are in very close contact, ensuring a high conductivity.
It is evident that metal flakes get similar sizes, dispersions, dimensions and orientations for all samples. The amount of printing passes does not affect flakes' distribution but the overall substrate cover, inducing discontinuities in the printed lines and consequently high electrical conductance. Curing temperature has been selected to get optimum condition of drying and solvent evaporation allowing contact among flakes.

The influence of the material structure on printed lines accuracy

The material structure and the printing direction strongly influence the thickness, width and accuracy of the printed lines. As can be seen in the optical images, the printing direction is along the warp. In the case of samples A with a 4/1 satin structure, four warping yarns interlaced with the filling yarns run over the one filling yarn followed by warp yarn passing below the filling yarns. On this type of structure, the most part of the conductive paste is deposited on these warping yarns. The silver paste fills almost all the pores and interspaces between the warping yarns. The filling yarns are only randomly spotted by printing paste interrupting the conductive lines. Another factor creating non-uniform surfaces, and, therefore, preventing the deposition of uniform, continuous lines silver on polyester fabric is the yarn itself, composed by a high number of filaments, which are less or more covered by silver.

The influence of the material structure on printed circuits' thickness

As the SEM images of the materials cross section show, the thickness of the printed lines is strongly

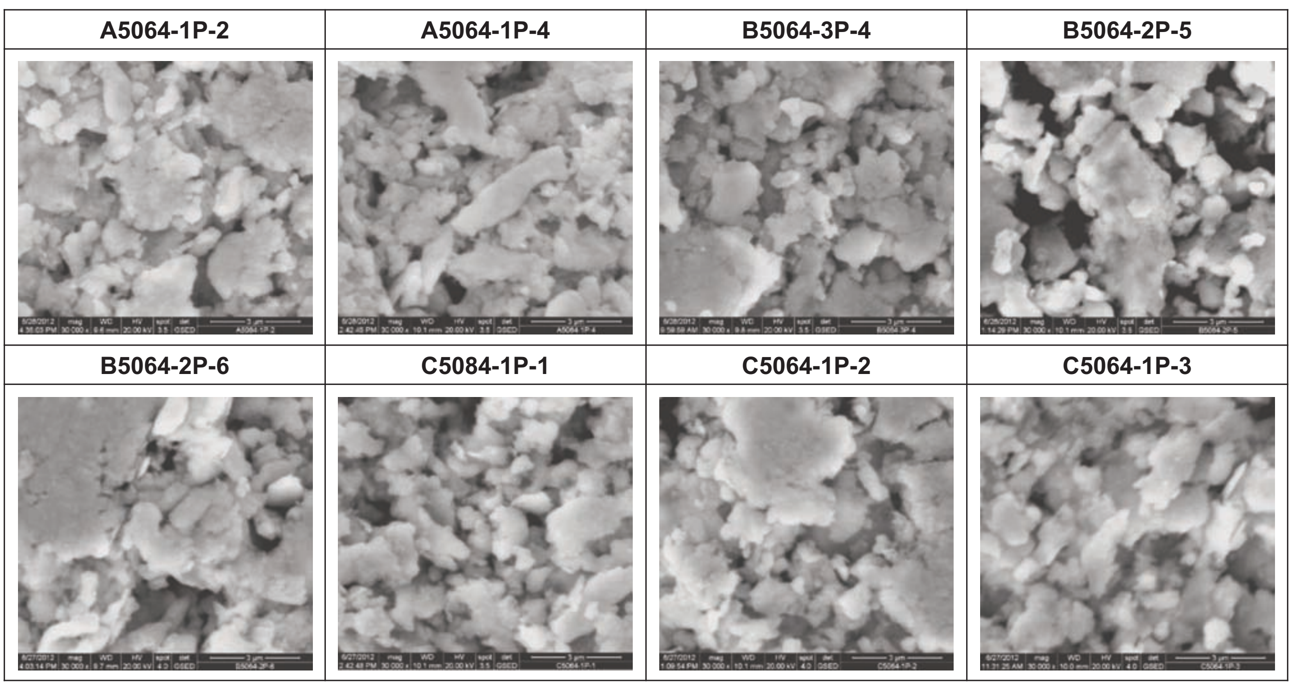

Fig. 1. SEM images of the conductive paste deposited on textile materials

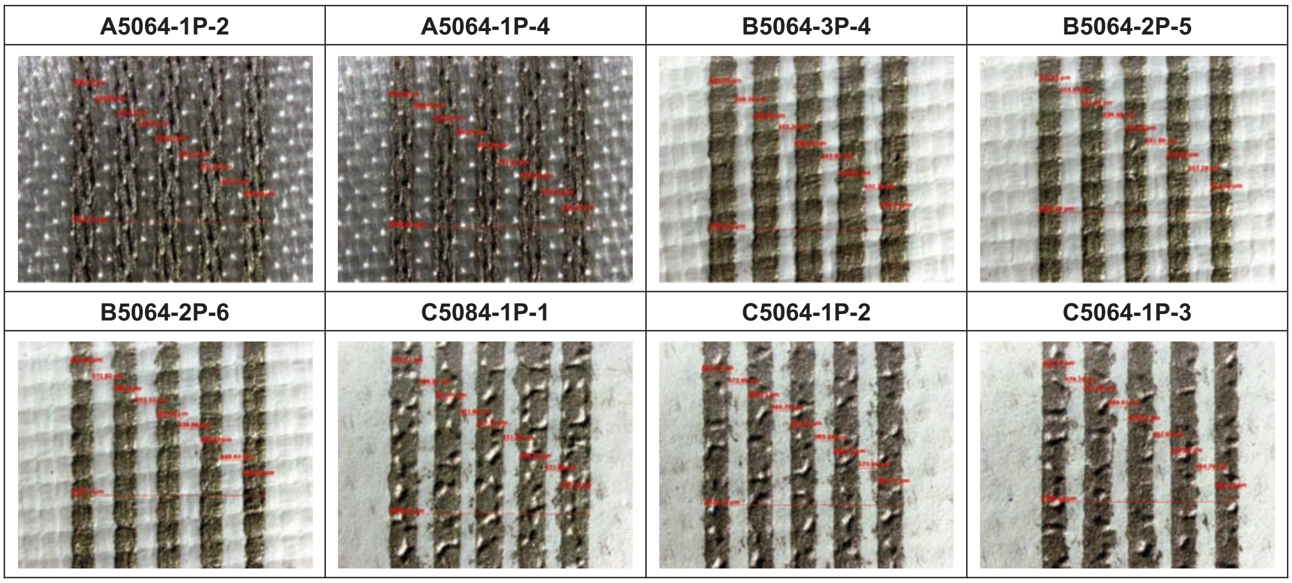

Fig. 2. Optical microscopic images of the printed lines

influenced by the material surface. Although a fabric with a smooth surface was chosen with parallel floats so no diagonal lines, with as few interlacings as possible and a tight structure (Satin 4/1) made of multifilament yarns in the warp with great finesse (7.6 tex) and relatively thick yarns (36 tex) in weave to give high strength, it was not possible to completely eliminate the pores in the material structure. As a consequence, the silver paste penetrates into material, filling the most of the empty spaces of the woven fabric. As the penetration is higher the circuits' thickness is lower as the SEM images demonstrate for the polyester samples, A5064-1P-2 and A5064-1P-4, where the printed circuits on sample A5064-1P-2 is lower than A5064-1P-4. Also, the silver printed lines on both polyester samples are thicker, more non-uniform and the edges look spread out than those printed on coated samples B and C, covered with polymeric layers. The thin polymers layers seal the pores and interspaces existing in the polyester woven material form a much smoother surface and minimize the penetration of the conductive paste into the substrate. SEM images show that, in both cases, the printing paste doesn't penetrate the materials B and C and the electrical lines are relatively uniform.

In the case of B material, the thickness increases in order: B5064-3P-4> B5064-2P-6> B5064-2P-5 and for C material: C5064-1P-1> C5064-1P-2> C5064-1P-1 as it is shown in figure 3.

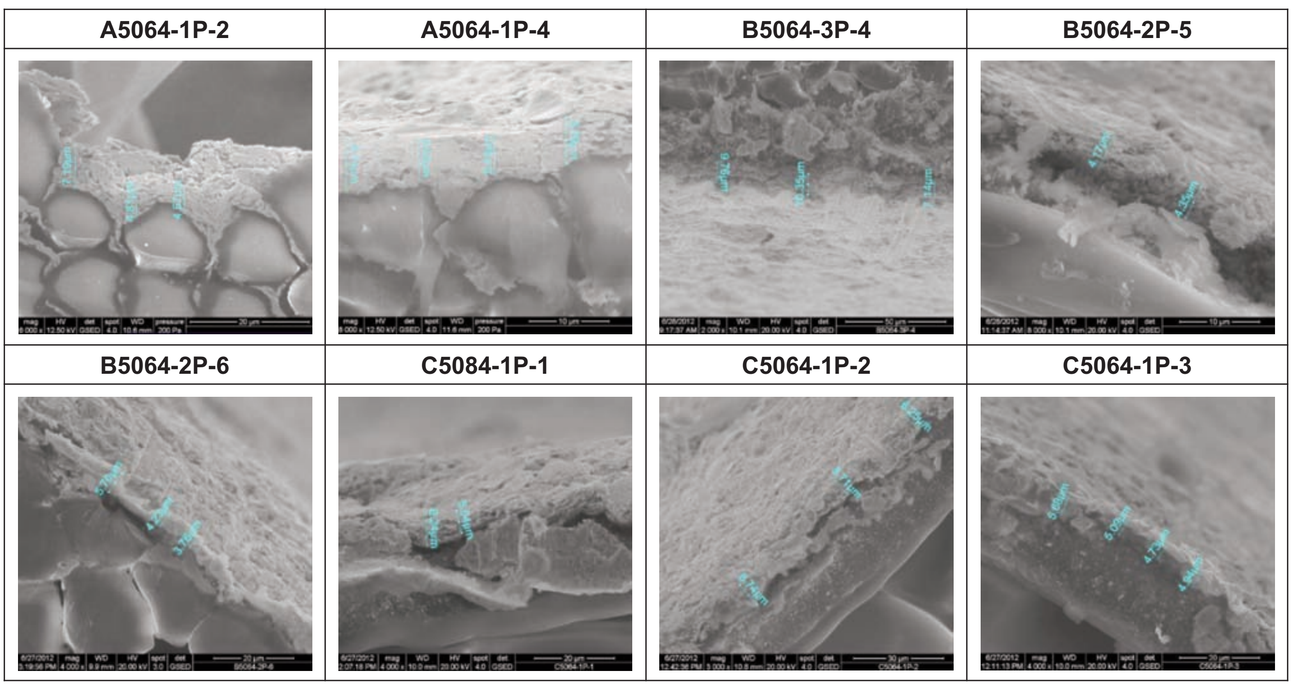

Fig. 3. SEM images of the silver circuits' cross-section

The influence of the material structure on printed lines width

The selection of satin 4/1 was effected to optimize the characteristics of the printed lines (thickness, width, distance between lines). We suppose that a compact structure produced from microfilament yarns, with small pore dimensions between the fibers inside the yarns and between yarns themselves and a high hydrophilicity will allow a fast penetration of a minimum amount of conductive paste so as to ensure a high adherence of the conductive paste simultaneous along with a high resolution of the printed lines (small width, high uniformity, reduced migration of silver paste).

As it can be seen from table 3, the contact angle was not possible to be measured due to rapid water absorption by material (contact angle is almost zero). It can be said that polyester fabric is super-hydrophilic which allows rapid absorption of printing paste. Indeed, the width of the printed coated polyester fabric is less than the printed circuits coated samples because a good amount of paste penetrates the polyester fabric (the silver particles fill up the gaps and pores of the polyester material and hence contribute less to increasing the thickness).

In the case of both samples, B and C, as printed silver lining thickness increases, the contact angle (the hydrophobia) is increasing due to the polymers hydrophobic character and the covering of the existing pores in polymeric layer.

Except samples B5064-3P-4 and C5064-1P-2, for all the analyzed samples, the contact angle decreases after printing. What is really important to notice is the effect of the printing parameters on the hydrophobic behavior of the printed and non-printed fabrics: both the substrates, B and C, are changing their hydrophobic behavior depending on the number of printing passes, drying temperature. Because both have

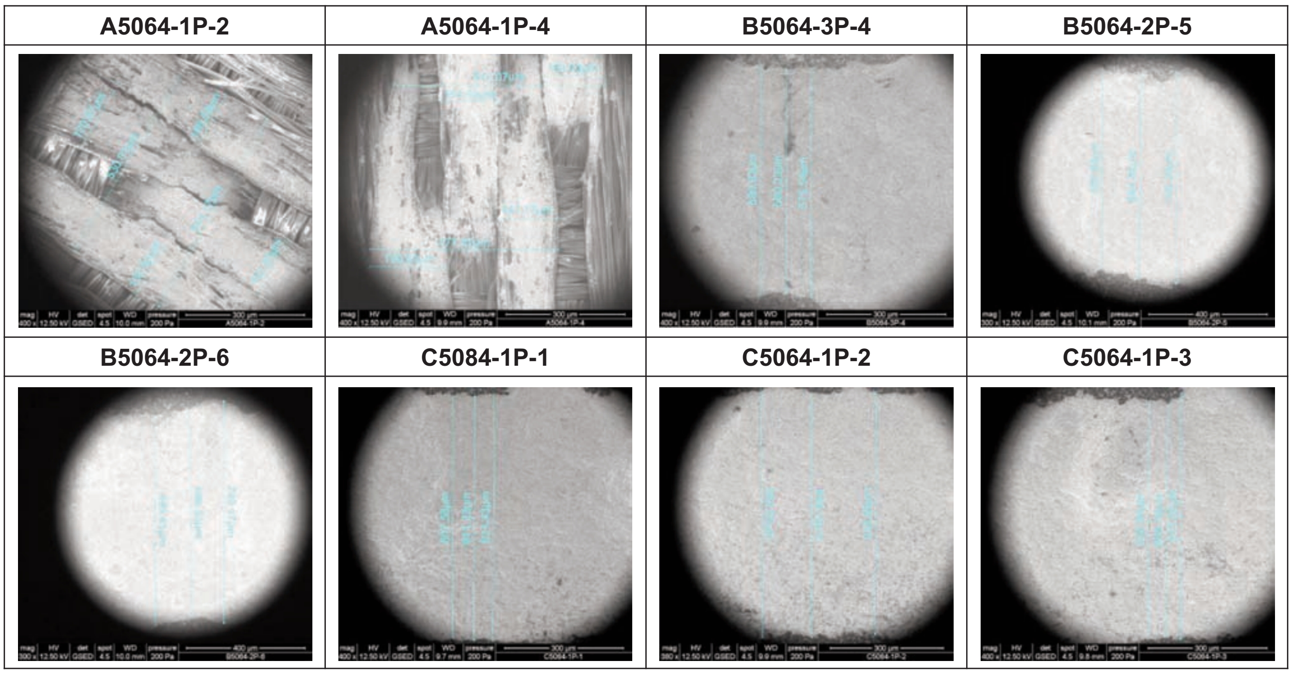

Fig. 4. SEM images of the printed lines

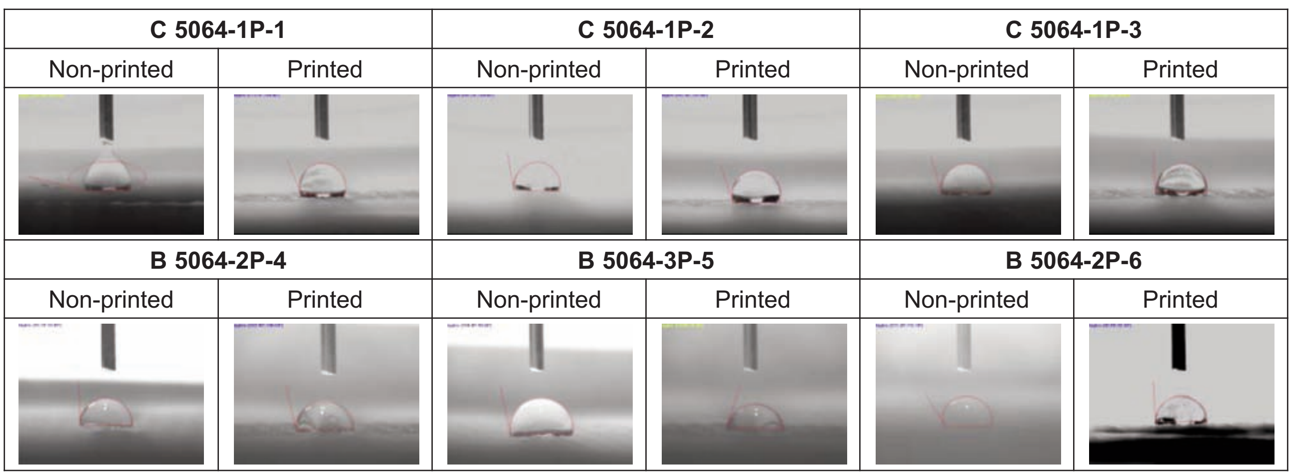

Fig. 5. Contact angle of the printed lines

Table 3

THE CHARACTERISTICS OF THE PRINTED LINES					
Sample	**Line thickness, µm**	**Line width, µm**	**Distance between 2 lines, µm**	**Contact angle**	
				Non-printed	Printed
A5064-1P-2	5.52	519.28	493.13	0	0
A5064-1P-4	5.90	529.54	468.40	0	0
B5064-3P-4	9.08	545.03	362.74	93.70; 93.80	102.90; 100.50
B5064-2P-5	4.26	687.40	278.20	100.40; 98.60	74.00; 78.30
B5064-2P-6	5.47	736.62	195.34	121.30; 116.10	92.90; 92.30
C5064-1P-1	6.94	604.52	381.32	163.70; 163.40	113.70; 109.40
C5064-1P-2	6.90	654.92	324.85	101.20; 104,60	107.90; 107.40
C5064-1P-3	5.11	593.03	388.60	106.20; 107.90	92.70; 98.40

Table 4

Ag CONCENTRATION IN WASHING WATER AFTER 5 WASHINGS					
Sample	**Printed samples weight, g**		**Weight difference**		**Ag leached in washing water, mg/l**
	Initial	**After 5 washings**	**[g]**	**[%]**	
A5064 1P-2	0.0521	0.0519	0.0002	0.385	0.259
A5064 1P-4	0.0502	0.0500	0.0002	0.398	**0.266**
B5064 3P-4	0.0644	0.0643	0.0001	0.155	***0.003***
B5064 2P-5	0.0604	0.0602	0.0002	0.331	0.008
B5064 2P-6	0.0589	0.0588	0.0001	0.169	0.009
C5064 1P-1	0.0619	0.0619	0	0	0.066
C5064 1P-2	0.0632	0.0631	0.0001	0.158	0.061
C5064 1P-3	0.0650	0.0650	0	0	0.068

coatings on top (PVC and PU) low absorption of inks is expected in these cases. According to the data included in the table, the best line resolution (minimum line width, no silver migration) was obtained for sample B5064-3P-4.

The amount of printings has been optimized because normally multiple passes get simultaneously increase of thickness and decrease of line precision. Only one pass generates lines with holes and discontinuities whereas more than 3 passes bring imprecise line and excess in materials usage not required for project target. Thus two or at least three passes allow high conductivity with right cover of overall line width. The whole thickness is approximately 10–15 µm even if precise measurements are challenging due to the basic roughness of the fabrics substrate.

The durability of the printed lines at washing

The materials have been cut in small pieces, 1.5 × 1.5 cm and were washed 5 × 30 minutes (simulating 5 washings), at 300 °C. After washing, the fabrics were removed from the containers and, the washing waters were analyzed on atomic absorption spectrophotometer to determine the Ag amount leached in water. The initial and final weights of the material after washing, and the quantity of Ag leached in washing water are summarized in table 4.

During washing, small amounts of Ag migrate in washing waters, the highest amount being recorded for sample A5064 1P-4 and the lowest for sample B5064 3P-4. After washing, the lines become brighter and more defined, the small particles existing between the lines being removed. No break in the lines was noticed after washing demonstrating the high adhesion and durability of the flexible printed circuits.

Electrical characterization

Electrical properties of the printed lines were analyzed before and after washing, the results being shown in the table 5. The resistance value was measured with an ohm-meter and is the average of 5 measurements.

All the resistances increase after washing, the highest increase being for sample A5064-1P-2, for which a high amount of silver is removed from the material. The resistance values depend on the type of material, length, width, and thickness of the printed wire. Theoretically, a longer wire has more resistance than a shorter wire, and a thicker wire has less resistance than a thinner wire of equal length.

Table 5

ELECTRICAL RESISTANCE OF THE PRINTED LINES, INITIAL AND AFTER 5 WASHINGS						
Sample	**Line thickness, μm**	**Wt (%) Ag found in the printed lines**	**Ag leached in washing water, mg/l**	**Initial Resistance, Ω**	**Resistance after 5 washings, Ω**	**Resistance increase after 5 washings, %**
A5064-1P-2	5.52	95.25	**0.259**	2.45	7.6	**210.20**
A5064-1P-4	5.90	94.66	0.266	1.75	2.5	42.86
B5064-3P-4	9.08	96.20	0.003	0.8	1.8	**125**
B5064-2P-5	4.26	93.30	0.008	1.25	1.3	4
B5064-2P-6	5.47	95.15	0.009	1.23	1.5	21.95
C5064-1P-1	6.94	95.67	0.066	1.0	1.3	30
C5064-1P-2	6.53	96.45	0.061	1.0	1.2	20
C5064-1P-3	5.11	97.25	0.068	1.1	1.3	20

Table 6

VOLUME RESISTIVITY OF THE PRINTED CIRCUITS						
Sample	**Line thickness, $\times 10^{-6}$ m**	**Line width, $\times 10^{-6}$ m**	**A, $\times 10^{-12}$**	**L, $\times 10^{-2}$m**	**Resistance, Ω**	**ρ, Ωm $\times 10^{-7}$**
A5064-1P-2	5.52	519.28	2866.4256	1	2.45	7.022
A5064-1P-4	5.90	529.54	3124.286	0.9	1.75	6.075
B5064-3P-4	9.08	545.03	4948.8724	1.2	0.8	3.299
B5064-2P-5	4.26	687.40	2928.324	1	1.25	3.660
B5064-2P-6	5.47	736.62	4029.3114	1.1	1.23	4.505
C5064-1P-1	6.94	604.52	4195.3688	1.2	1.0	3.496
C5064-1P-2	6.90	654.92	4516.188	1.2	1.0	3.763
C5064-1P-3	5.11	593.03	3030.3833	1	1.1	3.333

Table 7

WEIGHT RESISTIVITY OF THE PRINTED LINES								
Sample	**Material weight, g**		**ΔW, g**	**L1, $\times 10^{-2}$ m**	**L2, $\times 10^{-2}$ m**	**Resistance, Ω**	**$\rho_{w,}$ gΩ/m²**	**ρ, Ωm $\times 10^{-6}$**
	print	**non-printed**						
A5064-1P-2	0.0193	0.0173	0.002	1	1	2.45	49	4.67
A5064-1P-4	0.0102	0.0097	0.0005	0.9	0.9	1.75	10.8	1.03
B5064-3P-4	0.0323	0.0250	0.0073	1.3	1.2	0.8	37.43	3.56
B5064-2P-5	0.0241	0.0215	0.0026	1	1	1.25	32.5	3.01
B5064-2P-6	0.0231	0.0219	0.0012	1	1.1	1.23	13.42	1.27
C5064-1P-1	0.0225	0.0223	0.0002	1.1	1.2	1.0	15.15	1.45
C5064-1P-2	0.0254	0.0221	0.0033	1.1	1.2	1.0	2.5	0.24
C5064-1P-3	0.0230	0.0217	0.0013	1.1	1	1.1	14.3	1.36

As it can be seen from table 5, even when using the same print paste (DuPont 5064), the rule is observed only if the same print parameters and the same type of support are used. Because the resistance depends on the materials type and geometry of the system being measured, to compare different designs and materials, an intensive property known as resistivity is used instead of resistance [7]. The relationship between resistance and resistivity is expressed mathematically as:

$$\rho = A \times R/L, \qquad (1)$$

where: ρ is volume resistivity; *A* – cross-sectional area; *L* – length; *R* – resistance.

Starting from the value of bulk silver resistivity of 1.59×10^{-8} Ωm it can be observed that although the printed circuits' resistivity is 10 times higher, it may be considered small enough to ensure good conductivity for proposed purpose. The lowest resistivity is recorded in samples B5064 and C5064-3P-4-1P-3.

In the case of textile materials, it is very difficult to approximate the sectional area of the printed wire, and it is easier or more realistic to express resistivity as weight resistivity:

$$\rho_w = (W \times R) / L_1 \times L_2, [g\Omega/m2] \quad (2)$$

where:

W is the weight of test specimen (i.e., the conductor being measured, minus any substrate);

L_1 – the gage length used to determine the resistance, *R,* in meters;

L_2 – total length of test specimen, in m;

R – resistance, Ω.

The relationship between weight resistivity and volume resistivity is given by the equation:

$$\rho = \rho_w / density \quad (3)$$

The density of the printed silver is estimated of 80% of bulk silver density, 10.5 g/cm^3, due to porosity inherent as a result of the drying and sintering process. The results of the printed samples are shown in the table 7.

CONCLUSION

The results showed that the accuracy of the screen printed lines depends on the structure of the textile material and the surface roughness. By coating the material with a thin polymeric layer it is possible to control the ink penetration and the circuits' accuracy.

BIBLIOGRAPHY

[1] Kazani, I.; Hertleer, C.; De Mey, G.; Schwarz, A.; Guxho, G.; Van Langenhove, L. *Electrical Conductive Textiles Obtained by Screen Printing*, FIBRES & TEXTILES in Eastern Europe 2012, 20, 1(90) 57–63

[2] J. C. Lin, J. Y. Chan, *On the resistance of silver migration in Ag-Pd conductive thick films under humid environment and applied d.c. field*, Materials Chemistry and Physics 01/1996; 43(3): 256–265

[3] Pudas, M., Hagberg, J. & Leppavuori, S. (2004). *Printing Parameters and Ink Components Affecting Ultra-Fine-Line Gravure-Offset Printing for Electronics Applications*. J. Europ. Ceram. Soc., Vol. 24, pp. 2943–2950

[4] Matteo Stoppa and Alessandro Chiolerio, *Wearable Electronics and Smart Textiles: A Critical Review Sensors*, 2014, 14, 11957-11992; doi:10.3390/s140711957

[5] Sung Chul Joo, *Adhesion mechanism of nano-particle silver to electronic packaging materials, Advanced Packaging*, IEEE Transactions on, vol. 33, Issue:1, 2010, pp. 48–57

[6] http://www2.dupont.com/MCM/en_US/assets/downloads/prodinfo/5064.pdf, accessed on 10.3.2014

[7] Kim, Y.; Kim, H.; Yoo, J., *Electrical characterization of printed circuits on the fabric*. In: IEEE Trans. Adv. Packag. 2010, 33, 196–205

Authors:

Dr. eng. Iuliana Dumitrescu
Ovidiu George Iordache
National Research & Development
Institute for Textile & Leather, Bucharest
Lucretiu Patrascanu nr 16, sector 3, Bucuresti, Romania
e-mails: iuliana.dumitrescu@gmail.com;
iordacheovidiu.g@gmail.com

Li Pira Nello
C.R.F. SCPA, Italy
e-mail: nello.lipira@crf.it

Giusepe Bima
PERARIA S.r.l., Via Barberis 7, 12020 Vottignasco (CN) - Italy, Piedmonte
e-mail: giuseppe.bima@peraria.com

Pollution generated by cotton dyeing with direct dyes

IULIA STĂNESCU
ANIȘOARA BERTEA
ROMEN BUTNARU
ANDREI PETRU BERTEA

REZUMAT – ABSTRACT

Poluare generată de vopsirea bumbacului cu coloranți direcți

În acest studiu, au fost studiați parametrii ecologici ai apelor uzate obținute la vopsirea prin epuizare a țesăturilor de bumbac cu coloranți direcți. Nouă coloranți direcți, care fac parte din toate cele trei categorii de clasificare (SDC), au fost investigați prin determinarea gradului de epuizare, temperaturii apelor uzate, consumului chimic de oxigen, conținutului total de solide și conținutului de solide volatile. Au fost studiate atât apele uzate rezultate de la vopsire, cât și cele de la spălarea ulterioară vopsirii.

Cuvinte-cheie: coloranți direcți, vopsirea bumbacului, aspecte ecologice

Pollution generated by cotton dyeing with direct dyes

In this study, the ecological parameters of the wastewater obtained from the exhaust dyeing of cotton fabrics with direct dyes were studied. Nine direct dyes, belonging to all three categories (SDC classification), have been investigated, examining the exhaustion degree, wastewater temperature, chemical oxygen demand (COD), total solids and volatile solids content. Both dyeing and rinsing wastewater have been studied.

Key-words: Direct dyes, cotton dyeing, ecological aspects

INTRODUCTION

The textile finishing industry is one of the greatest fresh water consumer industries, and its wastewater has a substantial content of persistent organic pollutants [1], among which dyes, an important class of synthetic organic compounds, play a significant role [2]. More than 10 000 different textile dyes with an estimated annual production of 7 105 tons are commercially available worldwide [3] and 10–25% of these dyes are lost during the dyeing process, and 2–20% are directly discharged as aqueous effluents in different environmental components [4].

Cotton is one of most widely used raw materials in textiles and its processing requires numerous operations such as pre-treatment, dyeing and/or printing and finishing [5]. The cotton dyeing involves high water consumption and significant chemical pollution [6].

Cotton, as all cellulosic fibers, can be dyed using a wide variety of dyestuffs, including reactive, direct, vat and sulphur [7].

Direct dyes have been intensively used to dye cotton, but their use has declined in recent years as reactive dyes, with superior properties, have increased in popularity [8]. Nevertheless, as it can be seen from figure 1, a significant share in the market is still held by the direct dyes, which are anionic dyes with substantivity for cellulosic fibers that are generally applied from an aqueous dyebath containing an electrolyte [9]. The electrolyte (common salt – sodium chloride or Glauber's salt – sodium sulphate) lowers the electrostatic repulsion between the negatively charged dye anions and the negatively charged cellulosic fiber surface, disrupts the hydration of direct dyes and cellulosic dye sites and increases the potential for dye interactions [10].

They are named direct dyes because of their capacity to be applied directly to cellulosic fibers without mordants [11] and are mostly appreciated for the essential simplicity of the dyeing process, wide colour ranges, excellent dye penetration, low cost and short dyeing time [12]. The wet fastness of direct dyeing is poor, particularly to washing, but there are still many applications of direct dyes in the textile industry where good fastness is not of prime importance [13].

As the highly competitive environmental parameters become more severe, the main concern of the textile industry is to be aware of the environmental friendliness of their manufacturing processes. Many of the direct dyes are azo dyes. As the usage of the azo dyes that may cleave into potentially carcinogenic aromatic is banned according to the 19th amendment

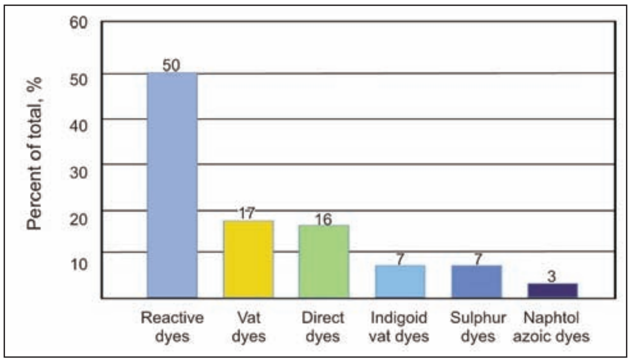

Fig. 1. Dyes used on cellulosic fibres (Lacasse and Bauman, 2004)

of Directive 76/769/EWG on dangerous substances [14], it may be assumed that the rest of the direct dyes pose no problem from the toxicological point of view [15]. Still, the dyeing process remains an important source of pollution and in this context, our study aims to analyze some of the most important ecological parameters in cotton dyeing with direct dyes, namely the organic load of wastewater (expressed by the chemical oxygen demand) and its solids load (total solids and volatile solids).

EXPERIMENTS

Dyestuffs

Nine direct dyes have been used: seven azo dyes: Dinamine Scarlet 4BS (Direct Red 23), Fast Yellow EPL (Direct Yellow 126), Crisofenine (Direct Yellow 12), Dinamine Red 5BR (Direct Red 80), Dinamine Fast Rubine BL (Direct Red 83), Dinamine Fast Blue 3R (Direct Blue 67), Dinamine Fast Green BGH (Direct Green 26), a stilbene dye – Direct Brown 3R (Direct Red 111), and Dinamine Turquoise Blue FBL (Direct Blue 199) – a phthalocyanine dye that contains a copper ion in its structure, all supplied by Dintex Dyechem Ltd.

Fabric

Scoured and bleached 100% cotton woven (weight 197 g/m^2) has been used.

Dyeing procedure

All dyes were used without purification. To obtain the dye solutions the dyestuff was pasted with cold water and dissolved in boiling water while stirring. The solutions were boiled to ensure complete dissolution and then filtered. Stock solutions of 10 g/L of dye were prepared, and the dyeing solutions of desired concentration were prepared by diluting these stock solutions.

All dyeing has been performed at liquor ratio 20:1. All dyeing processes have been performed in an Ahiba lab dyeing machine according to the recipes shown in table 1.

It can be appreciated from these recipes that direct dyes are beneficial from a pollution prevention perspective, as they use low amounts of salt compared with reactive dyes.

Direct dyes are classified according to their dyeing properties as follows:

(1) Class A – self-levelling (good migration or levelling properties).

(2) Class B – salt-controllable (dyes that can be controlled by addition of salt to give level results).

(3) Class C – temperature-controllable (the exhaustion of these dyes cannot sufficiently be controlled by adding only salt and require supplementary control by temperature).

Table 1

DYEING RECIPES

No.	Dye	Constitution number	Dye conc., % (owf)	Salt, % (owf)	Soda Ash, % (owf)
a b c	Crisofenine	C.I 24895	0.5 0.3 0.1	20 10 10	0.5 0.5 0.5
a b c	Dinamine Fast Blue 3R	C.I. 27925	4 1 0.1	25 15 7.5	2 1.5 1
a b c	Dinamine Fast Rubine BL	C.I. 29225	4 2 1	40 20 10	2 1.5 0.5
a b c	Dinamine Turquoise Blue FBL	–	2 1 0.5	40 20 10	2 1.5 0.5
a b c	Direct Brown 3R 133%	C.I. 40290	3 2 1	40 20 10	2 1 0.5
a b c	Dinamin Red 5BR	C.I. 35780	2 1 0.5	25 20 5	- - -
a b c	Dinamine Fast Green BGH	C.I. 34045	2 1 0.5	20 15 10	- - -
a b c	Fast Yellow EPL	–	1 0.5 0.2	40 20 10	2 1 0.5
a b c	Dinamine Scarlet 4BS	C.I. 29160	2.5 1 0.5	40 20 10	2 1.5 0.5

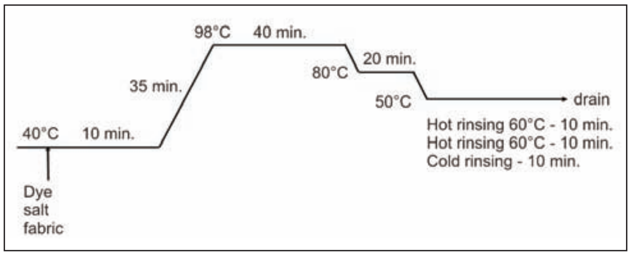

Fig. 2. Temperature course of the dyeing process for the A SDC classification direct dyes

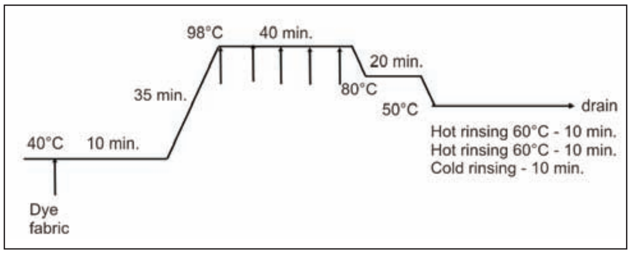

Fig. 3. Temperature course of the dyeing process for the B SDC classification direct dyes

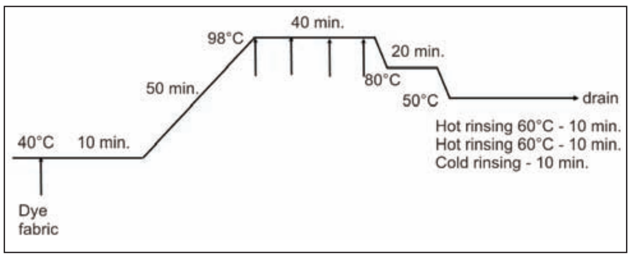

Fig. 4. Temperature course of the dyeing process for the C SDC classification direct dyes

The dyeing procedure, according to the SDC classification, is shown in figures 2 – 4.

MEASUREMENTS AND ANALYSIS

Exhaustion

Exhaustion, which is defined as the percent amount of dye that has migrated onto the substrate [16], has a major influence on the pollution load of the wastewater resulting in the dyeing process. The dyeing parameters that influence most the rate of absorption of the dye and its final exhaustion are intrinsic substantivity of the dye for the fiber, the quantity of salt used, the liquor ratio and the temperature of dyeing.

The dye exhaustion was calculated using spectroscopic analysis of the dye bath before and after dyeing [17]. In order to find dye concentration calibration curves have been used. The calibration curves have been obtained by measuring the absorbance of the dye solution of known concentrations. All measurements have been made at wavelength of maximum absorption using a Spectro UV/Vis Dual Beam Labomed UVS-2800 spectrophotometer.

% Exhaustion is a function of the initial and current concentrations [16] and was calculated from the formula:

$$E = \frac{c_1 - c_2}{c_1} \times 100, \% \qquad (1)$$

where:

E is the degree of dye exhaustion from the dyebath, in percentage,

c_1, c_2 – the concentration of the dye before and after dyeing, respectively [17].

Chemical oxygen demand

Chemical oxygen demand-Cr (COD), which indirectly measures the amount of organic compounds in water, represents the quantity of potassium dichromate that reacts with the sample under controlled conditions, expressed in terms of its oxygen equivalence [18]. COD-Cr was determined according to SR ISO 6060/1996 standard.

Reagents: Potassium dichromate solution, volumetric, 1/25 M (Sigma-Aldrich), Sulfuric acid reagent: 5.5 g Ag_2SO_4 dissolved in 1 kg H_2SO_4 (both Skonx and Co.), Ferroin indicator solution (Sigma-Aldrich), Standard ferrous ammonium sulfate 0.25M (Skonx and Co.).

In order to overcome the difficulties caused by the presence of chlorides, mercuric sulphate has been added before refluxing, with the purpose of binding the chloride ion as a soluble mercuric chloride complex.

Total solids

Total solids, which include total dissolved solids and total suspended solids (including colloidal), are the material residue left after evaporation of a sample and its subsequent drying in an oven at a defined temperature. The weight loss on ignition is called volatile solids [18].

The total solids have been determined using EPA 2540 B standard. A 100 mL sample of wastewater was evaporated in a weighed dish and dried to constant weight at 105°C. The total solids were calculated with the relation:

$$Total\ solids = \frac{(A - B) \times 1000}{V}, \text{ mg/L} \qquad (2)$$

where:

A = weight of dried residue + dish, mg;

B = weight of dish, mg;

V = sample volume, mL.

Volatile solids

The volatile solids have been determined according to EPA 2540 E standard. The residue from total solids determination was ignited to constant weight at 550°C and the weight lost on ignition is the volatile solids.

$$Volatile\ solids = \frac{(A - B) \times 1000}{V}, \text{ mg/L} \qquad (3)$$

where:

A = weight of residue + dish before ignition, mg;

B = weight of residue + dish or filter after ignition, mg;

V = sample volume, mL.

RESULTS AND DISCUSSIONS

For each dye and each dyeing variant, the exhaustion has been calculated. The results are reported in table 2. From this table it can be seen that the exhaust varies between 70–95 %, depending on the dye concentration. This means that as much as 30% of the dye is to be lost in the dyeing wastewater. In most cases, the exhaustion degree decreases with the dye concentration in the dyeing bath, but there are situations when this dependency is insignificant (Fast Yellow EPL, Crisofenine, Direct Brown 3R, Dinamine Fast Green BGH).

In order to reduce pollution with residual dye, it is recommended to use the dyes that exhaust poorly at high concentrations only for pale hues, while using the dyes with little influence of concentration on the exhaustion in deep hue dyeings.

Some major ecological characteristics of direct dyeing and rinsing wastewater are shown in table 3.

Analyzing the results, the following observations can be made:

- All dyeing wastewaters are colored, and the color degree is inversely proportional to the exhaustion of the dyes.
- Wastewaters from both dyeing and rinsing are hot or at least warm; the temperature of dyeing wastewater varied between 50 °C and 70 °C, and the temperature of rinsing wastewater varied between 30 and 35 °C.
- The values for the total residue (total dissolved and suspended solids) fluctuate significantly in all studied cases. High values are recorded when using a high dye concentration, when the amount of added processing aids (sodium chloride, sodium carbonate) increases accordingly. Therefore, it can be appreciated that the values for this parameter is due mainly to the additions of auxiliary substances used in dyeing process, these substances being found almost entirely in wastewater.
- The rinsing wastewater total solids content is at a much lower level (about 10–12 times lower than in dyeing wastewater). The rinsing wastewater contains besides the unexhausted dye some fiber and dye auxiliaries, but in much reduced amount. For example, for Dinamine Fast Blue 3R, with 100% exhaustion degree (at 0.1% dyeing concentration), the total solids amount in rinsing wastewater is only 124 mg/L, much lower than 4350 mg/L corresponding to the dyeing wastewater. In this regard, it can be appreciated that the contribution of the rinsing process to the dyeing pollutant load is low.
- The organic load, expressed in COD, is large for most dyeing wastewater. COD-Cr is a measure of the oxygen equivalent of the organic matter content capable of being oxidized with potassium dichromate in an acidic medium. It should be noted that both the volatile compounds (organochlorine) and a number of stable compounds (paraffins, pyridine, etc.) are only partially oxidized under the reaction conditions of the method. It can be seen that, in general, the COD of the dyeing wastewater increases with increasing concentration of dye used in dyeing.
- Since the dyeing wastewater contains no other organic compounds out of the dye, it can be appreciated that the organic load of the effluent is determined by the amount of the residual dye. The higher the residual dye content (i.e. the lower the exhaustion degree), the values of COD are higher. For the majority of lighter shades of color, the COD value is in accordance with the current Romanian regulations (NTPA 002/2005 indicates for COD a maximal value of 300 mg/L when wastewater is discharged in the sewage networks [19]).
- Regardless of the exhaustion degree achieved in dyeing, there is a certain quantity of dye which is poorly fixed to the surface of the material and that is removed during the rinsing operation. It was found that the same phenomenon occurs in the

Table 2

EXHAUSTION VALUES FOR THE ANALYSED DYES

No.	Dye	Variant	Dye concentration, %	Exhaustion, %
1.	Fast Yellow EPL	a	1	75.5
		b	0.5	77.7
		c	0.2	76.3
2.	Dinamine Scarlet 4BS	a	2.5	95
		b	1	95.2
		c	0.5	93.4
3.	Dinamine Fast Rubine BL	a	4	56.7
		b	2	75
		c	1	70.4
4.	Dinamine Turquoise Blue FBL	a	2	51.2
		b	1	66.8
		c	0.5	73.7
5.	Crisofenine	a	0.5	93.7
		b	0.3	90.7
		c	0.1	97
6.	Direct Brown 3R	a	2	88.8
		b	0.5	90.9
		c	0.05	87
7.	Dinamin Red 5BR	a	2	99.7
		b	0.5	99.3
		c	0.05	98.9
8.	Dinamine Fast Blue 3R	a	4	73.7
		b	1	97
		c	0.1	100
9.	Dinamine Fast Green BGH	a	2	88
		b	1	90.2
		c	0.5	91.8

Table 3

ECOLOGICAL CHARACTERISTICS OF DYEING AND RINSING WASTEWATER FROM COTTON DYEING WITH DIRECT DYES

No.	Dye	Variant	COD-Cr content, mg/L		Total solids, mg/L		Volatile solids, mg/L	
			Dyeing wastewater	Rinsing wastewater	Dyeing wastewater	Rinsing wastewater	Dyeing wastewater	Rinsing wastewater
1.	Fast Yellow EPL	a	330.60	19.80	21059.48	1579.92	18052.04	594.79
		b	165.30	7.52	11784.39	1189.59	9695.16	431.22
		c	93.540	2.49	7063.19	743.49	4921.93	223.04
2.	Dinamine Scarlet 4BS	a	196.27	14.74	20594.80	1040.89	16342.01	802.97
		b	122.71	11.05	11301.12	371.74	9695.16	594.79
		c	85.48	6.81	5966.54	185.87	5055.76	371.74
3.	Dinamine Fast Rubine BL	a	1357.03	101.95	19524.16	1263.94	14665.43	702.60
		b	383.09	31.97	10304.83	951.67	6769.51	323.42
		c	201.04	15.24	5918.21	594.79	4873.60	167.28
4.	Dinamine Turquoise Blue FBL	a	1472.07	127.77	21003.72	1579.92	17843.87	594.79
		b	500.37	43.63	10966.54	743.49	10156.13	446.09
		c	201.042	19.80	5966.54	539.03	5635.68	223.04
5.	Crisofenine	a	98.13	14.74	11626.39	520.44	9048.32	639.40
		b	75.72	11.05	8996.28	371.74	7605.94	297.39
		c	21.51	2.15	6236.05	278.81	6416.35	185.87
6.	Direct Brown 3R	a	412.88	37.63	21094.80	1020.44	18275.09	327.13
		b	127.69	14.240	10856.88	368.02	9026.02	223.04
		c	48.77	5.69	6423.79	250.92	4921.93	208.17
7.	Dinamin Red 5BR	a	86.59	6.26	12174.72	594.79	9955.39	215.61
		b	39.76	3.94	9916.35	269.51	8579.92	111.52
		c	11.69	1.52	2871.74	139.40	2386.61	74.34
8.	Dinamine Fast Blue 3R	a	1178.33	90.89	12914.50	724.90	9449.81	215.61
		b	146.12	13.60	8386.61	479.55	6646.84	156.13
		c	61.42	5.13	4483.27	234.20	2289.96	111.52
9.	Dinamine Fast Green BGH	a	375.27	34.17	10260.22	789.96	7933.08	215.61
		b	116.15	11.28	7862.45	566.91	7040.89	156.13
		c	58.45	2.01	5548.32	195.16	4520.44	111.52

case of the rinsing wastewater, where the amount of COD-Cr decreases with decreasing concentration of dye used in dyeing.

- The interval between the discharges of the two types of sources is relatively short (30 minutes without the time to charge-discharge), so mixing the two effluents could be a solution (if the total effluent treatment process is more effective).

CONCLUSIONS

The study revealed that different types of direct dyes, dyeing concentrations and procedures have an important impact on dye exhaustion. The exhaustion of the studied dyes ranges between 51.2% and 100%, the worse result being obtained for dark dyeings (4% dye owf).

The results show that organic load, expressed through COD depends strongly on dyes exhaustion and is significantly higher in dyeing wastewater than rinsing wastewater.

It has been found that the values for the total residue (total dissolved and suspended solids) fluctuate significantly in all studied cases. High values are recorded when using a high dye concentration, when the amount of added processing aids (sodium chloride, sodium carbonate) increases accordingly.

Because rinsing water have low organic and total solids load, it could be productive to treat them separately in order to recycle in new dyeing processes.

For some dyes, such as Dinamine Fast Rubine BL or Dinamine Turquoise Blue FBL, with poor exhaustion capacity, particularly in dark color dyeing, the dyeing bath could be reused through the replenishment technique in order to reduce water consumption (especially for the same shade to avoid reproducibility problems).

BIBLIOGRAPHY

[1] Le Marechal, A. M., Križanec, B., Vajnhandl, S., Valh, J. V., *Textile Finishing Industry as an Important Source of Organic Pollutants*, In: “Organic Pollutants Ten Years After The Stockholm Convention – Environmental And Analytical Update”, edited by T. Puzyn and A. Mostrag-Szlichtyng, InTech, Rijeka, Croatia, 2012, pp. 29–54

[2] Moga, I.C., Pricop, F., Iordanescu, M., Scarlat, R., Dorogan, A. *Quality monitoring for wastewater generated by the textile finishing*, In: Industria Textila, 2013, vol. 64, issue 3, pp. 222–228

[3] Chequer, F.M.D., De Oliveira, G.A.R., Ferraz, E.R.A., Cardoso, J.C., Zanoni, M.V.B., De Oliveira, D.P., *Textile Dyes: Dyeing Process and Environmental Impact,* In: Eco-friendly textile dyeing and finishing. Edited by Gunay, M., InTech, Rijeka, Croatia, 2013, pp. 151–176

[4] Zaharia, C., Suteu, D., *Textile Organic Dyes – Characteristics, Polluting Effects and Separation/Elimination Procedures from Industrial Effluents – A Critical Overview,* In: “Organic Pollutants Ten Years After The Stockholm Convention – Environmental And Analytical Update”, edited by Puzyn, T., Mostrag-Szlichtyng, A., InTech, Rijeka, Croatia, 2012, pp. 55–86

[5] Pricop, F., Scarlat, R., Iordanescu, M., Ghituleasa, C., Popescu, A., Moga, I.C., *Integrated systems of monitoring and controlling wastewater quality*, Industria Textila, 2013, vol. 64, issue 1, pp. 40–45

[6] Bertea, A.F., Butnaru, R., Berariu, R., *Reducing pollution in reactive cotton dyeing through wastewater recycling*, In: Cellulose Chem. Technol., 2013, vol. 47, issue 1–2, pp. 133–139

[7] Lacasse, K., Bauman, W., Textile Chemicals – Environmental Data and Facts, Springer-Verlag Berlin Heidelberg, 2004, pp. 166–167

[8] Fazeli, F., Hamadani, A.Z., Tavanai, H., *Application of Taguchi and full factorial experimental design to model the color yield of cotton fabric dyed with 6 selected direct dyes*, In: Industria Textila, 2011, vol. 62, issue 5, pp. 233–239

[9] SHORE, J., *Cellulosics Dyeing*, In: The Society of Dyers and Colourists, Perkin House, Bradford, West Yorkshire BD1 2JB, England, 1995, pp. 152–153

[10] EPA *Best Management Practices for Pollution Prevention in the Textile Industry*, U.S. Environmental Protection Agency, Center for Environmental Research Information, Cincinnati, Ohio,1996

[11] Cegarra, J., Puente, P., Valldeperas, J., *The dyeing of textile materials*, In: Textilia, Biella, Italy, 1992, p. 262

[12] Liu, X., Wang, W., XU, P., *Improving the Wash Fastness of Direct Dyes on Cotton by Si/Ti Composite Nanosol*, In: Fibres & Textiles in Eastern Europe, 2010, vol. 18, issue 1, pp. 93–96

[13] Sekar, N., *Direct Dyes*, In: Handbook of textile and industrial dyeing, Woodhead Publishing Limited, Sawston, Cambridge, 2011, pp. 425–445

[14] Raghavendra, K. R., Kumar, K. A., International Journal of ChemTech Research, 2013, vol. 5, issue 4, pp. 1 756–1 760

[15] Bertea, A.F., Butnaru, R., Bertea, A.P., *Response surface methodology applied for the optimization of reactive black 5 discoloration in a Fenton-like process*, In: Environmental Engineering and Management Journal, 2013, vol. 12, issue 5, pp. 1 091–1 099

[16] Gunay, M., *The Future of Dye House Quality Control with the Introduction of Right-First Dyeing Technologies*, in “Textile Dyeing”, edited by Hauser, P., InTech, Rijeka, Croatia, 2011, pp. 119–144

[17] Matyjas, E., Rybicki, E., *Novel reactive red dyes*, AUTEX Research Journal, 2003, vol. 3, issue 2, pp. 90–95

[18] Clesceri, L., Greenberg, A., Eaton, A., *Standard Methods for the Examination of Water and Wastewater*, In: American Public Health Association, American Water Works Association, Water Environment Federation, 1999

[19] NTPA 002/2005 *Standard on wastewater discharge conditions in the local sewerage*

Authors:

PhD student. eng. IULIA STĂNESCU

Prof. dr. eng. ROMEN BUTNARU

Prof. dr. eng. ANDREI-PETRU BERTEA

Conf. dr. eng. ANIȘOARA BERTEA

Technical University ”Gh. Asachi” of Iași

Faculty of Textiles, Leather and Industrial Management

Bd. Dimitrie Mangeron Nr. 29, 700050, Iaşi, Romania

e-mail: iuliastanescu@yahoo.com; rbutnaru@tex.tuiasi.ro;

apbertea@tex.tuiasi.ro; anibertea@tex.tuiasi.ro

The macroscopic equivalent resistance model of knitted sensor under strip biaxial elongation

JUAN XIE HAIRU LONG

REZUMAT – ABSTRACT

Model macroscopic de estimare a rezistenţei echivalente a senzorului din tricot supus alungirii biaxiale

În scopul investigării relaţiei dintre variaţia rezistenţei și proprietatea mecanică a tricoturilor conductoare supuse alungirii biaxiale, a fost propus un model teoretic macroscopic pentru estimarea acestei relaţii, care se bazează pe rezistenţa la tracţiune şi la deformare a ţesăturii. De asemenea, a fost determinat calculul rezistenţei ţesăturii cu ajutorul rezultatelor experimentale ale rezistenţei la tracţiune şi la deformare în timpul alungirii. Prin urmare, validitatea acestui macro-model a fost verificată atât experimental, cât și teoretic. În plus, modelul poate fi utilizat și pentru studierea proprietăților electromecanice ale senzorului electroactiv din tricot în timpul purtării.

Cuvinte-cheie: rezistenţă echivalentă, alungire biaxială, tricot conductor, model macroscopic

The macroscopic equivalent resistance model of knitted sensor under strip biaxial elongation

In order to investigate the relationship between resistance variation and mechanical property of conductive knitted fabric under strip biaxial elongation, a macroscopic theoretical model for predicting this relation was proposed, which is based on tensile forces and strain of fabric. And fabric resistance calculation was determined by experimental results of tensile load and strain during elongation. As a result, the validity of this macro-model was verified well both experimentally and theoretically. In addition, the model can also be used for studying the electro-mechanical properties of electroactive knitted sensor in wearing situation.

Key-words: equivalent resistance, strip biaxial elongation, conductive knitted fabric, macroscopic model

Applying wearable strain sensors to detect body posture and movement of a user makes our life convenient. Recent reports have suggested that integrating flexible devices into fabrics to realize its promising performance on body posture and gesture classification, and some of these unobtrusive sensors can supply abstract information about our current activity to other wearable computers [1–13]. Besides, the principle of these electronic devices is based on the fact that electrical properties of conductive sensors change with mechanical behavior, *i.e.* the relation between resistance and strain. Hence, the importance of exploring the electromechanical properties of flexible sensors, which play positive role in promoting the development of electronic devices. Some researchers have investigated distributive resistive networks consisting of contact resistors and length-related resistors to simulate the sensing mechanism of textile strain sensors in relaxed state and under unidirectional extension, and some macroscopic models like a sheet resistance method were proposed to compute the static resistance of conductive fabrics [14–20].

In practical use, however, tensile deformation of knitted fabric is subjected to a wide range of outside forces [21]. For example, the body part of a clothing is stretched by in-plane tensile force, while those curved parts (including elbows, knees and hip) are extended by three-dimension force (including in-plane extension, bending and shear). Thus, the relation between electronic behavior and in-plane tensile including biaxial and multidirectional (in three and even more axis) elongation, plays a major role in electro-mechanical properties of flexible sensors. To explore the in-plane tensile properties, several papers have reported on the deformation of non-conductive knitted fabric under strip biaxial elongation (SBE), and corresponding theoretical models of stress-strain have been proposed [22–25]. To date, however, few studies can give explanations for the connection between biaxial elongation and the electrical behavior of conductive fabric.

This paper is aiming at proposing a macroscopic theoretical model for predicting the relation between equivalent resistance and mechanical properties of conductive knitted fabric under strip biaxial elongation, and the connections between equivalent resistance and tensile forces and strain have been made. Experiments were conducted to verify the validity of the equivalent fabric resistance model and contact resistance theoretical method.

THEORETICAL PART

Load-strain theory of nonlinear materials

For nonlinear materials [22], the relationship between load and strain in principal axes is as follows:

$$F = E\,\varepsilon^{\mu} \tag{1}$$

where:

F is the load of nonlinear materials (N);

ε – the load and strain of nonlinear materials (m);
E – the tensile modulus (N/m);
μ – a dimensionless value representing the nonlinear tensile property of the knitted fabric.

Both of E and μ are the parameters concerned with tensile properties and structure of the materials.

Load-strain theory of knitted fabric under strip biaxial elongation

When fabric is stretched under SBE, major tensile force either F_x (N) or F_y (N) is to keep specimen extending in major axis, while the fixed force either F_y or F_x is to keep strain zero in vertical direction. And both forces are related to tensile strain ε (%). The relation between tensile forces and strain under SBE is shown as equation (2). Then the expression of strain ε determined by tensile forces can be deduced into equation (3).

$$\begin{cases} F_x = E_1\, \varepsilon^{\mu_1} \\ F_y = E_2\, \varepsilon^{\mu_2} \end{cases} \tag{2}$$

$$\varepsilon = f(F_x, F_y) \tag{3}$$

where:
E_i are tensile modulus;
μ_i – the constants.

Electrical resistance of conductive textile materials

For fiber materials made from conductive polymer, the resistance calculation [26] is as follows:

$$R = \rho \frac{L}{A^{\beta}} \tag{4}$$

where:
L is length of conductive fiber materials (mm);
A – cross-section area of conductive fiber materials (mm^2);
ρ – electric resistivity of conductive fiber materials (Ω/mm);
β – scaling exponent of conductive fiber materials.

Moreover, ρ and β are constants relative to the conductive character of conductive materials.

Equivalent resistance of electro-active knitted sensor under strip biaxial elongation

The length of conductive knitted fabric grows with increment of strain under elongation, while cross-section area decreases. Therefore, equation (4) can be rewritten to as follows, which is related to strain.

$$R_e = \rho \frac{L(\varepsilon, L_0)}{A(\varepsilon, A_0)^{\beta}} = f(\varepsilon) \tag{5}$$

where:
R_e is the electric resistance of conductive knitted fabric;
ε – strain of conductive knitted fabric;
L_0 – initial length of conductive knitted fabric;
A_0 – cross-section area of conductive knitted fabric.

To investigate the influence of strain on equivalent resistance, equivalent resistance is assumed to be expressed by Maclaurin formula in one variable. After merging the similar items in the expansion, the theoretical calculation of resistance is approximately equal to the sum of ε with various powers, shown as equation (6).

$$R_e = f(\varepsilon) = f(0) + \frac{f'(0)}{1!}\varepsilon + \frac{f''(0)}{2!}\varepsilon^2 + \\ + \dots + \frac{f^{(n)}(0)}{n!}\varepsilon^n + \frac{f^{(n+1)}(0)}{(n+1)!}\varepsilon^{n+1} = \sum_{i=0}^{n} \alpha_i \varepsilon^i \tag{6}$$

where:
$f_{(n)}(0)$ are constants, meaning the n-level derivative of the function at the initial state where the strain is zero.

According to the Maclaurin formula in two variables, the fabric equivalent resistance R_e with relation to tensile forces can be expressed as equation (7):

$$R_e = f(F_x, F_y) = \sum_{i=0}^{n}\sum_{j=0}^{n} \alpha_{ij} F_x^i F_y^j, \quad i + j \le n \tag{7}$$

where:
$i + j \le n$ is to make the level of each component no more than the maximum order n.

EXPERIMENTAL PART

Materials used

The flexible knitted sensor includes two kinds of non-conductive yarns (one is polyamide yarn and the other is polyamide/spandex core-spun filament), and one silver-coated conductive yarn with resistance of 0.5 Ω/mm and the line density is 100D/40F.

The electro-active knitted specimens (16 cm × 16 cm) including conductive and non-conductive areas were produced by plating technique on a seamless knitting machine of SANTONI SM8 Top2. Besides, the face yarns in both areas are silver-coated conductive yarn and polyamide yarn, respectively. While ground yarns in conductive and non-conductive areas are both polyamide/spandex core-spun yarns to improve the elasticity of specimens. The conductive area is 3 cm × 3 cm with course-wise density of 80 wales/50 mm and wale-wise density of 140 courses/50 mm. Figure 1 shows the technical front and back sides of an experimental sample in relaxed state.

Experimental setup

The outline of experimental setup is shown in figure 2. The load and strain of specimens were measured by DRong X-Y Biaxial Material Tester, where two pairs of clamp plates were used to fix specimens in x and y directions. Besides, the electrical resistances were recorded by Rigol Digital Multimeter 3068 with a four-wire sensing method (two red testing pens and two black ones are connected to two points across the conductive area) to minimize the effect of the resistance of the leads.

Experiment design

In SBE-X experiment, specimens were stretched in x direction and fixed in y direction. After that, fabric

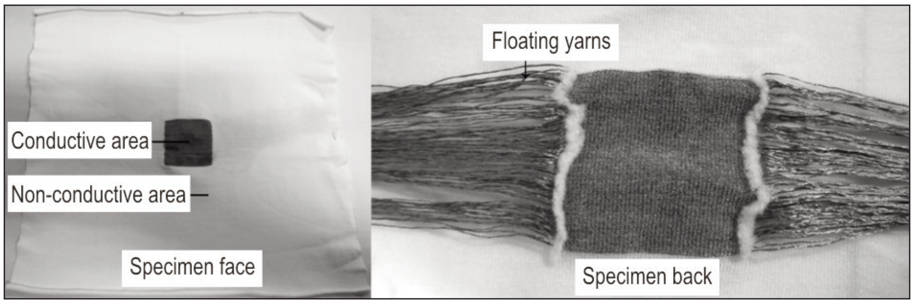

Fig. 1. The technical face and back of knitted sensor including conductive and non-conductive areas

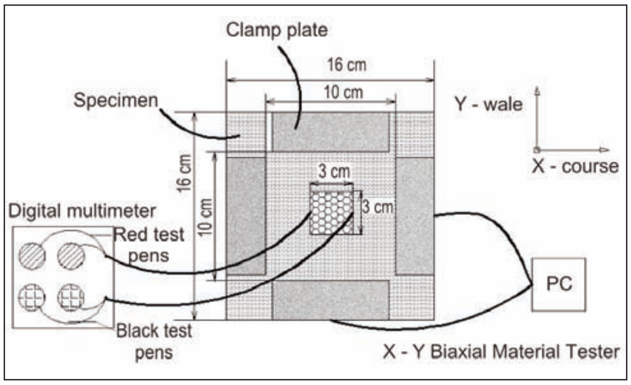

Fig. 2. Experimental setup measuring electrical resistance and force-strain of conductive knitted specimens

samples were tested under SBE-Y (stretching in *y* direction and fixed in *x* direction). In both experiments, the speed of clamps was 60 mm/min and the pre-load was 0.1 N. The experiments were not finished until ε_x under SBE-X and ε_y under SBE-Y came to 30%.

RESULTS AND DISCUSSIONS

Tensile force and strain under strip biaxial elongation

Figure 3 *a* and *b* elucidates the experimental and fitting results of tensile forces-strain under SBE-X (a) and SBE-Y (b), respectively. It can be found that the relations between tensile forces and strain are nonlinear, which accords with the nonlinear mechanical behavior of knitted materials. Besides, the maximum value of major load F_x under SBE-X is less than that of F_y under SBE-Y, which demonstrates the better extension in course direction of knitted fabric. The theoretical expressions of tensile forces-strain under SBE-X and SBE-Y are shown as equation (8), of which the determination coefficients r^2 are more than 0.95 to describe the high correlation between loads and strain.

$$\begin{cases} F_x = 0.08016\ \varepsilon_x^{1.21545}, & r^2 = 0.99529 \\ F_y = 0.11528\ \varepsilon_x^{0.74458}, & r^2 = 0.9655 \end{cases} \quad \text{SBE - X}$$
$$\begin{cases} F_x = 0.01743\ \varepsilon_y^{1.04901}, & r^2 = 0.95554 \\ F_y = 0.61332\ \varepsilon_y^{0.64112}, & r^2 = 0.99314 \end{cases} \quad \text{SBE - Y} \tag{8}$$

The relationship between resistance variation and strain under strip biaxial elongation

The connections between experimental results and fitting curves of resistance and strain under SBE-X and SBE-Y are displayed in figure 4 *a* and *b*, respectively. Fabric resistance grows nearly linearly with the increment of strain under SBE-X, while it experiences a nonlinear upward trend under SBE-Y. The fitting results in equation (9) show that determination coefficients are more than 0.998 when the maximum power of strain *n* is 2, meaning the effect of strain with high-order on fabric resistance can be ignored. Both fitting curves in figure 4 and equation (9) prove the theoretical model of resistance-strain shown as equation (6) can be used to calculate the equivalent resistance.

$$\begin{cases} R_e = 2.78863 + 0.01145\,\varepsilon_x - 0.0004\,\varepsilon_x^2, \\ \quad r^2 = 0.99814 \quad \text{SBE - X} \\ R_e = 2.80118 + 0.0021\,\varepsilon_x - 0.00004\,\varepsilon_y^2, \\ \quad r^2 = 0.99805 \quad \text{SBE - Y} \end{cases} \tag{9}$$

The relationship between resistance variation and tensile force under strip biaxial elongation

Being stretched by major tensile force and fixed force, the resistances of specimens change with strain. Then the effect of biaxial loads on resistance variation can be expressed by the combination of elements of F_x and F_y with various power. When taking the value of *n* as 2, the corresponding determination coefficients r^2 are as large as 0.99. The elements of tensile force with high-level, namely, make no significant difference in equivalent resistance calculation. It also can be found from equation (10) that the coefficients of 2-squared F_x and 2-squared F_y elements are not as significant as those of 1-level F_x and 1-level F_y, which is especially obvious under SBE-X. So the components of F_x and F_y with high-order are assumed to be ignored. Equation (11) can be obtained by refitting experimental data, and their large values of r^2(more than 0.98) makes practicable the method of excluding the high-rank components. More importantly, the equation (11) with fewer terms than (10) simplifies the theoretical resistance calculation in conjunction with tensile forces.

$$\begin{cases} R_e = 2.80015 + 0.06933\,F_x + 0.00009\,F_x^2 + 0.02294\,F_y + \\ \quad + 0.01215\,F_y^2 - 0.01581\,F_xF_y \;\; r^2 = 0.99593 \;\; \text{SBE - X}, \\ R_e = 2.79923 + 0.0644\,F_x + 0.06046\,F_x^2 + 0.00264\,F_y + \\ \quad + 0.00166\,F_y^2 - 0.02746\,F_xF_y \;\; r^2 = 0.99072 \;\; \text{SBE - Y}, \end{cases} \tag{10}$$

where $n = 2$

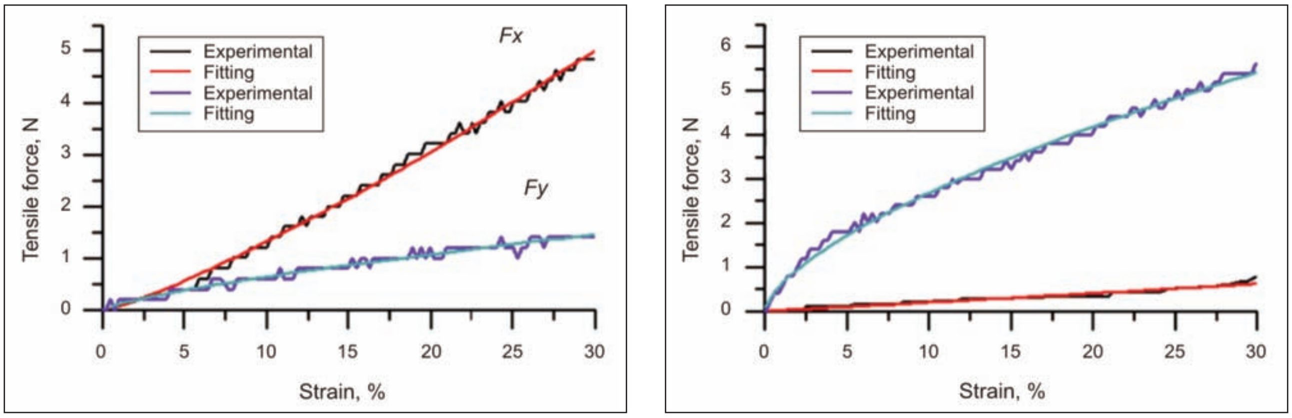

a *b*

Fig. 3. The experimental and fitting results of tensile forces-strain under SBE-X (a) and SBE-Y (b), respectively

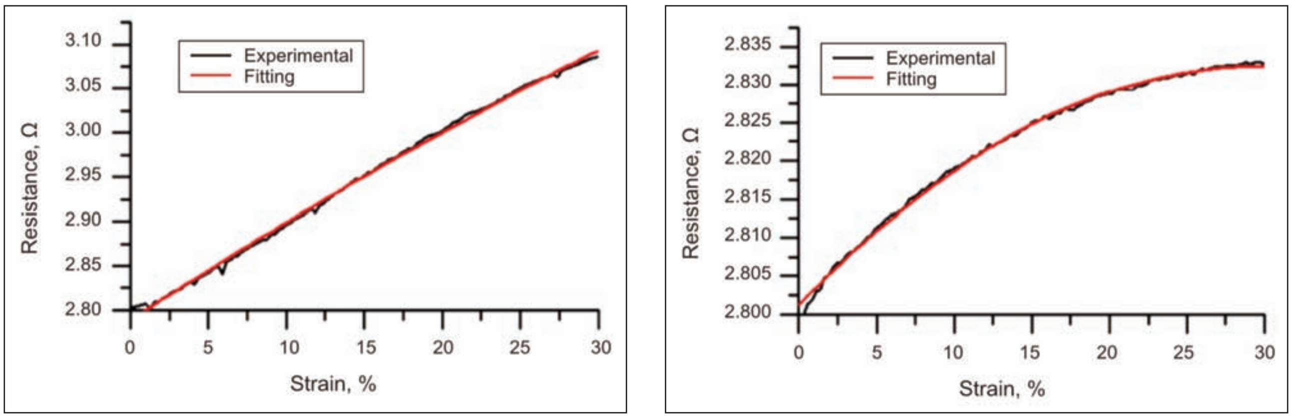

a *b*

Fig. 4. The connections between experimental results and fitting curves of resistance and strain under SBE-X (a) and SBE-Y (b), respectively

$$\begin{cases} R_e = 2.79875 + 0.0666 F_x + 0.03413 F_y - 0.01205 F_x F_y \\ \quad r^2 = 0.99591 \quad \text{SBE - X}, \\ R_e = 2.79698 + 0.02738 F_x + 0.00741 F_y - 0.00617 F_x F_y \\ \quad r^2 = 0.98884 \quad \text{SBE - Y}. \end{cases} \tag{11}$$

CONCLUSIONS

The electro-mechanical properties of knitted sensor under strip biaxial elongation have been explained clearly from a macroscopic perspective. Namely, the connection between equivalent resistance and either fabric strain or external load has been established directly. Besides, the results of resistance-load and resistance-strain models accord with the experimental data within a high accuracy. In future research, the model can be used for investigating the electro-mechanical properties of electro-active knitted sensor in wearing situation.

BIBLIOGRAPHY

[1] Tognetti, A., Bartalesi, R., Lorussi, F., Rossi, D. D. *Body segment position reconstruction and posture classification by smart textiles.* In: Transactions of The Institute of Measurement and Control, 2007, vol. 29, issue 3–4, pp. 215–53

[2] Wijesiriwardana, R. *Inductive fiber-meshed strain and displacement transducers for respiratory measuring systems and motion capturing systems.* In: IEEE Sensors Journal, 2006, vol. 6, issue 3, pp. 571–579

[3] Farringdon, J., Moore, A. J., Tilbury, N., Church, J., Biemond, P. D. *Wearable sensor badge & sensor jacket for context awareness.* In: the 3rd International Symposium on Wearable Computer, 1999, pp. 107–113

[4] Paradiso, R., Loriga, G., Taccini, N. *A wearable health care system based on knitted integrated sensors.* In: IEEE Transactions on Information Technology in Biomedicine, 2005, vol. 9, issue 3, pp. 337–344

[5] Bonfiglio, A., Rossi, D. D., Kirstein, T., Locher, I., Mameli, F., Paradiso, R., Vozzi, G. *A feasibility study of yarns and fibers with annexed electronic functions: The ARIANE Project.* In: Proceedings of International New Generation Wearable Systerm eHealth, 2003, pp. 258–264

[6] Paradiso, R., Gemignani, A., Scilingo, E.P., Rossi, D. D. *Knitted bioclothes for cardiopulmonary monitoring.* In: Engineering in Medicine and Biology Society, 2003, vol. 25, pp. 3720–3723
[7] Tognetti, A., Carpi, F., Lorussi, F., Mazzoldi, A., Orsini, P., Scilingo, E. P., Tesconi, M., Rossi, D. D. *Wearable sensory-motor orthoses for tele-rehabilitation.* In: Engineering in Medicine and Biology Society, 2003, vol. 25, pp. 3724–3727
[8] Paradiso, R., Loriga, G., Taccini, N., Gemignani, A., Ghelarducci, B. *WEALTHY-a wearable healthcare system: new frontier on e-textile.* In: Journal of Telecommunications and Information Technology, 2005, vol. 4, pp. 105–113
[9] Weber, L., Blanc, D., Dittmar, A., Comet, B., Corroy, C., Noury, N., Baghai, R., Vaysse, S., Blinowska, A. *Telemonitoring of vital parameters with newly designed biomedical clothing.* In: Wearable eHealth Systems for Personalised Health Management: State of the Art and Future Challenges, 2004, vol.108, pp. 260–265
[10] Carpus E., Scarlat R, Bonfert D, Ene A., Mihai C, Visileanu E., Donciu C, Popa A., Enache Ghe. *Investigation of two-layer knitted structures with conductive fibres content.* In: Industria Textila, 2014, vol. 65, issue 3, pp. 145–152
[11] Renzo, M. D., Rizzo, F., Parati, G., Brambilla, G., Ferratini, M., Castiglioni, P. *Magic system: a new textile-based wearable device for biological signal monitoring applicability in daily life and clinical settings.* In: Proc. 27th Annual Int. Conf. IEEE-Engineering in Medicine and Biology Society, 2005, pp. 7 167–7 169
[12] Pacelli, M., Caldani, L., Paradiso, R. *Textile piezoresistive sensors for biomechanical variables monitoring.* In: Proceedings 28th Annual International Conference IEEE Engineering in Medicine and Biology Society, 2006, pp. 5 358–5 362
[13] Helmer, R. J. N., Farrow, D., Ball, K., Phillips, E., Farouil, A., Blanchonette, I. *A pilot evaluation of an electronic textile for lower limb monitoring and interactive biofeedback.* In: Procedia Engineering, 2011, vol. 13, pp. 513–518
[14] Xue, P., Tao, X. M., Kwok, K. W. Y., Leung, M. Y., Yu, T. X. *Electromechanical behavior of fibers coated with an electrically conductive polymer.* In: Textile Research Journal, 2004, vol. 74, issue 10, pp. 929–936
[15] Zhang, H., Tao, X. M., Yu, T. X., Wang, S. Y. *Conductive knitted fabric as large-strain gauge under high temperature.* In: Sensors and Actuators A: Physical, 2006, vol. 126, issue 1, pp.129–140
[16] Xue, P., Tao, X. M., Tsang, H. Y. *In situ SEM studies on strain sensing mechanisms of PPy-coated electrically conducting fabrics.* In: Applied Surface Science, 2007, vol. 253, issue 7, pp. 3 387–3 392
[17] Yang, K., Song, G. L., Zhang, L., Li, L. W. *Modelling the electrical property of 1x1 rib knitted fabric made from conductive yarns.* In: 2rd International Conference on Information and Computing Science, 2009, pp. 382–385
[18] Li, L., Au, W. M., Wan, K. M., Wan, S. H., Chung, W. Y., Wong, K. S. *A resistive network model for conductive knitting stitches.* In: Textile Research Journal, 2010, vol. 80, issue 10, pp. 935–948
[19] Li, Q., Tao, X. M. *A stretchable knitted interconnect for three-dimensional curvilinear surfaces.* In: Textile Research Journal, 2011, vol. 81, issue 11, pp. 1 171–1 183
[20] Li, L., Au, W. M., Hua, T., Wong, K. S. *Design of a conductive fabric network by the sheet resistance method.* In: Textile Research Journal, 2011, vol. 81, issue 15, pp. 1 568–1 578
[21] Yokura, H., Nagae, S., Niwa, M. *Prediction of fabric bagging from mechanical properties.* In: Textile Research Journal, 1986, vol. 56, issue 12, pp. 748–754
[22] Wu, W. L., Hamada, H., Maekawa, Z. *Computer simulation of the deformation of weft-knitted fabrics for composite materials.* In: Journal of the Textile Institute, 1994, vol. 85, issue 2, pp. 198–214
[23] Niwa, M., Inamura, A., Inone, M., Yamashita, Y. *Validity of the 'linearizing method' for describing the biaxial stress-strain relationship of textiles.* In: Journal of the Textile Institute, 2001, vol. 92, issue 3, pp. 38–52
[24] Kageyama, M,, Kawabata, S., Niwa, M. *The validity of a linearizing method for predicting the biaxial-extension properties of fabrics.* In: Journal of the Textile Institute, 1988, vol. 79, issue 4, pp. 543–567
[25] Zhang, Y. P., Long, H. R. *The biaxial tensile elastic properties of plain knitted fabrics.* In: Journal of Fiber Bioengineering and Informatics, 2010, vol. 3, pp. 27–31
[26] He, J. H. *Allometric scaling law in conductive polymer.* In: Polymer, 2004, vol. 45, issue 26, pp. 9 067–9 070

Authors:

JUAN XIE
HAI-RU LONG
College of Textiles
Donghua University
2999 North Renmin Road, Shanghai 201620
P. R. China

Corresponding author:

HAI-RU LONG
e-mail: hrlong@dhu.edu.cn

Numerical study of the permeability effect on parachute working process

HAN CHENG
YA-NAN ZHAN
XUE YANG

LI YU
XIAO CHEN

REZUMAT – ABSTRACT

Studiu numeric al efectului permeabilităţii asupra funcţionării paraşutei

Pentru a studia efectul proprietăţilor de permeabilitate asupra funcţionării paraşutei, a fost utilizată funcţia de penalitate pentru a calcula diferenţa de presiune cauzată de porozitatea materialului textil. Pentru a reduce costurile computaţionale a fost utilizată o zonă de curgere mobilă, care urmăreşte materialul textil în mişcare. Procesul de frânare a paraşutei C9 (un exemplar tipic din material textil poros fabricat din poliamidă MIL-c-7020 tip III) a fost modelat matematic folosind această metodă, verificată prin experimentul paraşutării. Apoi au fost obţinute experimental proprietăţile poliamidei K29225 şi K58326, iar aceste materiale au înlocuit materialul iniţial. Efectul permeabilităţii asupra funcţionării materialului textil a fost analizat pe baza acestor rezultate numerice. Rezultatele cercetării şi metoda descrise în acest articol pot ghida procesul de proiectare a paraşutelor şi alegerea materialului din care acestea sunt confecţionate.

Cuvinte cheie: materiale textile poroase deformabile, macro-permeabilitate, mecanica materialelor, poliamidă

Numerical study of the permeability effect on parachute working process

In order to study the effect of permeability properties on parachute working process, the penalty function was used to calculate the pressure drop caused by the porous textile. To reduce the computational cost, the moving textile was followed by an unfixed flow field mesh. The deceleration process of C9 parachute (a typical porous textile sample made of polyamide MIL-c-7020 type III) was calculated by using this method, which was verified by the airdrop experiment. Then the permeability properties of the polyamide K29225 and polyamide K58326 were obtained by experiments and these materials were substituted for the original material. The effect of permeability on textile working process was analyzed based on these numerical results. The research results and method in this paper could be used to guide the parachute design and the material selecting.

Key-words: deformable porous textiles, macro permeability, materials mechanics, polyamide

As a kind of aerospace materials, the textile fabric is widely used in all types of parachute [1], and the parachute inherits the textile characteristics, being light and easy to fold. In a very short time, the folded parachute can rapidly expand and form an aerodynamic deceleration surface, which makes the textile materials irreplaceable in aerospace area. However, the textile materials are different from the other continuous media. The fibers cross each other and form a special connection relationship. Therefore the textile materials can be dealt with as a kind of deformable porous materials. The permeability of pores is influenced by the penetration velocity on macro view. While, the permeability influences the pressure drop between the internal and external side of the canopy and thus influences the aerodynamic performance of the parachute. At present, the researches focus on the effect of penetration velocity on pressure drop by experiments [2–3], or the permeability on micro-scale [4–5]. But the theoretical research achievements about the effect of permeability on the working process are too few to be found.

The textile moving in a flow field is a typical fluid-structure interaction and a strongly nonlinear time-varying process [6]. The textile materials deform largely under the influence of internal and external flow field, which is a structural dynamics problem with geometric nonlinear and material nonlinear change. While, the flow field change is also complicated, the internal flow field is in a turbulent state, and the external has serious separation phenomenon. The pressure drop changes all the time, which directly affects the permeability. This nonlinear change is very difficult to describe by theoretical formula. With the development of the computer hardware, the numerical methods used to study the permeability effect are realized. In 2006, Aquelet used the Euler Lagrange Coupling (ELC) method to simulate the channel tests of polyamide MIL-c-7020 type III the first time, and the results were compared with the experiments [7]. In 2009, Jia applied the same method to verify the results of Aquelet's work [8]. In 2012, Xiao developed micro-scale model to analyze the permeability of woven fabric [9]. In 2012, Cheng used porous domain to simulate the thin textile, the permeability of polyamide MIL-c-7020 type III in steady flow field was studied, but the dynamic relationship between the permeability and pressure drop cannot be obtained by this method [10].

In this work, the working process of C9 parachute was calculated by using Arbitrary Lagrange Euler (ALE) method, and the numerical results were compared with the airdrop experiment to verify the feasibility of this method. Then the permeability properties of polyamide K29225 and polyamide K58326 were obtained by experiments. The working processes of C9 parachute with the same structure and different materials were calculated.

MODEL DEVELOPING

Control equation of permeable textile

The textile materials in this work are described by using the continuous model which can reveal the mechanical characteristics of textile and is suitable for macro-scale, multi-configuration and complicated dynamic calculation. The continuous model of textile satisfies both the mass conservation equation and momentum conservation equation. The permeable textile described by the Lagrangian mesh can accurately track the material boundary. Therefore the mass conservation equation is satisfied naturally. The momentum equation applies the update Lagrangian discrete method [11]:

$$\int_{\Omega} B_{Ij}\,\sigma_{ji}\,d\Omega - \left(\int_{\Omega} N_I\,\rho\,b_i\,d\Omega + \int_{\Gamma_{t_i}} N_I\,\bar{t}_i\,d\Gamma\right) + \\ + \delta_{ij}\int_{\Omega} N_I N_J\,\rho\,d\Omega\,\dot{v}_{Ji} = f^{\text{int}} - f^{\text{ext}} + \boldsymbol{Ma} = 0 \qquad (1)$$

where:

$B_{Ij} = \dfrac{\partial N_I}{\partial x_j}$, N_I is the shape function;

x – the spatial coordinates;
Ω – the spatial configuration;
b_i – body force;
$\bar{t}_i$ – boundary force;
f^{int} – the internal force matrix;
f^{ext} – the external force matrix;
$\boldsymbol{M}$ – the mass matrix;
$\boldsymbol{a}$ – the acceleration matrix.

The boundary condition is:

$$\Gamma_{t_i}: n_j\sigma_{ji} = \bar{t}_i,\ \ \Gamma_{v_i}: v_i = \bar{v}_i,\ \text{and} \\ \Gamma_{t_i}\cap\Gamma_{v_i} = 0,\ \ \Gamma_{t_i}\cup\Gamma_{v_i} = \Gamma \qquad (2)$$

where:

Γ_{t_i} is mechanical boundary;
Γ_{v_i} – velocity boundary;
Γ – complete boundary.

The initial condition is:

$$\boldsymbol{v} = \boldsymbol{v}_0 \qquad (3)$$

The time discrete use the central difference scheme with second order accuracy:

$$\boldsymbol{v}^{n+\frac{1}{2}} = \boldsymbol{v}^{n-\frac{1}{2}} + \Delta t^n \boldsymbol{M}^{-1}(f^{\text{ext}}(\boldsymbol{d}^n,t^n) - f^{\text{int}}(\boldsymbol{d}^n,t^n)) = \\ = \boldsymbol{v}^{n-\frac{1}{2}} + \Delta t^n \boldsymbol{M}^{-1} f^n \qquad (4)$$

where:

$\boldsymbol{d}$ is the nodal displacement;
f^n – the resultant force matrix at n.

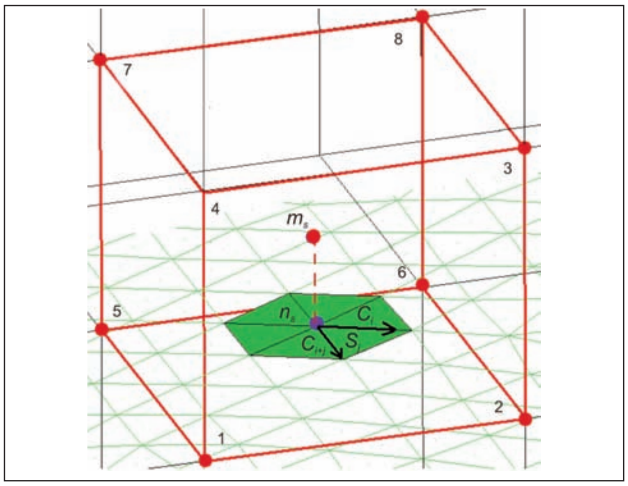

Fig. 1. The slave node and the master node

Mathematics description of permeability

The penalty function method is applied to calculate the coupling force f_{couple} between the permeable textile and flow field. In this method, the textile mesh node is defined as slave node n_S and the fluid materials node is defined as master node m_S.

In figure 1, the velocity and the location of master node can be interpolated by using shape function N_I:

$$\boldsymbol{v}_{m_S}(\xi_{m_S},t) = \boldsymbol{v}_I(t)\,N_I(\xi_{m_S}) \\ \boldsymbol{x}_{m_S}(\xi_{m_S},t) = \boldsymbol{x}_I(t)\,N_I(\xi_{m_S}) \qquad (5)$$

Except for the slave node and master node, the average vector $\boldsymbol{n}_{\text{average}}$ and the penetration depth vector $\boldsymbol{d}_p^n$ need to define:

$$\boldsymbol{n} = \frac{\boldsymbol{c}_i \times \boldsymbol{c}_{i+1}}{|\boldsymbol{c}_i \times \boldsymbol{c}_{i+1}|} \qquad (6)$$

where:

$\boldsymbol{n}$ is the unit normal vector of textile element;
$\boldsymbol{c}_i$ and $\boldsymbol{c}_{i+1}$ are edge vectors.

Therefore the vector $\boldsymbol{n}_{\text{average}}$ is built up by averaging normal vector of textile elements connected to the slave node.

The penetration depth vector at time $t = n + 1$ is updated:

$$\boldsymbol{d}_p^{n+1} = \boldsymbol{d}_p^n + \boldsymbol{v}_{\text{rel}}^{n+\frac{1}{2}}\cdot\Delta t \qquad \boldsymbol{v}_{\text{rel}}^{n+\frac{1}{2}} = \boldsymbol{v}_{n_S}^{n+\frac{1}{2}} - \boldsymbol{v}_{m_S}^{n+\frac{1}{2}} \qquad (7)$$

where

$\boldsymbol{v}_{\text{rel}}$ is relative velocity.

The coupling force is calculated only if $\boldsymbol{n}_{\text{average}}\cdot\boldsymbol{d}_p^n < 0$, the coupling force f_{couple} derived from the pressure drop p is distributed to the slave node:

$$\frac{dp}{dz} = a\cdot\boldsymbol{v}_{\text{rel}}\cdot\boldsymbol{n}_{\text{average}} + b\cdot(\boldsymbol{v}_{\text{rel}}\cdot\boldsymbol{n}_{\text{average}})^2 \\ \Rightarrow\ \ p = [a\cdot\boldsymbol{v}_{\text{rel}}\cdot\boldsymbol{n}_{\text{average}} + b\cdot(\boldsymbol{v}_{\text{rel}}\cdot\boldsymbol{n}_{\text{average}})^2]\cdot e \qquad (8)$$

where:

a is linear resistance coefficient;
b – quadratic resistance coefficient;
e – thickness (these parameters can be obtained by experiments).

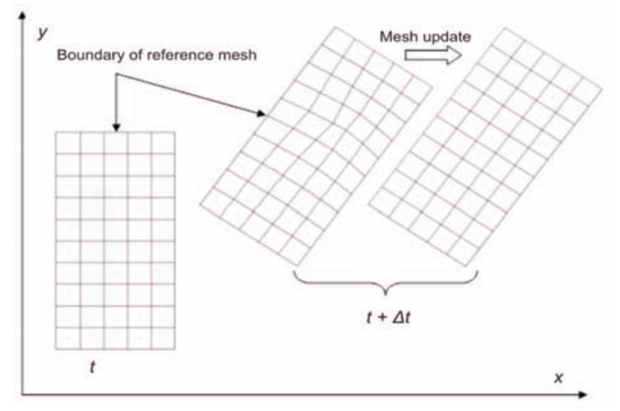

Fig. 2. Mesh update step

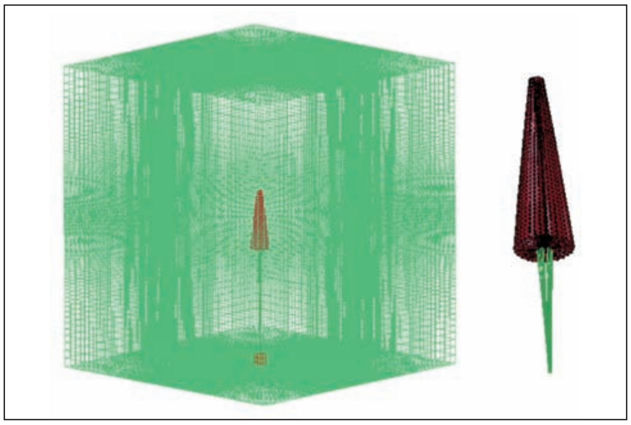

Fig. 3. Finite element model

According to the action and reaction principle, the master node is applied the same coupling force on opposite direction, then the reaction force distributed to the fluid element nodes by using shape function:

$$f_{coupleI} = -N_I(\xi_{m_s})f_{couple} \tag{9}$$

Both the forces on textile node and fluid node are taken as a part of external force f^{ext} in equation (1).

Flow field model

This research takes the free moving parachute in sky as subject. If the ELC method was applied, a huge number of elements need to be established. It is very hard to simulate the parachute working process in a fixed flow field. By using the ALE method, an unfixed flow field follows the movement of parachute, and then the computational time is reduced.
In ALE method, $\boldsymbol{v}$ is the velocity of flow field mesh, $\boldsymbol{v}$ is the velocity of fluid materials in spatial domain. The flow field mesh is taken as the reference, therefore the convective velocity can be defined as $\boldsymbol{c} = \boldsymbol{v} - \boldsymbol{v}$.
The total derivative of the variable in equation (1) is:

$$\frac{Df}{Dt} = f_{,t[\chi]} + f_{,t}\, c_j \tag{10}$$

The momentum equation based on ALE description:

$$\boldsymbol{Ma} + \boldsymbol{Lv} + \boldsymbol{f}^{int} = \boldsymbol{f}^{ext} \tag{11}$$

where $\boldsymbol{L} = \boldsymbol{I}[L_{IJ}] = \left(\int_\Omega \rho N_I c_i N_{J,i} d\Omega\right)\boldsymbol{I}$.

The other matrixes are similar with those in equation (1).
The asymmetric and nonlinear convective term in equation (11) can easily lead to an oscillatory result. Therefore, the operator split method including Lagrangian step, mesh update step and Eulerian step is applied.
a. Assuming that the flow field mesh follows the fluid deformation in Lagrangian step. Thus, the calculation process is the same with the explicit method used in textile deformation calculation.
b. The internal meshes in flow field often deform after the Lagrangian step. In mesh update step, the deformed meshes are updated by solving the inverse of a Laplace equation, and the original topological relationships are unchanged (figure 2).
c. The Van Leer MUSCL scheme with second order accuracy is applied in Eulerian step [12].

NUMERICAL EXAMPLE

Finite element model

In this paper, the C9 parachute made of polyamide MIL-c-7020 type III is used to verify this method. The structural parameters and material properties of C9 parachute are shown in table 1.
Figure 3 shows the finite element model. The canopy and lines are meshed by triangular elements (14 000) and bar elements (1 932). The hexahedral elements (921 600) are used to mesh the flow field. The canopy and fluid domain interpenetrate. The initial velocity (20.7 m/s) and the gravity acceleration (9.8 m/s^2) are given to the payload (100 kg).

RESULTS AND COMPARISON

The run takes about 200 hours on an Intel processor i7-3770. Figure 4 shows the parachute opening process. The bottom of the canopy is inflated first. As air

Table 1

MODEL PARAMETERS		
Structure of C9	Number of canopy gores	28
	Nominal diameter (m)	8.5
	Diameter of vent (m)	0.85
	Nominal area (m^2)	57.2
	Length of line (m)	7
Material properties of canopy	Density of canopy (kg/m^3)	533
	Young's modulus of canopy (pa)	4.3E+8
	Thickness of canopy (m)	1E-4
	Linear resistance coefficient (kg/m^3·s)	1.6E+6
	Quadratic resistance coefficient (kg/m^4)	4.8E+5
Material properties of line	Density of line (kg/m^3)	462
	Young's modulus of line (pa)	9.7E+10
Properties of air	Density of air (kg/m^3)	1.02
	Temperature of air (°)	25
	Ambient Pressure (pa)	8.12E+4

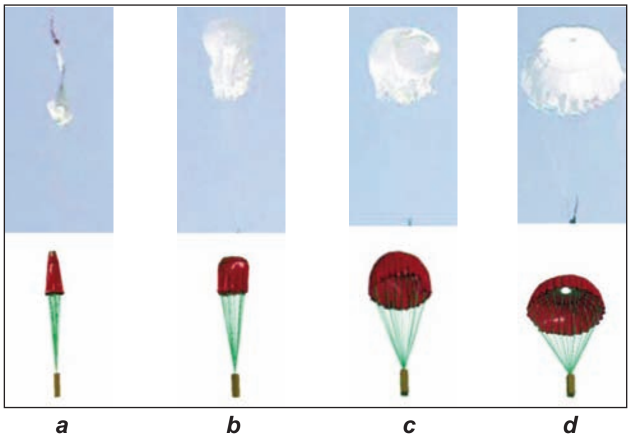

Fig. 4. Comparison between calculation and airdrop experiment

enters the canopy, the top opened quickly, and then the canopy has the classical 'bulb' state. At last, the fully inflated area gradually expands from the top to the bottom. Compared with the airdrop experiment (figure 4), both changes are similar.

In the steady dropping state, the parachute dropping velocity is 6.4 m/s and the drag coefficient is 0.82. The corresponding experimental values are 6–7 m/s and 0.8 [13]. The pressure drop between internal and external canopy is about 120 Pa (figure 5) and close to US standard value 124.5 Pa (the dropping velocity in steady state is 6–7 m/s). The numerical results show that it is feasible to simulate the deformable porous textile working process by using ALE method.

RESEARCH OF TEXTILE PERMEABILITY

Textile permeability experiment

The experiment is carried out according to the standard GB/T5453-1997, and the YG461D tester is used for getting the permeability parameters (figure 6). The instrument and principle are shown in figure 6. The pressure drop is obtained according to the difference of atmospheric pressure P_0 and front chamber pressure. The unit flow, which can be viewed as relative velocity, is obtained according to the nozzle diameter, the front and the rear chamber pressure.

The polyamide K29225 and polyamide K58326 are tested, and the experimental data are fitted to permeability curve. Table 2 shows the permeability parameters and figure 7 shows the fitted curves.

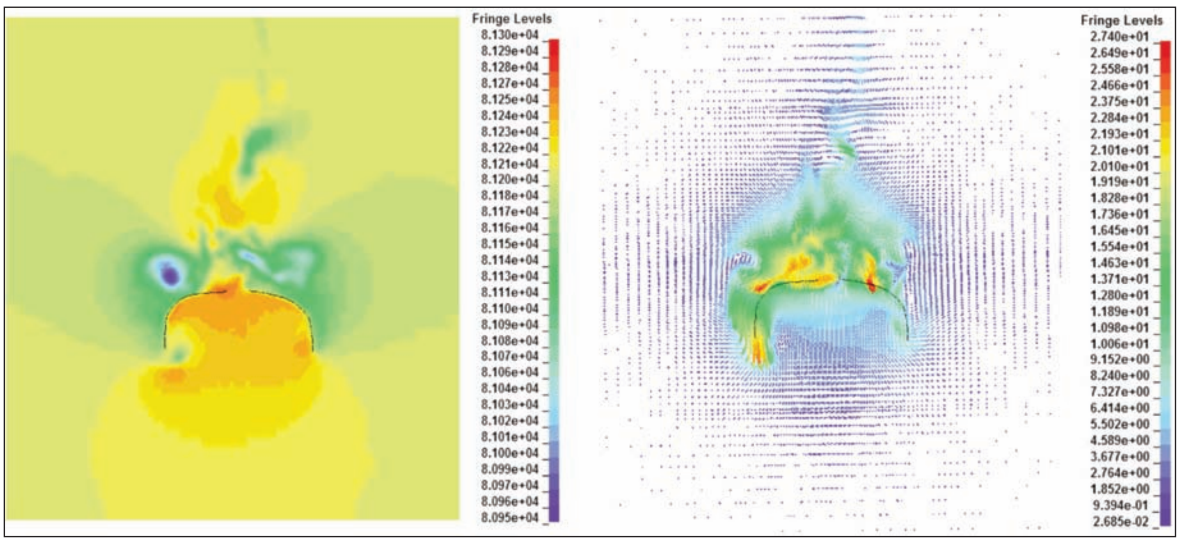

Fig. 5. Flow field results (in steady dropping state)

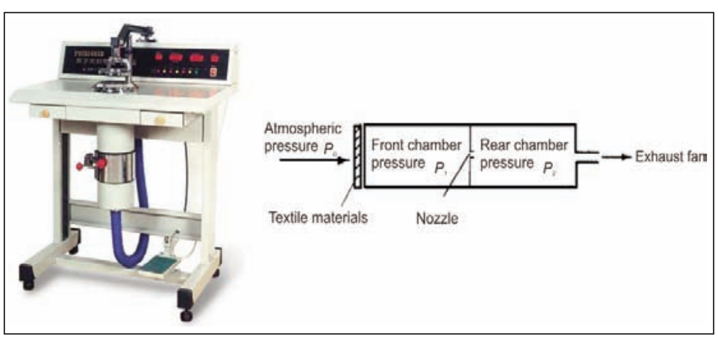

Fig. 6. Permeability tester (left: YG461D tester; right: principle)

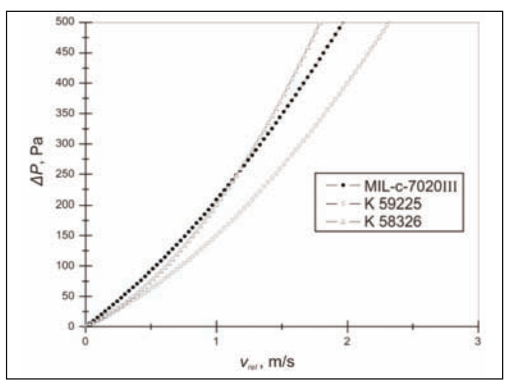

Fig. 7. Permeability change follows the pressure change

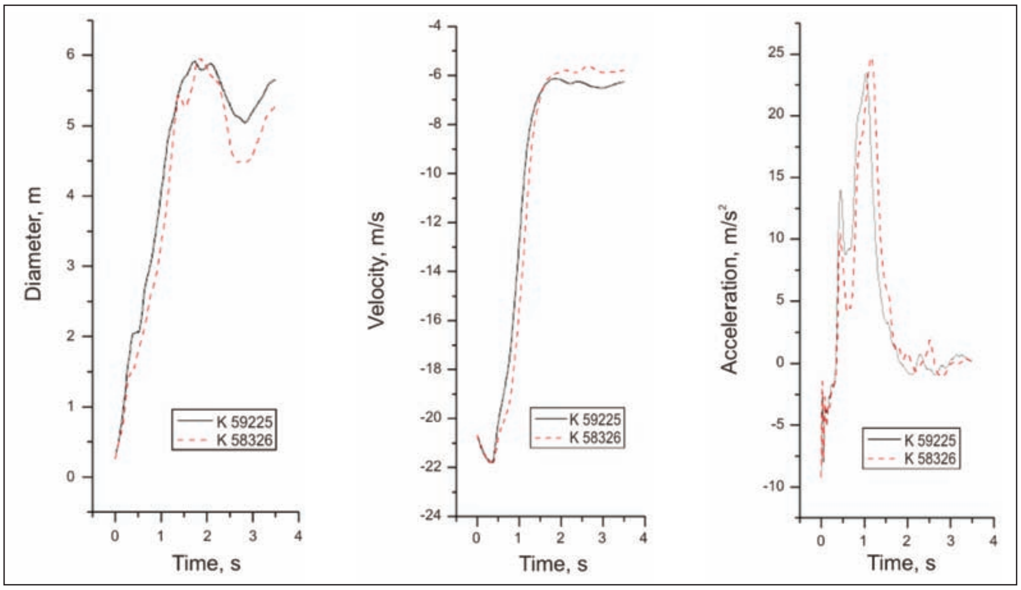

Fig. 8. Parachute performance (left: diameter change; middle: velocity; right: acceleration)

Table 2

PERMEABILITY PARAMETERS			
	Linear resistance coefficient ($kg/m^3 \cdot s$)	**Quadratic resistance coefficient** (kg/m^4)	**Thickness** (m)
K59225	1.05E+6	4.9E+5	1E-4
K58326	1.1E+6	1E+6	1E-4

Performances of the parachute made from different permeable materials

The textile materials used in C9 parachute are replaced by polyamide K29225 (Model A) and polyamide K58326 (Model B) respectively. The parachute performances are shown in figure 8.

The projected diameter of Model A is generally larger than that of Model B. When the parachute entered the steady dropping state (1.5 s later) and appears the breath phenomenon, the change magnitude of Model A drops. The steady dropping velocity of Model A (6.5 m/s) is faster than Model B (5.9 m/s). According to the equation of drag coefficient, the value of Model A (0.79) is smaller than that of Model B (0.96). Before the steady dropping state, the projected diameter and velocity of Model A are higher than Model B and also the acceleration is higher, but the maximum value is smaller (at about 1.5 s).

The result shows that the high permeability material can reduce the maximum dynamic load but the dropping velocity is higher, while the small permeability material gives the opposite results.

CONCLUSIONS

The numerical method used in this paper was verified by airdrop experiment. Then the same parachute made of different permeable textile material was calculated. The effect of permeability on parachute opening was analyzed, and the qualitative conclusions were obtained. The method used in this work could be used to guide the parachute design and material selection.

Acknowledgments

This paper is supported by the National Natural Science Foundation of China (No. 11172137) and the Aeronautical Science Foundation of China (No. 20122910001). The authors are grateful to Jiang LONG for his carefully polishing.

BIBLIOGRAPHY

[1] Niculescu, C., Butoescu, V., Salistean, A., Olaru, S., *Equipment for paraglider- the emergency parachute.* In: Industria Textila, 2010, vol. 61, issue 1, pp. 11–16

[2] Xiao, X. L., Zeng, X., S., Bandara, P., et al. *Experimental Study of Dynamic air Permeability for Woven Fabrics.* In: Textile Research Journal, 2012, vol. 82, issue 9, pp. 920–930

[3] Rowan, J., *Development of a High Differential Pressure Fabric Permeability Tester.* In: Report AIAA 2001-2071, Boston, US, 2001

[4] Yazdchi, K., Srivastava, S., Luding, S., *Microstructural effects on the permeability of periodic fibrous porous media.* In: International Journal of Multiphase Flow, 2011, vol. 36, pp. 956–966

[5] Melro, A., R., Camanho, P., P., Pinho, S., T., *Generation of random distribution of fibres in long-fibre reinforced composites.* In: Composites Science and Technology, 2008, vol. 68, pp. 2092–2102

[6] Yu, L., Ming, X., *Study on transient aerodynamic characteristics of parachute opening process.* In: Acta Mechanica Sinica, 2007, vol. 23, issue 6, pp. 627–633

[7] Aquelet, N., Wang, J., Tutt, B., A., et al. *Euler-Lagrange Coupling with Deformable Porous Shells*. In: ASME Pressure Vessels and Piping Division Conference. Vancouver, BC, Canada, 2006, pp. 23–27

[8] Jia, H., Rong, W., Chen, G., L., *The use of LS-DYNA to simulate the permeability parameters of the parachute canopy*. In: Spacecraft Recovery & Remote Sensing, 2009, vol. 30, issue 1, pp.15–20

[9] Xiao, X., L., Zeng, X., S., Long, A., et al. *An analytical model for through-thickness permeability of woven fabric.* In: Textile Research Journal, 2012, vol. 82, issue 5, pp. 492–501

[10] Cheng, H., Yu, L., Chen, X., et al. *Numerical study of flow around parachute based on macro-scale fabric permeability as momentum source term.* In: Industria Textila, 2014, vol. 65, issue 5, pp.271–276

[11] Belytschko, T., Liu, W., K., Moran, B., *Nonlinear Finite Elements for Continua and Structures.* John Wiley & Sons, Ltd.

[12] Souli, M., Ouahsine, A., Lewin, L., *ALE and Fluid-Structure Interaction problems*. In: Comput. Methods Appl. Mech. Engrg., 2000, vol. 190, pp. 659–675

[13] Ewing, E., G., Knacke, T., Bixby, H., W., *Recovery Systems Design Guide.* Beijing Aviation Industry Press.

Authors:

HAN CHENG
Aviation Engineering Institute
Civil Aviation Flight University of China
46 Nanchang Road
Sichuan Guanghan 618307
P. R. China
e-mail: chenghanstorm@sina.com

LI YU
YA-NAN ZHAN
XIAO CHEN
XUE YANG
College of Aerospace Engineering
Nanjing University of Aeronautics and Astronautics
29 Yudao Stress
Nanjing 210016
P. R. China

Corresponding author:

LI YU
e-mail: yuli_happy@163.com

Sewing needle temperature of an industrial lockstitch machine

ADNAN MAZARI

GUOCHENG ZHU
ANTONIN HAVELKA

REZUMAT – ABSTRACT

Temperatura acului unei mașini de cusut industriale în timpul coaserii

În acest articol este realizată o analiză de regresie multiplă folosind sistemul MATLAB, pentru a preconiza temperatura acului de cusut al unei mașini de cusut, în cazul unei țesături denim 100%. Variabilele, precum cusăturile/cm, viteza de coasere, numărul de straturi de material textil și momentul coaserii sunt alese ca parametri de intrare. Temperatura acului a fost măsurată experimental prin metoda termocuplului introdus. Un model experimental Box-Behnken cu patru factori și trei niveluri (construit cu ajutorul Minitab 16) este utilizat pentru a evalua efectele variabilelor independente selectate asupra răspunsului. Rezultatele experimentelor sunt utilizate pentru modelul statistic, care ne pot ajuta să identificăm condițiile experimentale optime și relațiile dintre temperatura acului și parametrii selectați. Se observă că viteza de coasere este cel mai important factor care influențează temperatura acului, urmată de timpul de coasere, numărul de straturi și densitatea cusăturii. Modelul are un procentaj de eroare mai mic de 10% și poate fi ușor de utilizat la coasere în calcularea temperaturii acului.

Cuvinte-cheie: ac de cusut, temperatura acului, măsurarea temperaturii acului

Sewing needle temperature of an Industrial lockstitch machine

In this article a multiple regression analysis is performed using MATLAB to predict the sewing needle temperature of a lockstitch machine for 100% denim fabric. The variables like stitches/cm, sewing speed, number of fabric layers, and the time of sewing are chosen as input parameters. Needle temperature was experimentally measured by Inserted thermocouple method. A three-level four factorial Box–Behnken experimental design (constructed using Minitab 16) is used to evaluate the effects of the selected independent variables on the response. The results from the experiments are used for statistical model, which can help finding the optimum experimental conditions and the relationships between needle temperature and selected parameters. It is observed that sewing speed is the most important factor for needle temperature followed by sewing time, number of layers and the stitch density. The model has error percentage of less than 10% and can be easily used at the sewing floor for calculating needle temperature.

Key-words: Sewing needle, needle temperature, needle heat measurement.

Industrial sewing is one of the most common manufacturing operations. Its application can be found in the manufacturing of garments, shoes, furniture and automobiles. Every day, millions of products ranging from shirts to automotive airbags are sewn. Hence, even small improvements may result in significant commercial benefits. Heavy industrial sewing, such as that used in the manufacture of automobile seat cushions, backs and airbags, requires not only high production but also high sewing quality. In recent years, in order to increase production, high-speed sewing has been extensively used. Currently, sewing speeds range from 16~100 stitches/sec. In heavy industrial sewing, typical sewing speeds range from 16~50 stitches/sec.

Depending on the sewing conditions, maximum needle temperatures range from 100°C~300°C [1]. This high temperature weakens the thread, since thread tensile strength is a function of temperature [1, 2]. In addition, the final stitched thread has 30–40% less strength than the parent threads [3].

Various methods for measuring needle temperature, such as infrared pyrometer, thermocouple and temperature sensitive waxes, have been used. As the needle is moving extremely fast during the sewing process, it is quite difficult to measure the exact temperature [4]. There are few theoretical models available to predict sewing needle temperature [4, 5, and 7], Trung et al [5] uses FEA model which shows better accuracy but it's complicated to be used at sewing floor, Q. Li et al [7] have studied two models; which has an average error of 25%. Recently Yukseloglu et al [12] have observed the needle temperature by thermal camera for polyester blend fabrics for sewing speed of 16~50 stitches/cm, using a chromium needle and therefore the emissivity was considered as 0.07; this was also stated by some other researchers [7]. For the infrared temperature measurement, there is a problem in calibration because the amount of radiation emitted at higher temperature depends on the surface characteristics. The emissivity of each needle must be determined individually and, indeed, the emissivity might change during high speed sewing process. Researchers have similarly tried different methods for measuring needle temperature in the past; Sondhelm [8] used a lacquer painted in the needle groove to observe a change of colour with temperature, Laughlin [9] tried to measure needle temperature through infrared measurement from the needle using a lead-sulphide photocell and another

Table 1

SEWING THREAD PROPERTIES					
Thread type	**Company name/product**	**Thread Count (tex)**	**Twist (t/m)**	**Twist direction (ply/single)**	**Coefficient of friction μ**
Polyester/polyester core spun	AMANN/Saba C-80	22*2	660	Z/S	0.14

Table 2

FABRIC PROPERTIES					
Fabric type	**Weave**	**Weight**	**Ends/cm**	**Picks/cm**	**Fabric Thickness**
100% Cotton Denim	2/1 Twill	257 g/m^2	25	20	0.035 cm

technique using thermocouples was later developed by Dorkin and Chamberlain [10]. In this current research, inserted thermocouple method [11] is used to measure the sewing needle temperature of a lock-stitch machine at different machine speeds (16~50 stitches/s).

EXPERIMENTAL PART

Material and methods

For this research inserted thermocouple method is used to measure the sewing needle temperature of an industrial lockstitch machine (BROTHER Industries). Conditions for all experiments were kept constant at 26°C and 65% RH. The devices and materials used for the experiments are listed below:

- Lockstitch machine (Brother Company, DD7100-905).
- Thermocouple by Omega (K type 5SC-TT-(K)-36-(36)) for the inserted method.
- Thermocouple by Omega-wireless device and receiver (MWTC-D-K-868).
- Needles (Groz-Becker 100/16) R-type.
- Sewing thread properties are shown in table 1.
- Denim fabric properties are shown in table 2.

Needle temperature measurement

There are many different ways of experimentally measuring the needle heat for industrial sewing machine but inserted thermocouple method proved to be the most efficient way of measurement. The previous work of author [11, 13] compares different experimental method of needle temperature measurement and shows the inserted thermocouple with highly repeatable results.

Figure 1 shows the sewing needle with the inserted thermocouple. A thin thermocouple is inserted inside the needle groove and needle temperature is measured wirelessly to computer during high speed sewing.

Box-Behnken design

A three-level four factorial Box–Behnken experimental design (constructed using Minitab 16) was used to evaluate the effects of the selected independent variables on the response. The number of experiments required to investigate the previously noted four factors at three levels would be 81. However, this was reduced to 27 by using a Box–Behnken experimental design. The results from this limited number of experiments provided a statistical model, which can help to find the optimum experimental conditions and the relationships between experimental results and parameters. The significant variables like stitch, speed of sewing, layer of fabric, and the time were chosen as the critical variables and designated as X_1, X_2, X_3, and X_4, respectively. The low, middle, and high levels of each variable were designated as −1, 0, and +1, respectively, as shown in table 3. Design of this experiment is given in table 4.

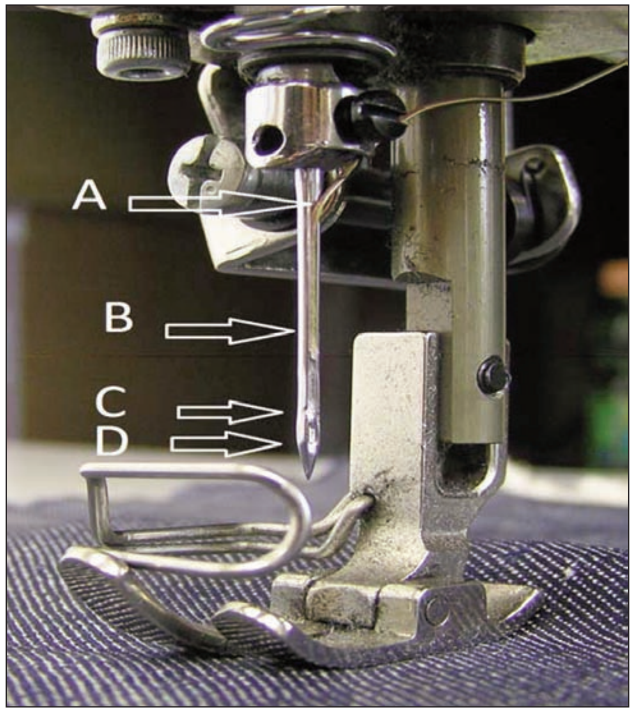

Fig. 1. Sewing needle with the inserted thermocouple
A – thermocouple wire connected to data logger,
B – needle groove, C – thermocouple tip, D – needle eye

Table 3

FACTORS AND FACTOR LEVELS STUDIED IN BOX-BEHNKEN EXPERIMENTAL DESIGN			
	Levels		
Factors	–1	0	1
X_1=number of stitches /2.54 cm	10	12	14
X_2=Speed of Sewing (stitches/60 s)	1000	2000	3000
X_3=Number of Denim fabric layers	2	3	4
X_4=Time of Sewing (s)	10	20	30

Table 4

THE DESIGN OF THE EXPERIMENT

Trial No.	X_1	X_2	X_3	X_4
1	–1	–1	0	0
2	–1	1	0	0
3	1	–1	0	0
4	1	1	0	0
5	0	0	–1	–1
6	0	0	–1	1
7	0	0	1	–1
8	0	0	1	1
9	–1	0	0	–1
10	–1	0	0	1
11	1	0	0	–1
12	1	0	0	1
13	0	–1	–1	0
14	0	–1	1	0
15	0	1	–1	0
16	0	1	1	0
17	–1	0	–1	0
18	–1	0	1	0
19	1	0	–1	0
20	1	0	1	0
21	0	–1	0	–1
22	0	–1	0	1
23	0	1	0	–1
24	0	1	0	1
25	0	0	0	0
26	0	0	0	0
27	0	0	0	0

RESULTS AND DISCUSSIONS

In a system involving four significant independent variables X_1, X_2, X_3, and X_4 the mathematical relationship of the response on these variables can be approximated by the quadratic polynomial equation:

$$Y = \alpha_0 + \alpha_1 x_1 + \alpha_2 x_2 + \alpha_3 x_3 + \alpha_4 x_4 + \alpha_{12} x_1 x_2 + \alpha_{13} x_1 x_3 + \alpha_{14} x_1 x_4 + \alpha_{23} x_2 x_3 + \alpha_{24} x_2 x_4 + \alpha_{34} x_3 x_4 + \alpha_{11} x_1^2 + \alpha_{22} x_2^2 + \alpha_{33} x_3^2 + \alpha_{44} x_4^2 + \alpha_5 x_1 x_2 x_3 + \alpha_6 x_1 x_2 x_4 + \alpha_7 x_1 x_3 x_4 + \alpha_8 x_2 x_3 x_4 + \alpha_9 x_1 x_2 x_3 x_4 \quad (1)$$

where:

Y is estimate response, α_0 is constant, α_1, α_2, α_3, and α_4 are linear coefficients, α_{12}, α_{13}, and α_{23} are interaction coefficients between the three factors, α_{11}, α_{22}, and α_{33} are quadratic coefficients.

In this model given in equation (1), interactions higher than second-order have been neglected. A multiple regression analysis is done to obtain the coefficients and the equation can be used to predict the response.

$$Y = -26 + 1.375X_1 - 0.0262X_1^2 + 1.2{*}10^{-5}X_2^2 + 0.2134X_3X_4 + 0.00123X_2X_4 \quad (2)$$

where:

Y is needle temperature (°C);

X_1 – stitch (number of stitches/2.54 cm);

X_2 – speed of sewing (number of stitches/60 s);

X_3 – number of denim fabric layers;

X_4 – time of sewing (s).

Adjusted R^2 = 0.994 and P-value = 1.24*10^{-24} ≈ 0.

In order to gain a better understanding of the interaction effects of variables on needle temperature. Selective three dimensional surface plots for the measured responses were studied.

It is clear from figure 2 that the needle temperature rises substantially with the increase of sewing speed. It might be due to higher friction between thread and machine part at higher speeds of sewing.

Figure 3 shows the 3D-surface plot for impact of number of layers and stitch density on needle temperature. It was observed that needle temperature is highly

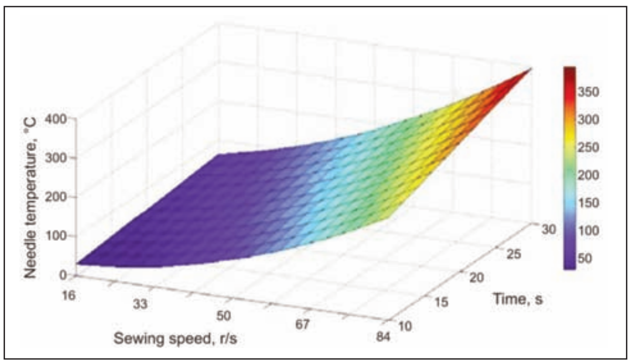

Fig. 2. Effect of sewing speed and sewing time on needle temperature

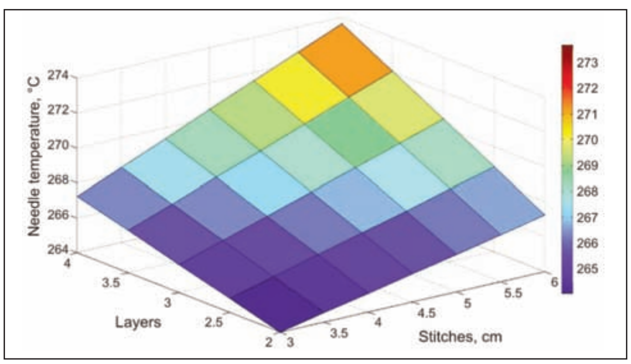

Fig. 3. Effect of number of fabric layers and stitch density on needle temperature

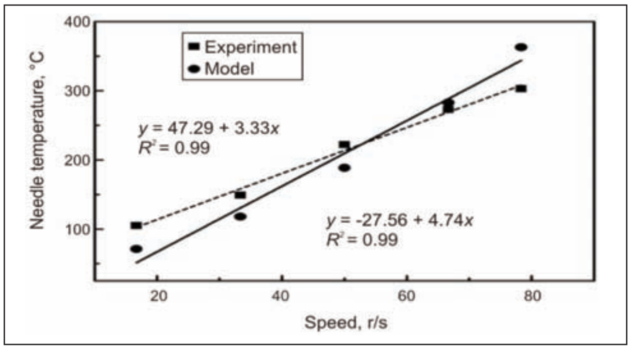

Fig. 4. Comparison of experimental and predicted needle temperature for different sewing speeds

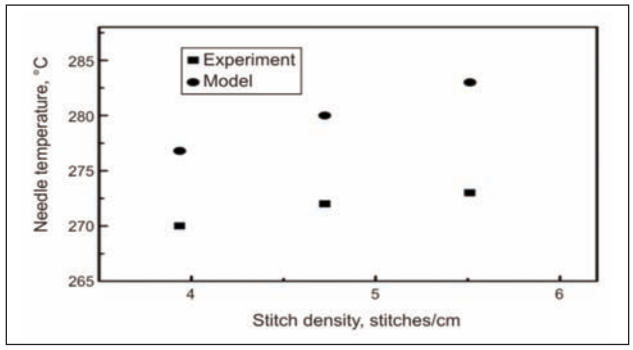

Fig. 6. Comparison of experimental and predicted needle temperature for different stitch density

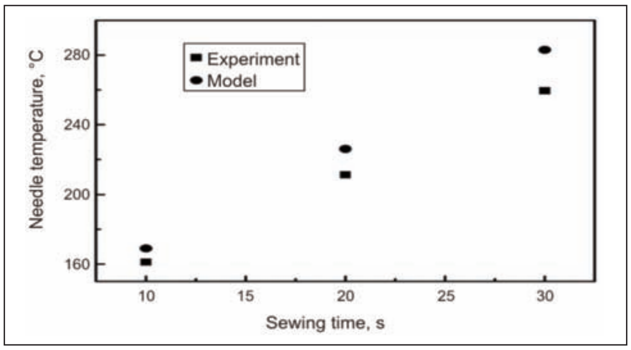

Fig. 5. Comparison of experimental and predicted needle temperature for different time of sewing

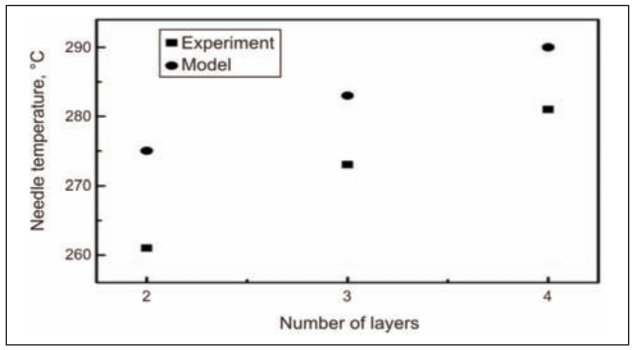

Fig. 7. Comparison of experimental and predicted needle temperature for different number of fabric layers

impacted by number of layers of fabrics, because with the increase of fabric thickness, higher friction occurs between needle and the fabric. Whereas the stitch density causes a minor increase in needle temperature which might be due to the fact that higher number of stitches in one second causes more friction but contact time with fabric to conduct the needle heat is also increased.

Figures 4–7 show the comparison of experimental and predicted sewing needle temperature at different speeds, sewing time, stitch density and number of layers.

Figure 4 shows the comparison of needle temperature at different speed of sewing by experiment, and the predicted values by the model developed. It is visible that needle temperature rises linearly with the increase of sewing speed. There is nearly 15°C rise in needle temperature with each 10 r/s increase in sewing speed.

Figure 5 shows the increase of needle temperature with respect to time for both experimental and the predicted values. It is visible that the needle temperature raises with the increase in sewing time, as friction between thread, needle and fabric for longer time period increases the needle temperature.

Figure 6 shows the effect of stitch density on needle temperature, there is a minor increase of needle temperature with increase of stitch density, higher stitch density represents more stitches per unit length which increases the friction time between needle, thread and fabric but also the contact time between needle and fabric is increased which helps in conducting needle heat to fabric.

Figure 7 shows the comparison of needle temperature for different layers of denim fabric. It is visible that there is nearly 10°C rise in needle temperature with each extra layer of fabric. As increasing the layer changes the thread tension and might cause higher friction between thread and fabric.

Figure 8 shows the comparison of needle temperature measured by experiment and by regression model. The needle temperature is shown for sewing speed of 50 r/sec at sewing time of 10, 20 and 30 seconds for 2, 3 and 5 layer of denim fabric. The secondary *y*-axis on the right side of graph shows the average percentage difference between the predicted and the experimental results. Results confirm that the model has error percent of less than 10% for all factors.

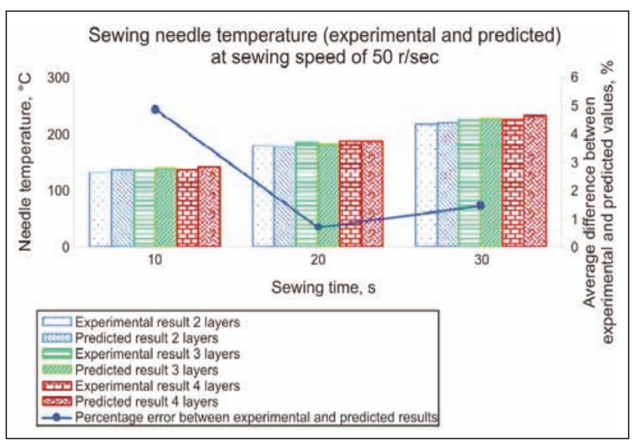

Fig. 8. Prediction of model at 50 r/sec of sewing

Needle temperature rises with longer time of sewing but the increase is dramatic till 10 seconds of sewing, as after this time the needle system get stabilize with the environment temperature. The needle heat is dissipated to surrounding through conduction through fabric, thread and needle holder and also by convection through airflow (surrounding airflow and air forced at the needle eye with the sewing thread), whereas the heat dissipation through radiation might be very low as needle is thin and shiny with emissivity of less than 0.08 (This value of emissivity is for needle made from chromium).

CONCLUSIONS

In this research, needle temperature for denim fabric is measured at different speeds of sewing, sewing time, stitch density and number of fabric layers. A multiple regression analysis is done to obtain the coefficients and the equation can be used to predict the needle temperature. Followings conclusion can be made:

- Needle temperature rises dramatically with the increase of sewing speed, there is nearly 80°C rise of needle temperature when speed of machine increases from 16 stitches/cm to 33 stitches/cm.
- Needle temperature rises with time of sewing; but after 10 seconds of sewing the rise of temperature is minor.
- Stitch density shows minor increase in the sewing needle temperature which may be due to the reason that needle is inserted more times inside the fabric causing higher friction but also increasing the heat transfer from needle to the fabric.
- Needle heat increases with the increase of number of fabric layers. There is nearly 20°C rise in needle temperature by increasing each layer of fabric.
- The model can be easily applied, for 100% denim fabric with sewing thread of 22*2 tex (PET-PET cores-pun) at any sewing floor, knowing the needle heat will always help in improving the productivity of sewing process. Sewing speed appeared to be the major factor impacting the needle temperature followed by sewing speed, number of layers and the stitch density. Our model prediction performance has error percentage of less than 10 % (see fig. 8.), which is believed much lower as compared to any other sewing needle heat model. Further work will be performed with different fabrics and thread types.

BIBLIOGRAPHY

[1] Qinwen, Li., and Liasi, E. *A study on the needle heating in heavy industrial sewing, part II.* In: International Journal of Clothing Science and Technology, 2001, vol.13, issue 5, pp. 351–367.
[2] Hersh, S., Grady, P. *Needle heating during high speed sewing.* In: Textile Research Journal, 1969, vol. 39, pp. 101–120.
[3] Midha, V., Mukhopadhyay, A., Chatopadhyay, R., Kothari, V. *Studies on the changes in tensile properties of sewing thread at different sewing stages.* In: Textile Research Journal, 2009, vol. 79, pp. 1 155–1 167.
[4] Qinwen, Li., Liasi, E. *A study on the needle heating in heavy industrial sewing, part I.* In: International Journal of Clothing Science and Technology, 2001, vol. 13, issue 2, pp. 87–105.
[5] Trung, N., Kus, Z. *Computer Simulation of Sewing Needle Heating.* In: CSCC'99 Proceedings, 1999, vol.1, pp. 1 991–1 994.
[6] Mazari, A., Havelka, A. *Tensile properties of sewing thread and sewing needle temperature at different speed of sewing machine*. In: Advanced Materials Research, 2013, vol. 627, pp. 456–460.
[7] Li, Q., Liasi, E., Simon, D., and Du, R. *Heating of industrial sewing machine needles, FEA model and verification using IR radiometry.* In: Thermosense XXI, 1999, vol. 3700, pp. 347–357.
[8] Sondhelm, W. *Causes of seam damage: Needle heating.* In: Journal of Textile Institute, 1953, vol. 44, pp. 580–585.
[9] Laughlin, R. *Needle temperature measurement by infrared pyrometry.* In: Textile Research Journal, 1963, vol. 33, pp. 35–39.
[10] Dorkin, C.,Chamberlain, N. *The facts about needle heating.* In: Clothing Institute Technical, 1963, Report no.13.
[11] Mazari, A., and Havelka, A. *Influence of needle heat during sewing process on the tensile properties of sewing thread.* In: Tekstilec, 2013, vol. 56, issue 4, pp. 345–352
[12] Yukseloglu, M., Citoglu, F., Cetinkaya, B. *A study on the needle heating in polyester blend upholstery fabrics.* In: Industria Textila, 2013, vol. 64, issue 5, pp. 246–253.
[13] Mazari, A., Havelka, A.,Hes, L. *Experimental techniques for measuring sewing needle temperature.* In: Tekstil ve konfeksiyon, 2014, vol. 24, issue 1, pp. 111–118.

Authors:

ADNAN AHMED MAZARI
ANTONIN HAVELKA
Technical University of Liberec,
Faculty of Textile Engineering,
Department of Textile Clothing, Studentska 2, Liberec,
461 17, Czech Republic

GUOCHENG ZHU
Technical University of Liberec,
Faculty of Textile engineering,
Department of Material Engineering,
Studentska 2, Liberec, Czech Republic

Corresponding author:

ADNAN AHMED MAZARI
e-mail: adnanmazari86@gmail.com;
adnan.ahmed.mazari@tul.cz

Investigation on compression properties of polyurethane-based warp-knitted spacer fabric composites for cushioning applications
Part II. Theoretical model and experimental verification

SI CHEN HAI-RU LONG

REZUMAT – ABSTRACT

Investigarea proprietăţilor de compresie ale compozitelor spacer tricotate din urzeală pe bază de poliuretan pentru aplicaţii de amortizare a şocului: Partea II. Model teoretic şi verificare experimentală

În acest studiu a fost stabilit un model experimental pentru anticiparea proprietăţilor de compresie ale compozitelor spacer tricotate din urzeală pe bază de poliuretan. Curbele de deformare la compresie ale simulărilor teoretice obţinute prin modelul derivat au fost realizate cu ajutorul Matlab. Pentru a verifica modelul de compresie propus, curbele de compresie ale simulării teoretice şi rezultatele experimentale au fost comparate şi reprezentate într-o diagramă, aceste două curbe prezentând o bună compatibilitate. Cu toate acestea, au existat unele abateri rezultate din reprezentările idealizate şi substituţiile ecuaţiilor firelor spacer, precum şi diferenţe între parametrii structurali teoretici şi cei reali.

Cuvinte-cheie: comportament la compresie, verificare experimentală, compozite pe bază de poliuretan, model teoretic

Investigation on compression properties of polyurethane-based warp-knitted spacer fabric composites for cushioning applications Part II: theoretical model and experimental verification

In this part, a theoretical model was established to predict the compression properties of polyurethane-based warp-knitted spacer fabric composites. The theoretical compression curves obtained by the derived model were simulated by Matlab. In order to verify the proposed compression model, the compression curves of theoretical simulations and experiment results were compared in a figure and these two curves exhibited good agreement with each other. However, there were still some deviations derived from the idealizations and substitutions of spacer yarn's status and equations, as well as the differences between theoretical and actual structure parameters.

Key-words: compression behaviors, experimental verification, polyurethane-based composites, theoretical model

In order to better understand the compression properties of polyurethane-based warp-knitted spacer fabric composites, the theoretical compression model was established to investigate its compression responses [1–4]. In the first part, the detailed experimental results of compression tests were given out. It can be found that the compression behaviors of polyurethane-based composites are obviously influenced by structure parameters. Based on these structure parameters and experimental results in the first part, the study presented in this second part will focus on establishing theoretical model of compression properties. And the compression curves of theoretical simulations and experiment results were compared in a figure to verify the proposed compression model. Firstly, some basic equations are established by structure parameters. Then, the compression models were generated based on these obtained equations and total compression force-displacement curves for each sample were calculated. Finally, the calculated curves are compared with experimental ones to verify the model. The differences between the simulations and experiments are also discussed.

EXPERIMENTAL PART

The mixing rule of composite materials

The mechanical and physical properties of composite materials depend on the volume percentage of each component in the condition that the mechanical and physical characteristics of each component are derived. It can be given as the equation (1):

$$P_c = \sum_{i=1}^{n} P_i V_i \tag{1}$$

where:

P_c is the mechanical and physical properties of composite materials;

P_i – the mechanical and physical characteristics of each component;

V – the volume percentage of each component;

i – the number of component.

As for the spacer fabrics, the thickness of outer layers is lower than the height of core area. The compression properties of spacer fabrics mainly depend on the anti-compression abilities of spacer yarns. To avoid the complicated analysis, it is assumed that the compression behaviors of spacer fabrics can be described by using the compression behaviors of spacer yarns [5–6]. In that case, according to equation (1), the total compression force (F) on the polyurethane-based composites, equals the sum of the compression forces withstood by the spacer yarns (F_1) and the polyurethane foams (F_2). It satisfies the equation (2):

$$F = V_f F_1 + V_p F_2 \tag{2}$$

where:

F is the total compression force;
F_1 – the forces withstood by the spacer yarns;
F_2 – compression load on polyurethane foams;
V_f – the volume percentage of spacer yarns;
V_p – the volume percentage of polyurethane foams.

Determination of structure parameters of spacer yarns

Spacer yarns are used to connect the two surface layers, the angle between spacer yarns and surface layers in weft direction is defined as inclination angle (α). Based on the figure 7 in Part I, it can be found that the chain notations of GB3 and GB4 are exactly symmetrical and the inclination angle decreases as the chain notations increase. To simplify the calculation, the chain notation of GB3 is chosen for analysis. The chain notation view of GB3 (type II) in a cycle process is given in figure 1. In figure 1, the X-, Y- and Z-axes indicate the direction of weft, wale, and thickness of spacer fabrics, respectively. All the points in the figure represent the junctions between spacer yarns and outer layers. Three adjacent courses are put in three planes: the white dots representing the first course are placed in the first plane, while the black and blue dots representing the second and third courses are placed in the subsequent two planes. Points A, C, D', B', A'' show the lapping movements of 1-0, 3-2, 3-2, 1-0, respectively. Moreover, areas ADD'A' and BCC'B' are the top and bottom layers. Moreover, the schematic of spacer yarn is shown in figure 2. In the diagram, L_z is the length of spacer yarn, H is thickness. L is the distance between two under-lapped loops, it can be obtained from the course-wise density (table 2, part I). The black dots represent points D' and B' exhibited in figure 1. The inclination angle (α) can be calculated by equation (3):

$$\alpha = \arctan\left(\frac{H}{L}\right) \tag{3}$$

In addition,

$$L_z = \frac{L}{\cos \alpha} \tag{4}$$

The values of α, H, L and L_z are presented in table 1.

Table 1

THE STRUCTURE PARAMETERS OF SPACER YARN				
Specimen	Inclination angle (degree)	Parameters (mm)		
		L	H	L_z
A1	69.54	2.86	7.68	8.19
A2	61.28	4.23	7.72	8.80
A3	61.07	4.26	7.71	8.81
A4	63.96	2.99	6.12	6.81
A5	75.02	2.84	10.62	10.98

Compression model derivation

According to the compression test results of polyurethane-based warp-knitted spacer fabric composites,

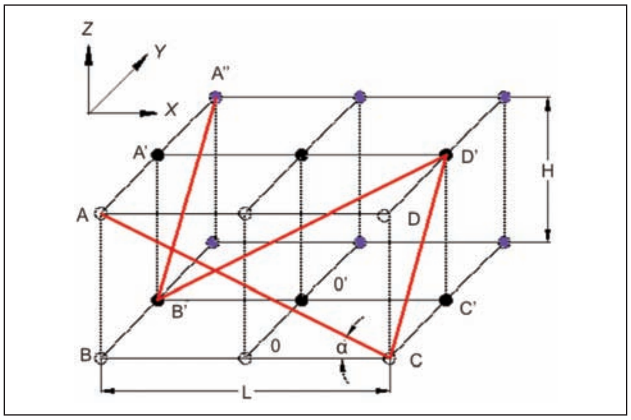

Fig. 1. Simplification model of spacer yarn arrangement (type II) in a cycle process

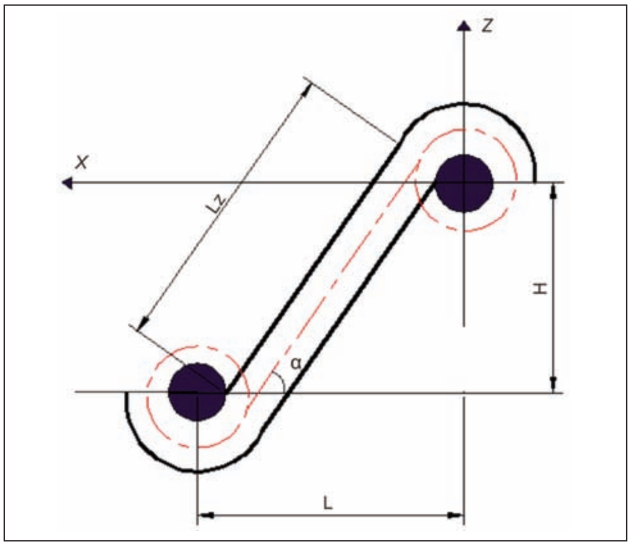

Fig. 2. The schematic of spacer yarn in X-Z plane

it is assumed that the deformation condition of composites was exponential function proximately, which can be described as equation (5):

$$x = e^z \tag{5}$$

The bending moment $M(x)$ and compression force load (F_1) of spacer yarns have the following relationship [7]:

$$\frac{x''}{(1 + x'^2)^{3/2}} = -\frac{M(z)}{EI} \qquad M(z) = F_1 x \tag{6}$$

where:
E (CN/dtex) is the Young's modulus of spacer yarn, the value of E is 286.5 CN/dtex;
I – rotary inertia.
According to Equations (5)–(6), the compression force on spacer yarn (F_1), can be given as equation (7):

$$F_1 = \frac{EI}{(1 + x'^2)^{3/2}} \tag{7}$$

According to Maclaurin formula, $(1 + x'^2)^{3/2}$ can be expressed as:

$$(1 + x'^2) = 1 + \frac{3}{2} \times x'^2 + \frac{3}{4} \times \frac{1}{2!} \times x'^4 \ldots \tag{8}$$

Using equation (8), equation (7) becomes:

$$x' = \sqrt{\frac{2}{3} \times (\frac{EI}{F_1} - 1)} \tag{9}$$

By integrating equation (9), the following equation is obtained:

$$\int_0^H x' \, d_z = \int_0^H \sqrt{\frac{2}{3} \times (\frac{EI}{F_1} - 1)} \, d_z \tag{10}$$

Equation (10) should meet the boundary condition: the horizontal displacement at the ends of spacer yarns is zero during compression test process, so the equation (10) becomes:

$$F_1 = EI \tag{11}$$

In addition:

$$V_f = \frac{n \pi d^2 L_z}{4H}, \qquad I = \frac{\pi d^4}{64} \tag{12}$$

where:

n is spacer yarn/cm^2 (table 2, part I);

d – the diameter of spacer yarn.

The value of V_f and V_p is presented in table 2.

Table 2

THE VOLUME PERCENT OF SPACER YARNS AND POLYURETHANE FOAM					
Sample	A1	A2	A3	A4	A5
V_f (%)	2.42	1.98	1.28	2.53	2.32
V_p(%)	97.58	98.02	98.72	97.469	97.68

Next, the aim is to get the compression force on polyurethane foam (F_2). The ends of spacer yarns are interlocked by surface layers of spacer fabrics. The constraint condition at ends of spacer yarns can be seen as the constraint of elastically hinged support. The polyurethane foams can be given as the elastic foundation that provides mechanical supports. According to the theory of elastic foundation, it is indicated that the compression force on the foams is directly proportional to the displacement function. Based on the above mentioned assumptions, the compression load on the polyurethane foams can be given as:

$$F_2 = kx \tag{13}$$

where:

F_2 is the compression force on polyurethane foams;

k – elastic foundation coefficient.

In addition, the elastic coefficient k is expressed as [8]:

$$k = \phi \frac{E_p L}{H} \tag{14}$$

where:

E_p is compression modulus of polyurethane foams; it can be obtained from compression test. The value of E_p is 13.96 Mpa. ϕ can be calculated by equation (15):

$$\phi = \frac{1}{2} e^{-10(1-\frac{L_w}{L})} \tag{15}$$

where:

L_w is the distance between two adjacent loops in wale direction. It can be calculated by wale-wise density. The value of L_w is given in table 3.

Table 3

THE VALUE OF L_W	
Sample	**L_w (mm)**
A1	1.83
A2	1.84
A3	1.77
A4	1.83
A5	1.78

According to equation (13)–(15), the compression force on polyurethane foam (F_2) can be given as equation (16):

$$F_2 = \frac{1}{2} e^{Z-10(1-\frac{L_w}{L})} \frac{E_p L}{H} \tag{16}$$

Therefore, according to equation (1), the total compression force of polyurethane-based composites can be give as equation (17):

$$F = V_f EI + \frac{V_p}{2} e^{Z-10(1-\frac{L_w}{L})} \frac{E_p L}{H} \tag{17}$$

Based on equation (17), the total compression force (F) on polyurethane-based composites can be simulated by Matlab.

RESULTS AND DISCUSSIONS

Comparison of simulation and experiment curves

Comparisons of the experimental results and theoretical estimates for five specimens are shown in figure 3. It is revealed that there are still some deviations between the experiment and simulation curves. Many factors contribute to the results. But the following reasons may be the critical ones. Firstly, the idealization of spacer yarns' status accounts for the deviations. To simplify the calculation, the status of spacer yarns in the polyurethane-based composites was assumed to be straight after filling PU foams, since spacer yarns were fully stretching and carried by PU foams. However, the real status of spacer yarns is not straight but a little buckled. Secondly, the simulation models are established by assuming the deformation curves of composites follow exponential function and that are frictionless. In fact, the curves are not a perfect exponential function and the friction existed. At last, the compression behaviors of spacer yarns were

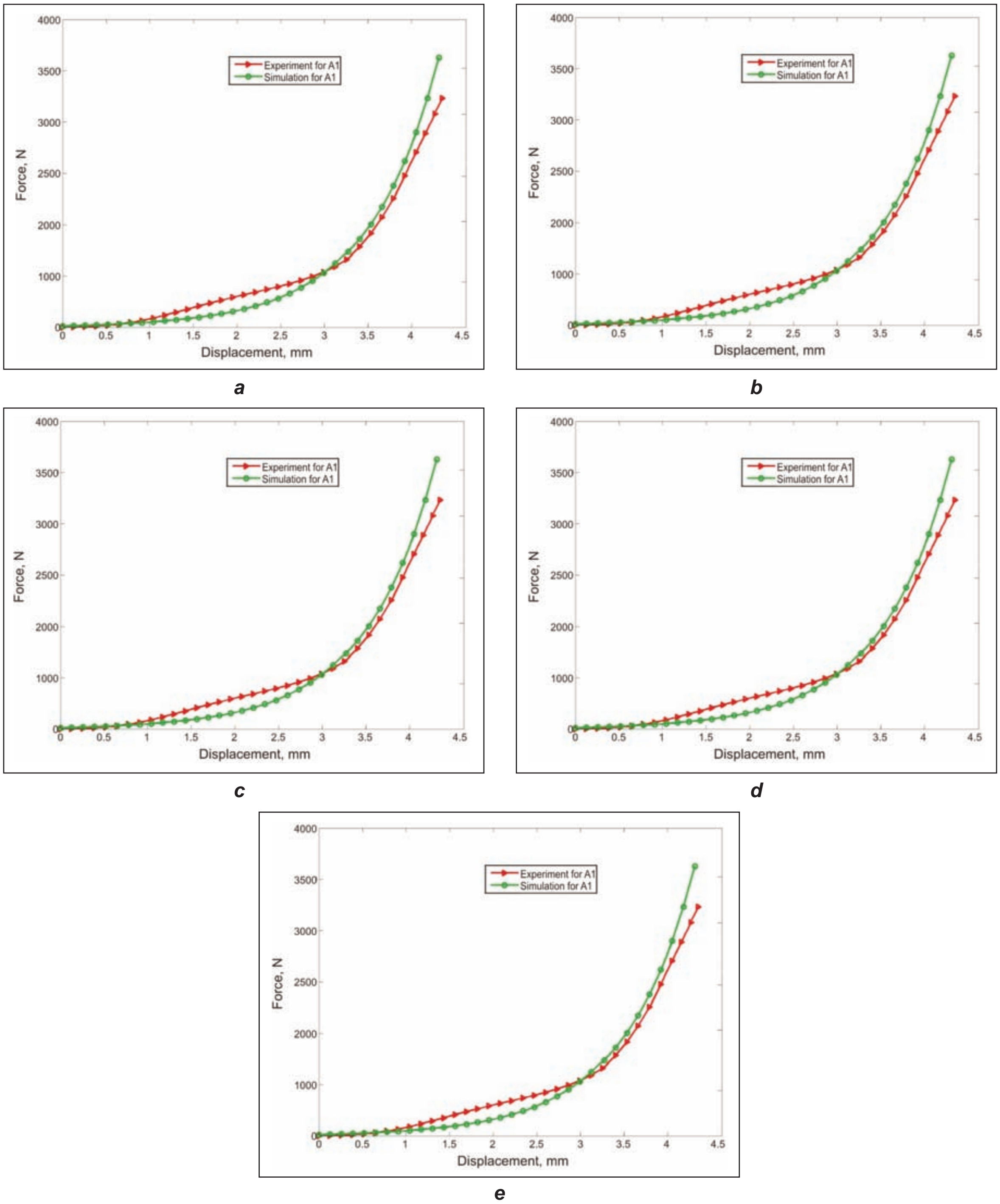

Fig. 3. Comparison of simulations and experiment results on compression behaviors

used to derive the compression behaviors of spacer fabrics in the process of model establishment, definitely influencing the precision of results.

CONCLUSIONS

Although there are still some deviations derived from some idealizations and substitutions in equation (17) such as the status of spacer yarns, outer layer density, etc., good correlations are obtained between the experimental results and the simulation ones. Therefore, the theoretical model of compression properties is validated and can be used to predict the anti-compression abilities of polyurethane-based warp-knitted spacer fabric composites and to establish the basic compression model is the initial stage of requirements. It can be the reference for further investigations on mechanical and other properties of polyurethane-based warp-knitted spacer fabric composites.

Acknowledgement

The authors would like to thank the Chinese Universities Scientific Fund for the financial support given to this work. [Grant number 13D310104].

BIBLIOGRAPHY

[1] Renkens W. and Kyosev Y. *Geometry modeling of warp knitted fabrics with 3D form.* In: Textile Research Journal, 2011, vol. 81, issue 4, pp. 437-443

[2] Vuure van A.W., Pflug J., Ivens J.A., Verpoest I. *Modeling the core properties of composite panels based in woven sandwich-fabrics performs*. In: Composites Part A. Applied Science and Manufacturing, 2000, vol. 60, issue 2, pp. 671–680

[3] Armakan D.M. and Roye A. *A study on the compression behavior of spacer fabrics designed for concrete applications*. In: Fibers and Polymers, 2009, vol. 10, pp.116–123

[4] Chen Y. *Compression resistance of warp knitted spacer fabric*. Dissertation, Jiang Nan University, 2007

[5] Miao X.H. and Ge M.Q*. Indentation force deflection property of cushioning warp-knitted spacer fabric.* In: Journal of Textile Research, 2009, vol. 30, issue 4, pp. 43–47

[6] Du Z.Q. and Hu H. *A study of spherical compression properties of knitted spacer fabrics Part I: Theoretical analysis.* In: Textile Research Journal, 2012, vol. 82, issue 15, pp. 1 569–1 578

[7] Zhang Y.M., Li S.Q. and Wang L.J. *Mid-point displacement after thin rod bending.* In: Mechanical Practice, 2002, vol. 24, issue 4, p. 36

[8] Hu X.G. *Calculating elastic foundation beam using Castigliao's second theorem.* Dissertation. Kunming University of Science and Technology. 2006

Authors:

SI CHEN
HAI-RU LONG
School Of Textile
Donghua University
2999 North Renmin Road, Shanghai 201620
P. R. China

Corresponding author:
HAI-RU LONG
e-mail: ansn9119@126.com, 40989087@qq.com

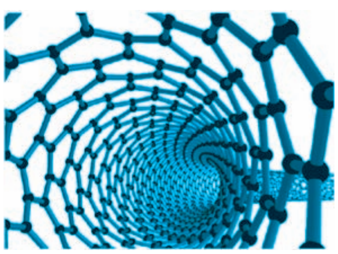

New Fortran subroutines used for biofluid parameters modeling and flow simulation thought artificial textile structures used in surgery

RALUCA MARIA AILENI
CARMEN MIHAI
ALEXANDRA ENE
COSMIN MEDAR

REZUMAT – ABSTRACT

Noi rutine Fortran utilizate pentru modelarea parametrilor biofluidului şi simularea curgerii prin structuri textile utilizate în chirurgie

În această lucrare este prezentată o nouă abordare a modelării parametrilor ce intervin în etapa de caracterizare a curgerii biofluidului în şi prin structuri tridimensionale de tip dispozitive medicale invazive obţinute prin tehnologii de prelucrare mecano-textilă. Obiectivul prezentat în lucrare este reprezentat de un produs software de tip console application pentru calculul vitezei de curgere a biofluidului, folosind programarea algoritmică în limbajul Fortran şi puterea de calcul oferită de reţeaua GRID.

Cuvinte cheie: rutine, Fortran, software, algoritm, textil, biofluid, viteză

New Fortran subroutines used for biofluid parameters modeling and flow simulation thought artificial textile structures used in surgery

This paper presents a new approach to modeling parameters involved in characterizing phase bio-fluid flow into and through the three-dimensional structure type invasive medical devices obtained by mechanic-textile processing technologies. The objective presented in this paper is console application type software for the calculation of bio-fluid flow velocity using Fortran algorithms programming language and the computing power obtained by using GRID NETWORK.

Key-words: subroutines, Fortran, software, algorithm, textile, bio-fluid, velocity

INTRODUCTION

Most programs are written by using algorithms, which contain the list of instructions in their proper execution order by the computer. The program is based on an algorithm [1], by the organization, and can use also some external data in main program. It can consider that the program is a package of data and algorithm.

Based on complex mathematical models, previously performed, which highlights the flow parameters in terms of the movement bio-fluid – solid coupling for Y textile structures [2], subroutines were developed to calculate the flow velocity for bio-fluid, by using the programming language FORTRAN [1] and power of the GRID Network.

As in the areas of bio-fluid flow artery bifurcation becomes difficult to determine the numerical simulation is required that flow rates using appropriate calculation routines.

To achieve this goal the following steps were made:

- mathematical modeling;
- writing the velocity.f program, by designing the adequate routines in FORTRAN programming language, using network GRID infrastructure for the benefit of speed and massive computing power in the execution of arithmetic complex;
- writing job for the program velocity.f;
- achieving results through program run velocity.f.

EXPERIMETAL PART

The goal was to create the console application software, writhed in FORTRAN, velocity.f.

The experimental part in this work it is represented by dividing the problem – biofluid velocity calculation:

– Mathematical modeling of the bio-fluid flow velocity [2] (4):

The start point in this application was the math formula for velocity (1):

$$v_z(r,z,t) = \frac{1}{\pi i R^2} \sum_j \frac{J_0(r s_j)}{[J_1(Rs_j)]^2} \int_{\gamma-i\infty}^{\gamma+i\infty} \Big[C_1(s_j,p)e^{-\omega z} + C_2(s_j,p)e^{-s_j z} + T(s_j,z,p) \Big] e^{pt}\, dp \quad (1)$$

where [3]:

$$C_2 = -\left\{ \frac{\dfrac{2\nu\alpha c''B\omega s}{i\alpha c''+p} - (2\nu s^2+p)\left[\dfrac{c''Bs}{i\alpha c''+p} - \dfrac{\alpha\beta^2}{\nu sp(p^2+\beta^2)}\right]}{\Delta} \right\} \times RsJ_1(Rs) \quad (2)$$

and:

$$\Delta = 4\nu\omega s^3 - \frac{1}{\nu}(2\nu s^2 + p^2) \quad (3)$$

In order to achieve the FORTRAN routine calculation were assumed C1 = 0 and T (s, z, p) = 0.

The formula for calculating the tangential velocity is:

$$v_z(r,z,t) = \frac{1}{\pi i R^2} \sum_j \frac{J_0(rs_j)}{[J_1(Rs_j)]^2} \int_{\gamma-i\infty}^{\gamma+i\infty} C_2(s_j,p) e^{-s_j z} \, dp \quad (4)$$

For calculation the velocity Vz by using the formula (4) it was done the software application velocity.f. In the program the formula (2) was calculated by using the variable SumaC2. The expression $\sum_j \frac{J_0(rs_j)}{[J_1(Rs_j)]^2}$ is calculated in program by using the variable SumaJ. The value of the mathematical expression $\frac{1}{\pi i R^2}$ is held by the variable Calc.

– Formulation of the logic programming concept – which consists in the execution of logic flow chart that is presented in figure 1.
– Using modularization by decomposing the complex problem [4] – bio-fluid flow velocity – in the subroutines and function by using the programming language Fortran [5].

The calculation of the velocity value is based on Bessel function roots [3].
For programming in FORTRAN the software application velocity.f were made the following subroutines and functions:

- Subroutine MembriIntegrala (N,NT,RJ0,RJ1,RY0,RY1,RY2,RY3,RY4,RY5, RY6,RY7,RY8,RY9,RI1,RI2,RI6,RI7);
- Subroutine functii (N,X,BJN,DJN,FJN,BYN,DYN, FYN,GYN, OYN, PYN,RYN,QYN,VYN,YYN,IYN, ZYN,ZY1,ZYP, ZY5,ZY6);
- Function : REAL Function FF(y), for calculating the integral value by using the trapezoidal method – it is calling an external function FF;

For input area, by using write and read instruction, it were used the next real or integer type parameters:

```
WRITE (*,*)'Enter Bessel function order n :'
READ(*,*)n
WRITE (*,*)'Enter Bessel function roots NT :'
READ(*,*)NT
WRITE (*,*)'Enter the blood pressure - mm Hg p :'
READ(*,*)p
WRITE (*,*)'Enter viscosity value - cm2/s v :'
READ(*,*)v
WRITE (*,*)'Enter density value - g/cm3 d :'
READ(*,*)d
.................................................................
WRITE (*,*)'Enter lower limit of integration aa :'
READ(*,*)aa
WRITE (*,*)'Enter upper limit of integration bb :'
READ(*,*)bb
WRITE (*,*)'Enter the interval number value :'
```

For output area it were displayed the calculated values for the integral and for velocity Vz:

```
SumaJ=0.0, SumaC2=0.0, Integral=0.0
DO 60 j=1,NT
SumaJ=SumaJ+RY3(j)
SumaC2=SumaC2+RY6(j)
Integral=Integral+RI6(j)
CONTINUE
..............................................................
Valoare=SumaJ*Integral*Calc          ! Valoare Vz(r,z,t)
PRINT 70, 'Velocity value in cm/s-Vz(r,z,t)=', Valoare
```

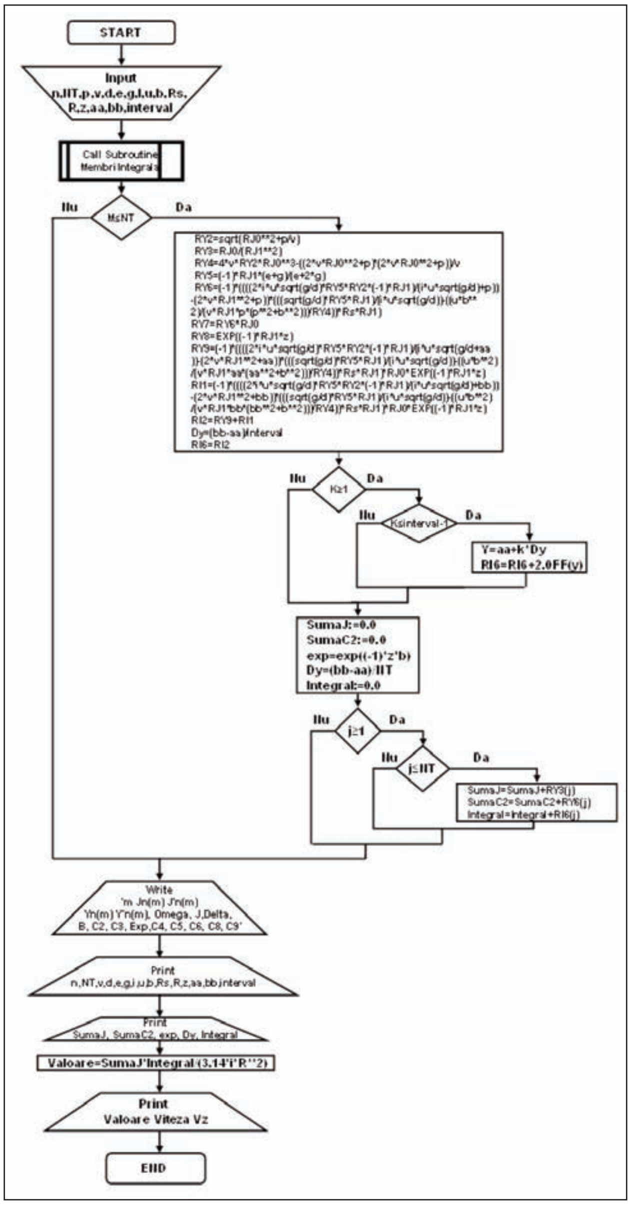

Fig. 1. Logical flow chart

Is important to note that the subroutine MembriIntegrala call is made in the main program and the subroutine Functii and the external function FF call is done in the subroutine MembriIntegrala.

RESULTS AND DISCUSSIONS

1. The mathematical modeling of the bio-fluid flow velocity

On the mathematical formula for velocity Vz (1) we were assuming the upper and lower integral limits to be done by the real variable aa – lower limit of integration and bb – upper limit of integration. Also we consider that the value C1=0 and T(s, z, p) =0.
In the formula (3) the value of the variable ω is done by using the formula: $\omega = \sqrt{s^2 + \frac{p}{v}}$,

where:
s is a Bessel root;
v – the cinematic viscosity
p – the Bio-fluid pressure.

```
[root@localhost ~]# gfortran velocity.f
[root@localhost ~]# gfortran -o velocity velocity.f
[root@localhost ~]# ./velocity
 Enter Bessel function order n :
0
 Enter Bessel function roots NT :
20
 Enter the blood pressure - mm Hg p :
0.201
 Enter viscosity value - cm2/s v :
0.000043
 Enter density value - g/cm3 d :
1059
 Enter constant elasticity lambda e :
0.87
 Enter constant elasticity mi g :
0.92
 Enter i :
0.05
 Enter alpha coefficient u :
1
 Enter beta coefficient b :
1
 Enter radius Rs in mm :
2
 Enter radius R in mm :
3
 Enter z :
3
 Enter lower limit of integration aa :
1
 Enter upper limit of integration bb :
6
 Enter the interval number value :
3
```

Fig. 2. The input parameters

WRAPPER (the agenda of the commands that must be executed).

JOB

[root@localhost ~]# cat job_incdtp.jdl
Type = "Job";
JobType = "Normal";
Executable = "wrapper.sh";
StdOutput = "std.out";
StdError = "std.err";
InputSandbox = {"wrapper.sh","viteza.f"};
OutputSandbox = {"std.out","std.err","fort.8","fort.9"};
RetryCount = 7;
Arguments = "";

WRAPPER

[root@localhost ~]# cat wrapper.sh

My wrapper !
echo "This is my wrapper !!!"
Check what was delivered
echo "Scanning landing zone...";echo -n "Current Worker node: ";hostname
echo -n "Current dir: "; startdir=$(pwd); echo $startdir; ls -l
Me=$0; echo "Me and my args: $0 $@"
if [! -f $me]; then
echo "Trouble ahead - cannot find myself."
fi
echo; gfortran viteza.f -o viteza.e; ./order.e; echo; echo "OK !!!"
rm order.f order.exe; echo "Finish "
ls -l
exit

```
 Velocity Vz(r.z.t)-Bessel functions. Integral
                          ( n = 0 )
  m       Jn(m)       J'n(m)      Yn(m)       Y'n(m)      OMEGA       J          delta         B          C2            C3                    EXP        C4         C5         C6         C8
 ..........................................................................................................................................................................................
  1      2.4048      3.8317      0.8936      2.1971      68.4120     0.1638     -944.0500     -2.5309   1659337.3899   3990416.9640         0.0000    46.6445    48.0474    94.6919    78.9099
  2      5.5201      7.0156      3.9577      5.4297      68.5922     0.1122     -962.2323     -4.6339  39653980.2581  218893068.4087         0.0000     0.1616     0.1623     0.3239     0.2699
  3      8.6537     10.1735      7.0861      8.5960      68.9152     0.0836     -993.0503     -6.7197 260014377.3722 2250093675.2237         0.0000     0.0001     0.0001     0.0003     0.0002
  4     11.7915     13.3237     10.2223     11.7492      69.3791     0.0664    -1035.1072     -8.8005 1013228254.107011947517032.0289        0.0000     0.0000     0.0000     0.0000     0.0000
  5     14.9309     16.4706     13.3611     14.8974      69.9811     0.0550    -1087.2786    -10.8791 2955507192.912344128434684.2170        0.0000     0.0000     0.0000     0.0000     0.0000
  6     18.0711     19.6159     16.5009     18.0434      70.7176     0.0470    -1148.6772    -12.9566 7161383981.9788****************        0.0000     0.0000     0.0000     0.0000     0.0000
  7     21.2116     22.7601     19.6413     21.1881      71.5846     0.0409    -1218.6156    -15.033415250891722.0190****************        0.0000     0.0000     0.0000     0.0000     0.0000
  8     24.3525     25.9037     22.7820     24.3319      72.5773     0.0363    -1296.5726    -17.1098295325398469.5105****************        0.0000     0.0000     0.0000     0.0000    -0.0000
  9     27.4935     29.0468     25.9230     27.4753      73.6906     0.0326    -1382.1623    -19.1859531684444452.0775****************        0.0000     0.0000     0.0000     0.0000    -0.0000
 10     30.6346     32.1897     29.0640     30.6183      74.9193     0.0296    -1475.1082    -21.2618903563663045.9719****************        0.0000     0.0000     0.0000     0.0000    -0.0000
 11     33.7758     35.3323     32.2052     33.7610      76.2576     0.0271    -1575.2204    -23.3376********************************        0.0000     0.0000     0.0000     0.0000    -0.0000
 12     36.9171     38.4748     35.3465     36.9036      77.7000     0.0249    -1682.3768    -25.4132********************************        0.0000     0.0000     0.0000     0.0000    -0.0000
 13     40.0584     41.6171     38.4878     40.0459      79.2407     0.0231    -1796.5071    -27.4888********************************        0.0000     0.0000     0.0000     0.0000    -0.0000
 14     43.1998     44.7593     41.6291     43.1882      80.8742     0.0216    -1917.5802    -29.5643********************************        0.0000     0.0000     0.0000     0.0000    -0.0000
 15     46.3412     47.9015     44.7705     46.3304      82.5949     0.0202    -2045.5940    -31.6397********************************        0.0000     0.0000     0.0000     0.0000    -0.0000
 16     49.4826     51.0435     47.9119     49.4725      84.3976     0.0190    -2180.5670    -33.7151********************************        0.0000     0.0000     0.0000     0.0000    -0.0000
 17     52.6241     54.1856     51.0533     52.6146      86.2769     0.0179    -2322.5321    -35.7905********************************        0.0000     0.0000     0.0000     0.0000    -0.0000
 18     55.7655     57.3275     54.1948     55.7565      88.2282     0.0170    -2471.5317    -37.8658********************************        0.0000     0.0000     0.0000     0.0000    -0.0000
 19     58.9070     60.4695     57.3362     58.8985      90.2466     0.0161    -2627.6140    -39.9411********************************        0.0000     0.0000     0.0000     0.0000    -0.0000
 20     62.0485     63.6114     60.4777     62.0404      92.3278     0.0153    -2790.8302    -42.0164********************************        0.0000     0.0000     0.0000     0.0000    -0.0000
 Bessel function order n=          0
 Bessel function roots NT=         20
Blood pressure inmm Hg  p=      0.201000
Viscosity value in cm2/s v=      0.000043
Density value in g/cm3 d=   1059.000000
Constant elasticity lambda e=       0.870000
Constant elasticity mi g=      0.920000
Value i=      0.050000
Alpha coefficient value u=      1.000000
Beta coefficient value b=      1.000000
Radius value in mm Rs=      2.000000
Radius value in mm R=      3.000000
 Value z=   3.00000000
 Lower limit of integration aa=   1.00000000
 Upper limit of integration bb=   6.00000000
 Interval number interval=         3
SumaJ=Jo/(J1**2)=      0.869509
 SumaC2=   1.23909765E+13
Integral Value=     79.180016
exp=      0.049787
Dy=     0.250000
Calc=1/pi*i*R**2=      0.707714
Velocity value in cm/s-Vz(r.z.t)=      48.728985
[root@localhost ~]#
```

Fig. 3. The results of the program velocity.f

2. The program velocity.f and the results

After compiling and execution of the source code, the user can input the parameters for bio-fluid and the specific coefficient like in figure 2. The program displays the results for velocity, integral like in figure 3.

3. Grid Network advantages

To access a powerful computation, the program was run external by using the grid network technologies (figure 4).

In this way for using the network GRID it was created a JOB (in job description language) and a

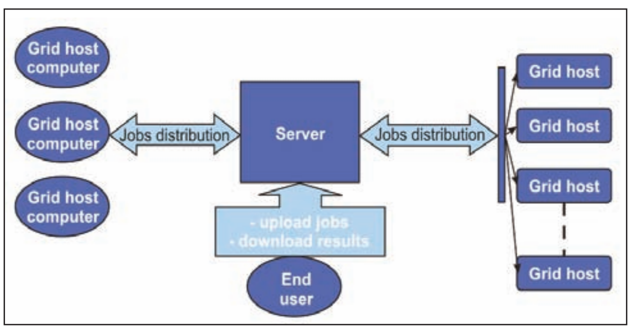

Fig. 4. Establishment of principles – GRID NETWORK

CONCLUSIONS

The objective of using the Grid Network was to obtain an upper computing power for parallel calculation of the complex mathematical formula for the bio-fluid flow velocity. The subroutines were done by using the algorithmic programming language FORTRAN. In this way it can conclude that is was obtained:

– a computing power for parallel calculation [5];
– time saving;
– precision calculation;
– logic programming execution based on operations based on modularization.

This software application can be used by researches and can be start-up for developing another complex software application.

BIBLIOGRAPHY

[1] Bacotiu, C., Gobesz, Z.F. *Initiere in programare si in limbajul Fortran*, Ed. U.T. PRES, Cluj-Napoca, 2003

[2] Ene, A. *Contributii teoretice si experimentale privind caracteristicile biomedicale si biofunctionale ale implanturilor textile destinate chirurgiei cardiovasculare*, Facultatea de Textile Pielarie si Management Industrial, Iasi, 2005

[3] Pontrelli, G. *A mathematical model of flow in liquid-filled visco-elastic tube*, In: Medical & Biological Engineering & Computing, Vol.40, pp. 550-556, 2002

[4] Chivers, I., Jane Sleightholme, J. *Introduction to Programming with FORTRAN*, Springer Verlag, ISBN 978-0-85729-232-2, 2012

[5] Press,W. H., Teukolsky, S. A., Vetterling, W. T., Flannery, B. P. *Numerical Recipes in Fortran 90: The Art of Parallel Scientific Computing, Volume 2 of Fortran Numerical Recipes*, Second Edition, United States, 1996

[6] *Fortran Programming Guide 0 Forte Developer 6 ,* (Sun WorkShop 6 update 2), Sun Microsystems, US, 2001

Authors:

Senior researcher eng. AILENI RALUCA MARIA, PhD
Senior researcher eng. ENE ALEXANDRA, PhD
Senior researcher eng. MIHAI CARMEN, PhD

The National Research & Development Institute for Textiles and Leather

16 Lucretiu Patrascanu, 030508, Bucharest, Romania

e-mail: raluca.aileni@certex.ro;

alexandra.ene@certex.ro; carmen.mihai@certex.ro;

MD COSMIN MEDAR, PhD

"Carol Davila" University of Medicine and Farmacy, Bucharest

e-mail: cosmin78@gmail.com

Fashion consumer behaviour patterns prompted by the youngest layer of Generation Y. Evidence from Romania

TUDOR EDU OANA PREDA ILIUŢĂ COSTEL NEGRICEA

REZUMAT – ABSTRACT

Modele de comportament al consumatorului de articole vestimentare regăsite în cadrul celui mai tânăr strat al Generaţiei Y. Situaţia din România

Generaţia Y, unul din cele patru grupuri generaţionale, manifestă trăsături distincte cu influenţe semnificative asupra comportamentului de cumpărare şi consum deja resimţite puternic pe diferite pieţe. Industria modei trebuie să înţeleagă modul de gândire al membrilor Generaţiei Y, deoarece aceştia vor fi cei mai mari cheltuitori pentru mulţi ani de acum încolo, dar această oportunitate importantă aduce provocări datorită eterogenităţii existente între diferitele intervale de vârstă, fiecare căutând beneficii distincte în achiziţiile efectuate. Acest studiu, realizat pe 400 de persoane din Bucureşti, cu vârsta între 20 şi 24 de ani şi cu un nivel educaţional minim la nivel de liceu, aduce lămuriri în privinţa beneficiilor căutate de consumatorii tineri din România în achiziţiile de îmbrăcăminte. De asemenea, studiul clarifică aspecte legate de criterii decizionale de cumpărare a articolelor vestimentare şi modul de corelare a diferitelor variabile în vederea explicării dimensiunilor comportamentului de consum. Acest segment de populaţie manifestă mai degrabă un comportament raţional de cumpărare pentru articolele de vestimentaţie, dar cu acordarea unei importanţe ridicate valorii sociale a mărcii. Deşi prezenta cercetare oferă informaţii importante, ea trebuie tratată ca un studiu longitudinal, fiind necesare date ulterioare pentru determinarea persistenţei acestor dimensiuni comportamentale şi descoperirea noilor dezvoltări provocate de schimbări de natură endogenă şi exogenă.

Cuvinte-cheie: comportamentul consumatorului, articole vestimentare, Generaţia Y, straturi de vârstă, România

Fashion consumer behaviour patterns prompted by the youngest layer of Generation Y. Evidence from Romania

Generation Y, one of the four generational groups, prompts distinct traits with a significant influence on the buying and consumption behaviour already greatly impacting various markets. The fashion industry must tap into the minds of the Generation Y individuals as they will be the biggest spenders for many years to come but this huge opportunity comes together with challenges induced by the heterogeneity between the different age layers, each seeking distinct benefits in their purchases. This study, performed on 400 individuals from Bucharest between 20 and 24 years old with at least a high school education, sheds light on what the young Romanian consumers look for when buying apparel. It also clarifies aspects related to fashion buying decision criteria and how different variables correlate to explain dimensions of the consumption behaviour. This population segment prompts a rather rational purchasing behaviour for clothes with a significant consideration for the brand's social value. Although the present research delivers significant insight it needs to be treated as a longitudinal study subsequent data being needed to determine the persistence of these behavioural dimensions and to unveil any new developments prompted by changes of hexogen and endogen nature.

Key-words: consumer behaviour, fashion, Generation Y, age layers, Romania

Understanding the consumer is the main concern of any business regardless the market or company size and, as a consequence, significant resources are directed to studying needs, wants, perceptions, attitudes, motives, awareness, image and buying decision criteria. Academics and researchers have successfully proposed pervasive approaches for consumer behaviour but from different angles and with distinct touches enriching the literature. The extant literature outlines that consumer behaviour entails everything that happens to an individual or within a group or organisation prior, during and after a purchase [1] in regard to seeking, selecting, acquiring, using and disposing of merchandise [2]. Consumer behaviour is centred on the decision-making process as a consumer uncovers a particular need, seeks options to satisfy it, evaluates these options based on buying criteria, makes a decision (to buy, postpone buying or not to buy) and, finally, evaluates the entire process being satisfied or dissatisfied [3], [4]. Individuals undergo such a process faster or slower and consciously or not every time a purchase is made and although the stages depicted above are common, significant differences occur in the evaluation stage as buying criteria are usually different even in the case of the same product category based on geographic, demographic, psychographic and behavioural perspectives [5].

Generation Y – definition and consumer behaviour dimensions

Generation, as a market segmentation criterion, has been used for decades by practitioners and academics for its comprehensive output. The extant literature prompts four generational groups bearing a wide variety of names: Veterans, also known as the

Silent Generation, Matures or Traditionalists; Baby Boomers; Generation X, also found as the Baby Busters or Lost Generation, and Generation Y, also known as the Millennials, Nexters, Echo Boomers [6]. If these groups are widely accepted in theory and practice, it is not the case for their time frame. There are different approaches related to Generation Y, which is under study here, being considered to comprise, according to some authors, the individuals born between 1977 and 1994 [7]. Others consider appropriate to include the individuals born between 1982 and 2002 [8], while others support the idea of including the individuals born between 1978 and 2002 [9]. Another scientific approach focuses on the individuals born between 1980 and 2000 [10]. A distinct approach underlines the use of narrow (individuals born between 1978 and 1989) and broad (individuals born between 1977 and 2002) definitions of Generation Y, as mentioned in USA Today (11 June 2005).

For this study, the time frame between 1977 and 1994 will be considered because of its wide acceptance and because this generation is a heterogeneous one [11] comprising three distinct age groups [12]: group no. 1 between 1977 and 1983, group no. 2 between 1984 and 1989 and group no. 3 between 1990 and 1994 based on encounters and experiences with ideas, technologies and means which brought about significant changes in the individual behaviour.

Generally speaking, Generation Y is considered to be socially and ethnically diverse [13] and better educated, its members mastering the latest IT&C technologies better than their parents [14] due to early-age encountering with them [15]. Also, the Generation Y individuals are entrepreneurial or in search of a flexible job [16] and most of all are more connected [17], interacting in ways unseen before [18], displaying a clear desire to work in teams [19].

From a consumption and purchase behaviour, Generation Y is marked by specific traits, such as an emotional buying decision [20], openness towards innovation and product early adoption and a high social influence [21], a materialistic approach [22] and a strong propensity towards buying brands [23] with a particular identity. The Generation Yers (as its members are named by different authors) are rather centred on acquiring hedonic satisfaction and status recognition [24] putting considerable effort and emotions into high-involvement purchases [25].

In conclusion, Generation Y prompts distinct traits with a significant influence on the buying and consumption behaviour already greatly impacting various markets, Anyway, there are significant differences within Generation Y induced mainly by the technological progress, social changes, political issues, conflicts and globalization, as a pervasive phenomenon, these factors rendering changes in values, goals and ideas especially amongst the youngest individuals.

Fashion – dimensions and peculiarities of the buying decision

At present fashion is a ubiquitous term. Due to its broad usage, there are various definitions appropriate for different contexts. Mostly, fashion is connected with style, the term being applied to a wide array of goods, such as furniture, architecture, watches, dishes, wine and, of course, clothing, as stated by Dr. Elliott Morss on www.morssglobalfinance.com. Other definitions match fashion with clothing emphasizing the style/styles of apparel considered by individuals during a period of time as found in some dictionaries, such as Encyclopaedia Britannica and Merriam-Webster. Also, fashion is connected with manner, according to the Oxford Dictionaries, portraying the making of a particular object or performing of an action, or behaviour, depicting ways in which an individual should act in a certain context. Another approach for fashion is centred on its relation to change and added value regardless of the output type [26]. Another perspective places fashion in connection with creativity extending from a basic level to a premium one [27].

It is said that fashion renders a high impulse purchase [28] due to its strong connection with style and social significance, as individuals try to blend in a particular group or a group differentiate from others through a conspicuous behaviour portrayed in a particular outfit, a gathering venue or a specific way of acting.

In this paper, fashion is associated with clothing as the scientific endeavour targets the consumption behaviour of the youngest layer within Generation Y. Nowadays people acquire apparel for other reasons than satisfying the basic needs expressed by Abraham Maslow. Individuals buy clothes to be associated with other people, to stand out in a crowd, many times dressing for other people [29] or for prestige [30]. A tremendous role in establishing and preserving this conspicuous behaviour should be attributed to the development of fashion brands [31] belonging to manufacturers and retailers and to the expansion of the globalization process.

The impact of Generation Y on the fashion industry is tremendous due to its consistent cumulative spending power, openness to product adoption and strong brand loyalty [32]. The industry must tap into the minds of these individuals as they will be the biggest spenders for the next decades but this huge opportunity comes along with challenges induced by the heterogeneity between the different age layers, each seeking distinct benefits in their purchases.

Fashion in Romania – a consumer behaviour perspective

Romanians spend around 11 billion lei per year on apparel, accessories and footwear or 11 EUR/month, according to Ziarul Financiar (10 Aug 2013). Foreign brands, such as H&M, those ones sold by Inditex and C&A recorded in 2013 a total turnover of more than 350 million EUR due to their aggressive strategy

prompted especially by the strong propensity towards brand value from the Romanian consumers, as pointed out in Ziarul Financiar (27 Sep 2013). Conversely, Romanian brands, such as TinaR and House of Art, were marked by losses and downsizing.
The most important ten foreign brands present in Romania – H&M, Zara, Bershka, Pull&Bear, Stradivarius, Oysho, Massimo Dutti, C&A, New Yorker and Kenvelo- position themselves as delivering affordable "chich" apparel. For example, H&M is positioning in the global market and Romania as a "massclusivity" brand while Zara as a brand where someone can buy cheap apparel but through a captivating customer experience rendered by trendy clothes and interesting centrally-located stores [33]. The Romanian consumers value their self-image and group identity more than price when choosing clothing items, a particular brand being the means for conveying a certain message. The foreign brands are so successful in Romania, as indicated in Business Magazin (07 Aug 2012), because they can deliver such a message based on an image built over decades in various parts of the world. This image is reinforced in Romania through the wide usage of the online tools, such as blogs and forums, and online social networks especially by the young consumers expressing and exchanging opinions about their fashion experiences [34]. These young consumers are also open to new experiences and excited to be concurrent with individuals form other parts of the world, as mentioned in the Telegraph (27 Oct 2013). Most Romanian brands focus on niche markets, as described in Ziarul Financiar (27.09.2013). This narrow focus is caused by the fierce competition from the multinational retailers but it can also be the outcome of managerial errors, as the inappropriate use of marketing tools such as the sales promotion techniques [35] and consumer behaviour mutations.
The Romanian fashion market will continue to grow for the next years due to an improvement in consumer income and a stronger switching propensity to modern retail and the expansion of the foreign fashion retailers, such as H&M and Inditex, as forecasted by Euromonitor in the 2013 Country Report.

The importance of this research

The youngest Romanian Generation Y consumers (20–24 years old) are either under recent employment or they will be very soon. They are very important fashion buyers, allocating a significant percentage of their disposable income on apparel. The suppliers, either big retailers or small companies, need to understand how these individuals inform themselves, appraise fashion items, make decisions and buy to be able to adjust their offerings as this age segment will become one of the most important ones in the fashion market for many years to come.

RESEARCH METHODOLOGY

The purpose of this study was to uncover purchasing behaviour patterns for clothing items prompted by the educated individuals between 20 and 24 years old residing in Bucharest as this group could be considered prone to trend setting in fashion and other markets considering its size (8,5%) and the behavioural changes caused by the challenges faced by these individuals caused by leaving the protective parental environment, entering employment or starting a business endeavour.
The study was built pursuing several objectives pertaining to the buying decision process for fashion products, commencing with sought-after information sources, purchasing venues, buying frequency, budgetary allocations, shopping motivation, buying criteria, brand awareness and buying intentions. Being of an explanatory type, the study was designed as a survey using a questionnaire.
A representative sample of the population between 20 and 24 years old residing in Bucharest was drawn. The sample was defined based on gender and education and built through the use of a random stratified sampling procedure. Based on the 2011 Census data for Bucharest, about gender structure (Male – 48,35% and Female – 51,65%) and academic level (High school graduates – 67,56% and University graduates – 32,44%), the sample had the following structure:

Table 1

RESEARCH SAMPLE STRUCTURE

	High school graduates	University graduates	Total
Male	131	62	193
Female	139	68	207
Total	270	130	400

The data collection was performed in Bucharest through the use of the designed questionnaire applying a systematic sampling procedure.

RESULTS AND DISCUSSIONS

Based on the applied questionnaire, data were collected uncovering interesting aspects about the garment usage and purchasing behaviour of the population under study.
The collected data displayed that the budget allocation for clothes was outranked by the rent/instalment, household, food and education expenses but surpassed the telecommunication and leisure ones. Connected to these findings, 73% of the respondents mentioned they would spend annually on clothes up to 3000 lei, with 27,5% spending between 1001 and 2000 lei. Also, considering the purchasing timeframe, 64,5% of the respondents said they would buy on monthly basis. The ranking of the garment expenses, the actual expenditure and the buying frequency should be appraised in relation with the income sourcing. Based on the findings, 45,2% of the respondents mentioned they would source the monthly income from a job and/or from a business endeavour, while 48,2% said they would benefit from

parental financial aid. These findings entitles us to believe that the young and educated individuals residing in Bucharest are rather rational than emotional decision makers, probably because of the significant percentage of them being employed or running their own business.
As to the shopping venues, 39,4% of the respondents mentioned they would buy clothes from stores selling several brands, while 24,5% mentioned they would purchase garments from stores specialized on one brand, 15,9% mentioned online stores and 0,4% other types of venues. An interesting outcome was that only 19,8% of the respondents selected outlet venues and cheap stores (in our questionnaire we used “stores selling below a certain price level”). Having 63,9% of the respondents purchasing from specialized stores, leads us to the conclusion that either the young and educated individuals residing in Bucharest are value-orientated or the social significance of the brand prevails in their buying decision.
The respondents mentioned a wide variety of information sources starting with store web sites (30,8%) and online social network pages (12,5%), followed by relatives/friends (16,6%), magazines (12,2%), store flyers (6,9%), in-store product comparisons (6,8%), role-models (Music, Movie, TV stars) (5,6%), Fashion TV channels (4,8%) and TV advertisements (3,8%). This wide variety of information sources considered together with the shopping venues strengthens our belief that the respondents are either value-orientated or focused on the brand’s social significance.
Related to the information sources to a certain extent, the awareness of the Romanian fashion brands was tested. In this regard, 56% of the respondents answered they didn’t know at least one Romanian fashion brand. The most mentioned Romanian brands by the other respondents (44%) were: TinaR, House of Art, Jolidon, Catalin Botezatu, Picioru Gras, Tatal si Fiul, Nissa. On the other hand, 58,3% of the respondents said they would definitely buy a particular clothing item if it were of Romanian origin, while 33,8% said they would consider doing so, while 5,1% said they didn’t know and 2,8% said they would definitely not buy. This low level of brand awareness is caused by the fact that only a few fashion brands bear Romanian names and the ones bearing foreign names very seldom communicate that they originate from Romania. On the other hand, this openness towards Romanian brands must be judged in connection with the core buying decision factors envisaged by this age group, especially value-for-money, and the fact that the young and educated individuals try their best in surfacing as a distinct group especially through conspicuous elements, succeeding in many instances to set trends.
Regarding the number of fashion brands bought in the past 12 months the answers varied from 1 to 30 brands, but the extremes were poorly represented. To understand the meaning of the scores obtained for this question, two correlations were performed, one with the purchasing frequency and the other one with the sum of money spent annually on clothes. The first set of scores indicated a weak negative correlation between purchasing frequency and the number of fashion brands purchased in the last twelve months. It means that if one increases, the other one decreases. Anyway, considering Somer’s d directional measure, we can estimate that the purchasing frequency can explain the number of brands purchases in the last 12 month in a proportion of 11,9% but with an error of +/– 5,7% (table 2).
The second set of scores indicated a weak positive correlation between the sum of money spent annually on clothes and the number of fashion brands purchased in the last 12 months. As an observation, although the correlation is weak, the scores are at least twice as high in comparison with the first correlation. According to the Somer’s d asymmetric value, the sum of money spent annually on clothes can explain the number of brands purchased in the last 12 months in a proportion of 26,2% with an error of +/– 3,8% (table 3).
To comprehend the motivation for shopping, six dimensions were considered: desire of acquiring a new item, seasonal wardrobe change, desire to be trendy, self-image, socializing and leisure. All these dimensions were analyzed using 5-point semantic

Table 2

DIRECTIONAL MEASURES

			Value	Asymp. Std. Error[a]	Approx. T[b]	Approx. Sig.
Ordinal by Ordinal	Somers' d	Symmetric	–0,092	0,044	–2,057	0,040
		How frequently do you buy clothes? Dependent	–0,075	0,036	–2,057	0,040
		How many brands from the same product category did you buy in the last 12 months? Dependent	–0,119	0,057	–2,057	0,040

a. Not assuming the null hypothesis.
b. Using the asymptotic standard error assuming the null hypothesis.

Table 3

DIRECTIONAL MEASURES						
			Value	**Asymp. Std. Error[a]**	**Approx. T[b]**	**Approx. Sig.**
Ordinal by Ordinal	Somers' d	Symmetric	0,251	0,037	6,853	0,000
		Money spent on clothes annually Dependent	0,241	0,035	6,853	0,000
		How many brands from the same product category did you buy in the last 12 months? Dependent	0,262	0,038	6,853	0,000

a. Not assuming the null hypothesis.
b. Using the asymptotic standard error assuming the null hypothesis.

differential scales. The respondents considered, based on the modal values, in the highest proportion the seasonal wardrobe change and self-image to be very important as shopping motives or reasons and the desire of acquiring a new item, the desire to be trendy, socializing and leisure to be important shopping motives. As a fact, at least half of the answers were recorded for the important and very important points on the scale for the desire of acquiring a new item, desire to be trendy, seasonal wardrobe change and self-image and for the very important, important and neutral points for socializing and leisure based on the median values. For a better understanding of the findings, these six dimensions were correlated with gender and education. Due to the fact that none of the 6 scales rendered a normal distribution, these variables were tested using contingency coefficients. It was uncovered according to Cohen's theory [36] that gender had a medium effect on the desire of acquiring a new item and leisure and a small effect on socializing, desire to be trendy and seasonal wardrobe change. There was no correlation between gender and self-image. As to the correlations between education and the 6 motivational dimensions, it was uncovered a small correlation between education and the desire to be trendy, leisure and self-image. There were no correlations between education and the desire of acquiring a new item, seasonal wardrobe change and socializing (tables 4 and 5).
For a wider comprehension of the purchasing behaviour, a complex model was proposed and tested based on the findings. The model is centred on the decision-making criteria used by young and educated individuals residing in Bucharest in purchasing different number of brands, on one hand and in purchasing items belonging to the same brand. The model's hypothesis was constructed on the idea that individuals used similar decision criteria for both types of purchases. For testing the model, linear regressions were used, based on the fact that all variables assumed a normal distribution, first between the number of brands purchased in the last twelve months and decision criteria and, secondly, between the tendency of buying items belonging to the same brand and decision criteria.
The first part of the model revealed a significant statistical connection between the variables but of a weak strength, the decision-making criteria being responsible for buying several fashion brands from

Table 4

CORRELATION BETWEEN MOTIVATIONAL DIMENSIONS AND GENDER				
Correlation	**Contingency coefficient**	**Approx. Sig**	**Rejecting the null hypothesis**	**Strength of correlation**
Desire of acquiring a new item and gender	0,319	0,000	Yes	Medium effect
Seasonal wardrobe change and gender	0,223	0,000	Yes	Small effect
Desire to be trendy and gender	0,233	0,000	Yes	Small effect
Self-image and gender	0,116	0,065	No	-
Socializing and gender	0,270	0,000	Yes	Small effect
Leisure and gender	0,305	0,000	Yes	Medium effect

Table 5

CORRELATION BETWEEN MOTIVATIONAL DIMENSIONS AND EDUCATION				
Correlation	**Contingency coefficient**	**Approx. Sig**	**Rejecting the null hypothesis**	**Strength of correlation**
Desire of acquiring a new item and education	0,051	0,793	No	-
Seasonal wardrobe change and education	0,097	0,282	No	-
Desire to be trendy and education	0,229	0,000	Yes	Small effect
Self-image and education	0,147	0,120	Yes	Small effect
Socializing and education	0,114	0,264	No	-
Leisure and education	0,182	0,009	Yes	Small effect

the same product category only in the range of 5%. Based on the unstandardized coefficients, only two decision criteria were relevant for buying several fashion brands from the same product criteria, meaning "matching with another item" and "manufacturing (cutting, printing, labelling etc.)" (tables 6–8).

This part of the model is defined by the following equation:

Buying several brands = 10,196 – 0,730 Matching – – 0,787 Manufacturing.

Table 6

MODEL SUMMARY				
Model	**R**	**R Square**	**Adjusted R Square**	**Std. Error of the Estimate**
1	0,223[a]	0,050	0,033	4,539

a. Predictors: (Constant), Manufacturing (cutting, printing, labelling etc.), Price, Wearing occasion, Brand reputation, Matching with another item, Design, Fabric

Table 7

ANOVA[b]						
Model		**Sum of Squares**	**df**	**Mean Square**	**F**	**Sig.**
1	Regression	422,689	7	60,384	2,931	0,005[a]
	Residual	8075,188	392	20,600		
	Total	8497,877	399			

a. Predictors: (Constant), Manufacturing (cutting, printing, labelling etc.), Price, Wearing occasion, Brand reputation, Matching with another item, Design, Fabric

b. Dependent Variable: How many brands from the same product category did you buy in the last 12 months?

Table 8

COEFFICIENTS[a]						
Model		**Unstandardized Coefficients**		**Standardized Coefficients**	**t**	**Sig.**
		B	Std. Error	Beta		
1	(Constant)	10,196	1,200		8,497	0,000
	Price	–0,018	0,310	–0,003	–0,059	0,953
	Brand reputation	–0,095	0,285	–0,017	–0,333	0,739
	Wearing occasion	–0,354	0,350	–0,053	–1,012	0,312
	Matching with another item	–0,730	0,281	–0,136	–2,595	0,010
	Fabric	0,199	0,350	0,033	0,569	0,570
	Design	–0,165	0,381	–0,023	–0,433	0,666
	Manufacturing (cutting, printing, labelling etc.)	–0,787	0,329	–0,140	–2,390	0,017

a. Dependent Variable: How many brands from the same product category did you buy in the last 12 months?

The second part of the model pointed out a stronger significant statistical connection between the variables, the decision-making criteria being responsible for buying items belonging to the same brand in proportion of 11,1%. Based on the unstandardized coefficients, three decision criteria were relevant for buying items sold under the same brand, “price”, “brand reputation” and “fabric”.

This part of the model is defined by the following equation:

Buying the same brand = 1,900 – 0,161 Price + + 0,111 Brand reputation + 0,190 Fabric.

Table 9

MODEL SUMMARY				
Model	**R**	**R Square**	**Adjusted R Square**	**Std. Error of the Estimate**
1	0,333[a]	0,111	0,095	0,611

a. Predictors: (Constant), Manufacturing (cutting, printing, labelling etc.), Price, Wearing occasion, Brand reputation, Matching with another item, Design, Fabric

Table 10

ANOVA[b]						
Model		**Sum of Squares**	**df**	**Mean Square**	**F**	**Sig.**
1	Regression	18,166	7	2,595	6,962	0,000[a]
	Residual	146,131	392	0,373		
	Total	164,297	399			

a. Predictors: (Constant), Manufacturing (cutting, printing, labelling etc.), Price, Wearing occasion, Brand reputation, Matching with another item, Design, Fabric
b. Dependent Variable: Do you usually buy items sold under the same brand?

Table 11

COEFFICIENTS[a]						
Model		**Unstandardized Coefficients**		**Standardized Coefficients**	**t**	**Sig.**
		B	Std. Error	Beta		
1	(Constant)	1,900	0,161		11,772	0,000
	Price	–0,161	0,042	–0,186	–3,869	0,000
	Brand reputation	0,111	0,038	0,144	2,899	0,004
	Wearing occasion	0,087	0,047	0,093	1,854	0,065
	Matching with another item	–0,050	0,038	–0,067	–1,315	0,189
	Fabric	0,190	0,047	0,224	4,023	0,000
	Design	–0,041	0,051	–0,040	–0,791	0,429
	Manufacturing (cutting, printing, labelling etc.)	–0,011	0,044	–0,014	–0,242	0,809

a. Dependent Variable: Do you usually buy items sold under the same brand?

As it can be noticed, buying several brands and buying one brand are rendered by different decision criteria, which is an interesting outcome as all these criteria are common denominators in individual purchasing. This model is relevant from a statistical perspective and uncovers dimensions of the purchasing behaviour of this population segment.

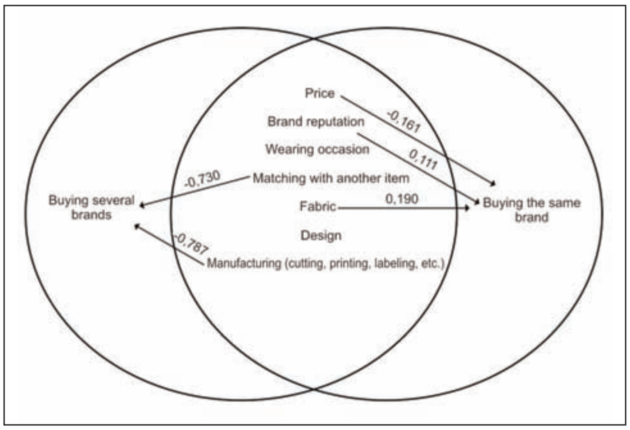

Fig. 1. Buying decision model consisting of two sections

CONCLUSIONS

This research offers purchasing and consumption behaviour guidelines of a very dynamic population segment with a tremendous impact on the future of the clothing demand. This age segment of 20 to 24 years old is on the verge of major life changes as the individuals are either still involved in the educational system and/or are in their employment infancy or at the beginning of entrepreneurial endeavours, living with their parents or have just departed and moved on their own. They are the group setting new trends and establishing new benchmarks and as a consequence shaping the supply in the garment industry for many years to come.

This research provides significant input for the garment industry, manufacturers and traders, pointing out the types of purchasing venues, information sources, shopping motivation, decision criteria and brand awareness and buying intentions pertaining to a population segment which will be at the forefront of the future purchasing and usage behaviour of the fashion products. This population segment prompts a rather rational purchasing behaviour for clothes with a significant consideration for the brand's social value. An interesting outcome of this research is the lack of awareness in relation with Romanian fashion brands but a considerable buying intention for these brands. The correlations between the number of brands purchased in the last twelve months and purchasing frequency and the sum of money allocated for clothes provide other relevant pieces of information about the rational usage and purchasing behaviour. Also, the small and medium correlations between gender and education on one side and some of the shopping motivation dimensions on the other side shed light as to what this population segment values and regards as being important. The model tested in this study unveils which decision criteria are of importance when individuals pursue one brand and which criteria are important when individuals pursue more brands.

Although the present research delivers significant insight about the usage and purchasing behaviour of fashion items amongst young and educated individuals residing in Bucharest it needs to be considered as a starting point and, as a consequence, treated as a longitudinal study subsequent data being needed to determine the persistence of these behavioural dimensions and to unveil any new developments prompted by changes of hexogen and endogen nature.

BIBLIOGRAPHY

[1] Strydom, J. *Introduction to Marketing*. 3rd ed., Juta, Cape Town, 2004

[2] Hawkins, D. I., Best, R. J., Coney, K. A. *Consumer Behavior: Building Marketing Strategy*. 7th ed., McGraw-Hill, Boston, 1998, pp. 7

[3] Peter, J. P., Olson, J. C. *Consumer Behavior and Marketing Strategy*. 7th ed., McGraw-Hill Irwin, Boston, 2005, pp. 169

[4] Catoiu, I., Teodorescu, N. *Comportamentul consumatorului*. ed. 2, Uranus, Bucuresti, 2004, pp. 34

[5] Kotler, Ph., Armstrong, G. *Principles of Marketing.* 12th ed., Prentice Hall, NJ, 2008, pp. 185–190

[6] Parry, E., Urwin, P.- *Generational Differences In Work Values: A Review of Theory and Evidence*. In: International Journal of Management Reviews, 2011, vol. 13, pp. 79–96

[7] Sheahan, P. *Generation Y: thriving (and surviving) with Generation Y at work*. Hardie Grant Books, Prahran, 2010

[8] McCrindle, M. *Understanding Generation Y*. In: Principal Matters, 2003, no. 55, pp. 28–31

[9] Sommer, K., Trudy, S. *Managing Generation Y: Stop resisting and start embracing the challenges Generation Y brings to the workplace*. In: Human Resources Magazine, 2006, vol. 51, no. 5

[10] Erickson, T. *Plugged In: The Generation Y Guide to Thriving at Work*. Harvard Business Press, Boston, 2008, pp. 5–6

[11] Foscht, T., Schloffer, J., Maloles, C., Chia, S.L. *Assessing the outcomes of Generation Y customers' loyalty*. In: International Journal of Bank Marketing, 2009, vol. 27, issue 3, pp. 218–241

[12] Paul, P. *Getting Inside Gen Y.* In: American Demographics, September 1st, 2001

[13] Howe, N., Strauss, W. *Millennials Rising: The Next Greatest Generation.* Vintage Books, NY, 2000

[14] Neuborne, E., Kerwin, K. *Generation Y*. In: Business Week, 14 Feb. 1999

[15] Djamashi, S., Siegel, M., Tullis, T. *Generation Y, web design and eye tracking*. In: International Journal of Human-Computer Studies, 2010, no. 68, pp. 307–323

[16] Martin, C.A. *From high maintenance to high productivity. What managers need to know about Generation Y*. In: Industrial and Commercial Training, 2005, vol. 37, no. 1, pp. 39–44

[17] Boase, J., Horrigan, J.B., Wellman, B., RAINIE, L. *The Strength of Internet Ties*. Pew Internet and American Life Project, 25 January 2006

[18] Westlake, E. J. *Friend Me if You Facebook Generation Y and Performative Surveillance*. In: The Drama Review, Winter 2008, vol. 52, no. 4, pp. 21–40

[19] Oblinger, D.G., Oblinger, J.L. (editors) *Educating the Net Generation*. Educase, 2005

[20] Kim, E. Y., Knight, D. K., Pelton, L. E. *Modeling Brand Equity of a US Apparel Brand as Perceived by Generation Y Consumers in the Emerging Korean Market*. In: Clothing and Textiles Research Journal, October, 2007, vol. 27, no. 4, pp. 247–258

[21] Parment, A. *Generation Y vs Baby Boomers: Shopping behavior, buyer involvement and implications for retailing*. In: Journal of Retailing and Consumer Services, 2013, no. 20, pp. 189–199

[22] Yingjiao, X. *The influence of public self-consciousness and materialism on young consumers' compulsive buying*. In: Young Consumers: Insight and Ideas for Responsible Marketers, 2008. vol. 9, issue 1, pp. 37–48

[23] Loroz, P. S. *The Generation Gap: A Baby Boomer vs Gen Y Comparison of Religiosity*, *Consumer Values and Advertising Appeal Effectiveness*. In: Advances in Consumer Research, 2009, vol. 33, eds. Pechmann Connie and Price Linda, Duluth, MN: Association for Consumer Research, pp. 308–309

[24] Mueller, S., Remaud, H., Chabin, Y. *How strong and generalisable is the Generation Y effect? A cross-cultural study for wine*. In: International Journal of Wine Business Research, 2011, vol. 23, issue 2, pp. 125–144

[25] Parment, A. *Generation Y in Consumer and Labour Markets*. Routledge, NY, 2011

[26] Kawamura, P. *Fashion-ology: An Introduction to Fashion Studies*. Berg, Oxford, 2005, pp. 4–5

[27] Easey, M. *Fashion marketing*. 3rd. ed., Wiley-Blackwell, Oxford, 2009

[28] Bhardwaj, V., Fairhurst, A. *Fast fashion: response to changes in the fashion industry*. In: The International Review of Retail, Distribution and Consumer Research, 2010, vol. 20, pp. 165–172

[29] De Lace, J. *The Psychology and Behavior of Consumers in the Fashion Industry*. Senior Honors Paper 234, 2011

[30] KORT, M.P., CAULKINS, P.J., HARTL, F.R., FEICHTINGER, G. *Brand image and brand dilution in the fashion industry*. In: Automatica, 2006, no. 42, pp. 1363–1370

[31] Rajagopal, M. *Consumer culture and purchase intentions toward fashion apparel in Mexico*. In: Database Marketing & Customer Strategy Management, 2011, vol. 18, issue 4, pp. 286–307

[32] Noble, S.M., Haytko, D.L., Phillips, J. *What drives college-age Generation Y consumers*. In: Journal of Business Research, 2009, no. 62, pp. 617–628

[33] Tungate, M. *Fashion brands, Brand Style from Armani to Zara*. 2nd ed., Kegan Page Ltd., London, 2008, pp. 47–48

[34] Orzan, G., Iconaru, C., Popescu, I. C., Orzan, M., Macovei, O. I. *PLS-based SEM analysis of apparel online buying behaviour. The importance of eWOM*. In: Industria Textila, 2013, vol. 64, nr. 6, pp. 362–367

[35] Popescu, D. I., Popa, I., Cicea, C., Iordanescu, M. *The expansion potential of using sales promotion techniques in the Romanian garments industry*, In: Industria Textila, 2013, vol. 64, nr. 5, pp. 293–300

[36] Cohen, J. *A Power Primer*. In: Psychological Bulletin, 1992. Vol. 112, issue 1, pp. 155–159

Authors:

Associate Professor PhD. TUDOR EDU

Associate Professor PhD. OANA PREDA

Associate Professor PhD. ILIUŢĂ COSTEL NEGRICEA

Romanian-American University

Faculty of Management-Marketing

1B Expozitiei Blvd., Bucharest

e-mail: tudoredu@yahoo.com, ocpreda@yahoo.com,

negricea@yahoo.com

INFORMATION FOR AUTHORS

Industria Textila magazine is an international peer-reviewed journal published by the National Research & Development Institute for Textiles and Leather – Bucharest, in print editions.

Aims and Scope: *Industria Textila* magazine welcomes papers concerning research and innovation, reflecting the professional interests of the Textile Institute in science, engineering, economics, management and design related to the textile industry and use of fibres in consumer and engineering applications. Papers may encompass anything in the range of textile activities, from fibre production through textile processes and machines, to the design, marketing and use of products. Papers may also report fundamental theoretical or experimental investigations, practical or commercial industrial studies and may relate to technical, economic, aesthetic, social or historical aspects of textiles and the textile industry.

Submission of Manuscripts

The paper submitted for publication shall concern problems associated with production and application of fibers and textiles.

Please include full postal address as well as telephone/fax/e-mail details for the corresponding author, and ensure that all correspondence addresses are included. Also include the scientific title of the authors.

Industria Textila magazine considers all manuscripts on the strict condition that they have been submitted only to the *Industria Textila* journal, on this occasion, and that they have not been published already, nor are they under consideration for publication or in press elsewhere. Authors who fail to adhere to this condition will be charged with all costs which *Industria Textila* magazine incurs and their papers will not be published.

Manuscripts

Manuscripts of the following types are accepted:

Research Papers – An original research document which reports results of major value to the Textile Community

Notes – see below

Book Reviews – A brief critical and unbiased evaluation of the current book, normally invited by the Editor

Correspondence – Communications based on previously published manuscripts

Manuscripts shall be submitted in English in double-spaced typing, A4 paper, size font 12, Times New Roman, margins 2 cm on all sides, under electronic version in Word for Windows format.

The volume of the submitted papers shall not exceed 10 pages (including the bibliography, abstract and key words), typescript pages including tables, figures and photographs.

All articles received are reviewed by a reviewer, renowned scientist and considered expert in the subject the article concerns, which is appointed by the editorial board. After the article has been accepted, with the completions and the modifications required by the reviewer or by the editorial staff, it will be published.

The submission of the above-mentioned papers is by all means the proof that the manuscript has not been published previously and is not currently under consideration for publication elsewhere in the country or abroad.

There may also be published papers that have been presented at national or international scientific events, which have not been published in volume, including the specification related to the respective event.

The articles assessed as inappropriate by the reviewer or by the editorial staff, concerning the subject matter or level, shall not be published.

The manuscript shall be headed by a concise title, which should represent in an exact, definite and complete way the paper content. Authors should also supply a shortened version of the title, suitable for the running head, not exceeding 50 character spaces.

The manuscript shall also be headed by complete information about the author(s): titles, name and forename(s), the full name of their affiliation (university, institute, company), department, city and state, as well as the complete mailing address (street, number, postal code, city, country, e-mail, fax, telephone).

Tables and figures (diagrams, schemes, and photographs) shall be clear and color, where possible.

The photographs shall be sent in original format (their soft), or in JPEG or TIF format, having a resolution of at least **300 dpi**.

All tables and figures shall have a title and shall be numbered with Arabic numerals, consecutively and separately throughout the paper, and referred to by the number in the text.

Generally, symbols and abbreviations shall be used according to ISO 31: specifications for quantities, units and symbols. SI units must be used, or at least given comprehensive explanations or their equivalent.

Cited references shall be listed at the end of the paper in order of quotation and contain: **for a paper in a periodical** – the initials and surname of the author(s), title of journal and of the article, year and number of issue, number of volume and page numbers; **for a book** – the initial and surname of the author(s), full name of the book, publisher, issue, place and year of publishing, and the pages cited; **for patents** – the initial and surname of the author(s), the title, the country, patent number and year.

[1]. Grégory, P., Marketing, 2e edition, Édition Dalloz, Paris, 1996

Authors are requested to send an abstract of the paper, preferably no longer than 100 words and a list of 5-6 key words (preferably simple, not compound words, in alphabetical order). Avoid abbreviations, diagrams and direct reference to the text.

All manuscripts with the material proposed for publication, shall be sent to:

marius.iordanescu@certex.ro

Complimentary issue – The corresponding author will receive a complimentary print copy of the issue in which his/her article appears. It will be up to the corresponding author if he/she decides to share or route his/her copy to his/her co-author(s).